

CHAPTER 5

Climate-Ozone Connections

Lead Authors:

M. Baldwin
M. Dameris

Coauthors:

J. Austin
S. Bekki
B. Bregman
N. Butchart
E. Cordero
N. Gillett
H.-F. Graf
C. Granier
D. Kinnison
S. Lal
T. Peter
W. Randel
J. Scinocca
D. Shindell
H. Struthers
M. Takahashi
D. Thompson

Contributors:

D. Battisti
P. Braesicke
R. Garcia
P. Haynes
E. Manzini
K. Matthes
G. Pitari
V. Ramaswamy
K. Rosenlof
B. Santer
R. Scott
A. Stenke
C. Timmreck

Final Release: February 2007
From *Scientific Assessment of Ozone Depletion: 2006*

CHAPTER 5

CLIMATE-OZONE CONNECTIONS

Contents

SCIENTIFIC SUMMARY	5.1
5.1 INTRODUCTION	5.3
5.2 COUPLING OF THE STRATOSPHERE AND TROPOSPHERE	5.3
5.2.1 Radiation	5.3
5.2.2 Dynamics	5.6
5.2.2.1 Role of Waves	5.6
5.2.2.2 How the Stratosphere Affects Its Own Variability	5.6
5.2.2.3 Transport of Air into the Stratosphere	5.7
5.2.2.4 Modeling and Parameterization of Small-Scale Waves	5.7
5.2.2.5 Annular Modes	5.8
5.2.2.6 Effects of Stratospheric Variability on the Troposphere	5.8
5.2.3 Tropospheric Composition	5.8
5.2.4 Stratospheric Aerosols	5.10
5.2.5 Past Changes in Stratospheric Water Vapor	5.12
5.2.6 Past Changes in Stratospheric Temperature	5.13
5.2.7 Impact of Ozone Changes on Surface Climate	5.16
5.2.7.1 Southern Hemisphere	5.16
5.2.7.2 Northern Hemisphere	5.18
5.3 EFFECTS OF ANTHROPOGENIC CLIMATE CHANGE AND OF EMISSIONS ON STRATOSPHERIC OZONE	5.18
5.3.1 Stratospheric Temperature Changes Due to Shifts in Radiative Forcing	5.18
5.3.2 Stratospheric Temperature Changes Due to Additional Effects	5.23
5.3.3 Troposphere-Stratosphere Exchange and the Brewer-Dobson Circulation	5.26
5.3.4 Changes in the Tropical and Extratropical Tropopause Layer	5.29
5.3.4.1 The Tropical Tropopause Layer (TTL)	5.29
5.3.4.2 The Extratropical Tropopause Layer (ExTL)	5.31
5.3.5 Impact of Future Water Vapor Changes on Ozone Chemistry	5.31
5.3.6 Impact of Temperature Changes on Ozone Chemistry	5.32
5.3.6.1 Upper Stratosphere	5.32
5.3.6.2 Polar Lower Stratosphere	5.33
5.3.7 Impact of Climate Change on Ozone Recovery	5.34
REFERENCES	5.38
APPENDIX 5A: AOGCMs Used in Chapter 5	5.49

SCIENTIFIC SUMMARY

Climate change will affect the evolution of the ozone layer through changes in transport, chemical composition, and temperature. In turn, changes to the ozone layer will affect climate through radiative processes, and consequential changes in temperature gradients will affect atmospheric dynamics. Therefore, climate change and the evolution of the ozone layer are coupled. Understanding all of the processes involved is made more complex by the fact that many of the interactions are nonlinear.

Impact of Climate Change

- **The stratospheric cooling observed during the past two decades has slowed in recent years.** Satellite and radiosonde measurements reveal an overall cooling trend in the global-mean lower stratosphere of approximately 0.5 K/decade over the 1979-2005 period, with a slowdown in the temperature decline since the late 1990s. The overall temperature decrease is punctuated by transient warmings of the stratosphere associated with the major volcanic eruptions in 1982 and 1991. Model calculations suggest that the observed ozone loss is the predominant cause of the cooling observed over this period. The lower stratospheric cooling is evident at all latitudes, in particular in both Arctic and Antarctic winter/spring lower stratosphere but with considerable interannual variability. Satellite observations show larger temperature trends in the upper stratosphere, with values of -1 to -2 K/decade, but little additional decline since the middle 1990s. Model calculations suggest that the upper stratosphere trends are due, roughly equally, to decreases in ozone and increases in CO_2 .
- **Future increases of greenhouse gas concentrations will contribute to the average cooling in the stratosphere.** Estimates derived from climate models (AOGCMs, coupled ocean-atmosphere general circulation models) and Chemistry-Climate Models (CCMs) with interactive ozone consistently predict continued cooling of the global average stratosphere. The predicted cooling rate within the next two decades is dependent on the prescribed scenario and the type of model used for the assessment. At 50 hPa an average of all AOGCMs gives approximately 0.1 K/decade, while CCMs predict a larger cooling of about 0.25 K/decade caused by the interactive consideration of ozone changes. All models calculate a stronger cooling at 10 hPa, averaging approximately 0.5 K/decade. Polar temperatures in the future are less certain than global mean temperatures because of greater natural variability.
- **Chemical reaction rates in the atmosphere are dependent on temperature, and thus the concentration of ozone is sensitive to temperature changes.** Decreases in upper stratospheric temperature slow the rate of photochemical ozone destruction in this region. Hence the concentration of upper stratospheric ozone increases in response to cooling. Cooling of the polar lower stratosphere would lead to more efficient chlorine activation on aerosol and polar stratospheric clouds and enhanced ozone destruction. Therefore, the concentration of ozone in the springtime polar lower stratosphere would decrease in response to cooling.
- **Greenhouse-gas-induced temperature and circulation changes are expected to accelerate global ozone increases in the next decades.** Two-dimensional latitude-height models, as well as CCMs, show that 1980 global mean total ozone values will be reached several years earlier than in a constant-temperature stratospheric environment.

Impact on the Troposphere

- **Changes to the temperature and circulation of the stratosphere affect weather and climate of the troposphere.** The response is seen largely as changes to the strength of the surface westerly winds in midlatitudes, and is found in both observations and model results. The strongest evidence for coupling is seen in the Northern Hemisphere during winter and in the Southern Hemisphere during spring. We do not have a complete understanding of the mechanisms that cause the stratosphere to affect the troposphere.
- **Stratospheric ozone depletion in the Southern Hemisphere appears to have caused circulation changes not only in the stratosphere, but in the troposphere as well.** The observed cooling of the Antarctic lower stratosphere has led to an increase in the speed of the stratospheric westerly winds and an associated delay in the seasonal breakdown of the stratospheric polar vortex. Observations and model results suggest that the changes to the lower

CLIMATE-OZONE CONNECTIONS

stratosphere have contributed to the observed strengthening of midlatitude tropospheric winds and to cooling over the interior of Antarctica during December-February. As ozone recovers, tropospheric changes due to ozone loss are expected to reverse. However, temperature changes due to increasing greenhouse gas concentrations may offset this reversal.

Importance of Tropospheric Changes

- **Human activities are expected to affect stratospheric ozone through changes in emissions of trace gases.** Enhanced methane (CH_4) emission (from wetter and warmer soils) is expected to enhance ozone production in the lower stratosphere, whereas a climate-driven increase in nitrous oxide (N_2O) emission is expected to reduce ozone in the middle and high stratosphere. Also, changes in nonmethane hydrocarbons and nitrogen oxide (NO_x) emissions are expected to affect the tropospheric concentrations of hydroxyl radical (OH) and, hence, impact the lifetime and concentration of stratospheric trace gases such as CH_4 and organic halogen species.
- **The exchange of air between the troposphere and the stratosphere is predicted to increase due to climate change.** Model studies predict that the annual mean troposphere-to-stratosphere mass exchange rate is expected to increase significantly, which will also decrease the average time that air remains within the stratosphere. Another possible consequence is a counterbalance of the stratospheric cooling associated with increasing greenhouse gases by an increase in the descent and adiabatic heating in the polar stratosphere during winter and spring. The net effect could result in local stratospheric temperature increases confined to high northern latitudes during winter and spring.

Importance of Water Vapor

- **Updated datasets of stratospheric water vapor concentrations now show differences in long-term behavior.** Recent trend analyses, which are based on only two available multiyear datasets, casts doubt on the positive stratospheric water vapor trend that was noted in the previous Assessment. Balloonborne measurements at Boulder, Colorado, for the period 1980-2005 show a significant increase of 5-10% per decade over altitudes of 15-28 km. Global measurements from the Halogen Occultation Experiment (HALOE) satellite instrument for 1991-2005 do not show corresponding positive lower stratospheric trends. Interannual water vapor changes derived from HALOE data exhibit quantitative agreement with temperature variations near the tropical tropopause. In contrast, the long-term increases inferred from the Boulder data are larger than can be explained by observed tropopause temperature changes or past increases in tropospheric methane.
- **Future changes of stratospheric water vapor concentrations are uncertain.** If water vapor concentration increases in the future, there will be both radiative and chemical effects. Modeling studies suggest increased water vapor concentrations will enhance odd hydrogen (HO_x) in the stratosphere and subsequently influence ozone depletion. Increases in water vapor in the polar regions would raise the temperature threshold for the formation of polar stratospheric clouds, potentially increasing springtime ozone depletion.

Importance of Volcanoes

- **If a major volcanic eruption occurs while stratospheric halogen loading is elevated, ozone will temporarily be depleted.** Strong volcanic eruptions enhance stratospheric aerosol loading for two to three years. A global average increase of lower stratospheric temperature (about 1 K at 50 hPa) was observed following the eruptions of El Chichón and Mt. Pinatubo, and globally averaged total ozone significantly decreased by about 2% before recovering after about two to three years. Ozone destruction via heterogeneous reactions depends on halogen loading, so the effects on ozone of a major eruption are expected to decrease in the coming decades. For sufficiently low halogen loading, a large volcanic eruption would temporarily increase ozone. Long-term ozone recovery would not be significantly affected.

5.1 INTRODUCTION

The purpose of this chapter is to assess the effects of human-induced climate change and greenhouse gases on stratospheric ozone. Investigations of the relationships and feedbacks between ozone depletion and climate change processes have demonstrated that it is not possible to achieve a complete understanding of ozone changes without the consideration of climate change. This chapter primarily concentrates on how climate change affects stratospheric ozone. The effect of stratospheric ozone depletion on climate was a focus of the Intergovernmental Panel on Climate Change/Technology and Economic Assessment Panel special report (IPCC/TEAP, 2005).

An increase of well-mixed greenhouse gas concentrations in the atmosphere leads to higher tropospheric temperatures (the greenhouse effect) and lower stratospheric temperatures. The rates of many chemical reactions are temperature dependent, and these reaction rates affect the chemical composition of the atmosphere. Reduced stratospheric temperatures lead to a slowing of some gas-phase reactions that destroy ozone, but also lead to intensified depletion of ozone in the lower polar stratosphere due to increased activation of halogens on polar stratospheric clouds (PSCs).

Since climate change processes influence the dynamics of the troposphere and the stratosphere, dynamically induced temperature changes could locally reinforce or oppose the temperature changes caused by radiative processes. These future changes are highly uncertain, with some models projecting that temperature will increase in the polar regions during northern winter and spring. The net effect of radiative, chemical, and dynamical interactions and feedbacks (many of which are nonlinear) is poorly understood and quantified at present.

Results of investigations presented in this chapter are based on observations and numerical modeling studies. Although atmospheric models have improved in recent years, they are still subject to uncertainties due to an incomplete description of atmospheric processes, their forcing, and their feedbacks. Weaknesses of models must be considered when evaluating calculated future changes, in particular for the assessment of the future evolution of the stratospheric ozone layer, as discussed in Chapter 6.

A summary description of the types of models used in this Assessment is given in Box 5-1. Section 5.2 provides an overview of stratospheric processes and a basic description of the coupling of the stratosphere and the troposphere. It contains background information about mechanisms and key processes that are relevant to describe and explain climate-ozone connections and feedbacks. In addition, it describes the influences of water vapor and of

its changes, sulfate aerosol, changes in source gases, temperature trends, their feedbacks on both chemistry and dynamics, and comparisons to results derived from numerical models describing atmospheric processes. Section 5.3 focuses on interactions between human-induced climate change and ozone depletion. At the end a detailed discussion of results derived from Chemistry-Climate Models is presented, which specifically addresses the question of how climate change will affect the evolution of the ozone layer.

5.2 COUPLING OF THE STRATOSPHERE AND TROPOSPHERE

5.2.1 Radiation

Greenhouse gases (GHGs), mainly carbon dioxide (CO_2) and water vapor, warm the troposphere by absorbing outgoing infrared (IR) radiation from the Earth in the well-known greenhouse effect. The dominant balance in the troposphere is between latent heating and radiative cooling by greenhouse gases. In the stratosphere, however, increased greenhouse gases lead to a net cooling as they emit more IR radiation out to space than they absorb. IR emission increases with local temperature, so the cooling effect increases with altitude, maximizing near the stratopause, where stratospheric temperatures are highest. The stratospheric cooling effect of greenhouse gases varies with latitude, as it depends on the balance between absorption of IR from below and local emission. The net cooling effect of greenhouse gases extends to lower levels at high latitudes, roughly following the tropopause.

Any change in radiatively active gas concentrations will change the balance between incoming solar (shortwave) and outgoing terrestrial (longwave) radiation in the atmosphere. The change of this balance due solely to the species in question, keeping other climate variables fixed, is termed radiative forcing (WMO, 2003; IPCC/TEAP, 2005). Radiative forcing is conventionally given as the net change in radiative fluxes at the tropopause, which can be a reasonable indicator of the surface temperature response.

Ozone absorbs both shortwave and longwave radiation. To determine radiative forcing from stratospheric ozone changes, it is important to distinguish between instantaneous effects and the effects after the stratospheric temperature has adjusted. Depletion of ozone in the lower stratosphere causes an instantaneous increase in the shortwave solar flux at the tropopause and a slight reduction of the downwelling longwave radiation. The net instantaneous effect is a positive radiative forcing. However, the

Box 5-1. Atmospheric Models

Numerical models are useful for investigations of the composition and the thermal and dynamical structure of Earth's atmosphere. They allow evaluation of different processes and mechanisms as well as feedbacks. Scientific progress can be achieved by understanding the discrepancies between observations and results derived from model simulations. Assessments of the future development of atmospheric dynamics and chemistry are typically based on scenario simulations and sensitivity studies. In this 2006 Assessment, results of the following model systems have been used:

- **Two-Dimensional (2-D) Photochemical Model:** *Zonally averaged representation of the atmosphere, with detailed chemistry but simplified transport and mixing.* Chemical reactions are included in the model according to the physical characteristics: pressure, temperature and incident solar radiation. In each model box, the movement of air into and out of each box is simulated, representing advection and dispersion. Advection by three-dimensional (3-D) motion and sub-grid scale mixing are parameterized. Some models include emissions from different sources, particularly for tropospheric pollutants, otherwise they use imposed tropospheric concentrations. In an "interactive" model, changes in the chemical composition of the atmosphere cause changes in temperatures and hence transport, whereas in a "non-interactive" model, this feedback is missing and temperatures are unaffected by changes in chemical composition.
- **Chemical Transport Model (CTM):** *Simulation of chemical processes in the atmosphere employing meteorological analyses derived from observations or climate models.* A CTM is a non-interactive model that does not consider the feedback of chemistry to dynamical and radiative processes. It uses winds and temperatures from meteorological analyses or predictions to specify the atmospheric transport and temperatures and to calculate the abundances of chemical species in the troposphere and stratosphere. A CTM can be used to simulate the evolution of atmospheric composition and help interpret observations.
- **Atmospheric General Circulation Model (AGCM):** *Three-dimensional model of large-scale (spatial resolution of a few hundred km) physical, radiative, and dynamical processes in the atmosphere over years and decades.* An AGCM is used to study changes in natural variability of the atmosphere and for investigations of climate effects of radiatively active trace gases (greenhouse gases) and aerosols (natural and anthropogenic), along with their interactions and feedbacks. Usually, AGCM calculations employ prescribed concentrations of radiatively active gases, e.g., carbon dioxide (CO₂), methane (CH₄), nitrous oxide (N₂O), chlorofluorocarbons (CFCs), and ozone (O₃). Changes of water vapor (H₂O) concentrations due to the hydrological cycle are directly simulated by an AGCM. Sea surface temperatures (SSTs) are prescribed. An AGCM coupled to an ocean model, commonly referred to as an AOGCM or a climate model, is used for investigation of climate change. More recently, climate models may also include other feedback processes (e.g., carbon cycle, interaction with the biosphere).
- **Chemistry-Climate Model (CCM):** *An AGCM that is interactively coupled to a detailed chemistry module (see Figure 5-1).* In a CCM, the simulated concentrations of the radiatively active gases are used in the calculations of net heating rates. Changes in the abundance of these gases due to chemistry and advection influence heating rates and, consequently, variables describing atmospheric dynamics such as temperature and wind. This gives rise to a dynamical-chemical coupling in which the chemistry influences the dynamics (via radiative heating) and vice versa (via temperature and advection). Not all CCMs have full coupling for all chemical constituents; some radiatively active gases are specified in either the climate or chemistry modules. Ozone is always fully coupled, as it represents the overwhelmingly dominant radiative-chemical feedback in the stratosphere. *Transient* simulations consider observed or predicted gradual changes in concentrations of radiatively active gases and other boundary conditions (e.g., emissions). The temporal development of source gas emissions and SSTs are prescribed for a specific episode (years to decades). In *time-slice* simulations, the internal variability of a CCM can be investigated under fixed conditions, e.g., for greenhouse gas (GHG) concentrations and SSTs, to estimate the significance of specific changes.

decrease in ozone causes less absorption of solar and long-wave radiation, leading to a local cooling. After the stratosphere has adjusted, the net effect of ozone depletion in the lower stratosphere is a negative radiative forcing (IPCC/TEAP, 2005). In contrast, ozone depletion in the middle and upper stratosphere causes a slight positive radiative forcing (IPCC/TEAP, 2005). The maximum sensitivity of radiative forcing for ozone changes is found in the tropopause region, and the maximum sensitivity of surface temperatures to ozone changes also peaks near the tropopause (Forster and Shine, 1997).

Quantifying the impact of stratospheric ozone changes on surface temperatures is less straightforward than estimating radiative forcing (RF). This is because a climate sensitivity term, λ , has to be introduced to translate radiative forcing to changes in surface temperatures (T_{surf}). The relationship between λ and T_{surf} changes is generally given by $\Delta T_{\text{surf}} = \lambda \text{ RF}$ (see Box 1.3 in IPCC/TEAP, 2005), where λ is in units of $\text{K} (\text{W m}^{-2})^{-1}$. ΔT_{surf} is the equilibrium response of global mean surface temperature and RF is the radiative perturbation. The assumption of linearity between radiative forcing and the surface temperature change made in this equation is found to hold well for ozone depletion (Forster and Shine, 1999).

λ is poorly constrained by observations and is conventionally evaluated in climate models as the equilibrium global mean temperature response to a radiative forcing change equivalent to a doubling of CO_2 . λ is dependent on the strength of climate feedbacks, such as those associated with clouds, water vapor, and ice albedo, and its magnitude varies considerably from model to model. Its value is likely to lie in the range 1.5 to $4.5 \text{ K} (\text{W m}^{-2})^{-1}$ (IPCC, 2001). λ can depend significantly on the nature of the forcing, particularly in the case of stratospheric ozone changes, and can differ from that for a doubling of CO_2 . Section 5.2.7 discusses dynamic responses in more detail.

Eleven-year solar ultraviolet (UV) irradiance variations have a direct impact on the radiation and ozone budget of the middle atmosphere (e.g., Haigh, 1994; see also Chapter 3, Section 3.4.4). During years with maximum solar activity, the solar UV irradiance is enhanced, which leads to additional ozone production and heating in the stratosphere and above. By modifying the meridional temperature gradient, the heating can alter the propagation of planetary and smaller-scale waves that drive the global circulation. Although the direct radiative forcing of the solar cycle in the upper stratosphere is relatively weak, it could lead to a large indirect dynamical response in the lower atmosphere through a modulation of the polar night jet and the Brewer-Dobson circulation (Kodera and Kuroda, 2002). Such dynamical changes can feed back on the chemical budget of the atmosphere because of the

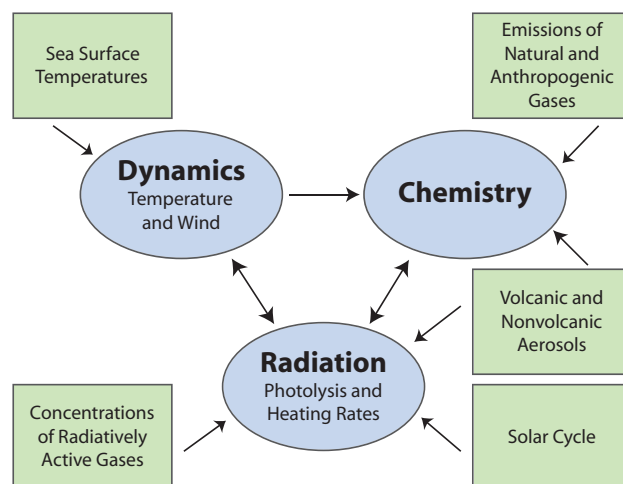


Figure 5-1. Schematic of a Chemistry-Climate Model (CCM). The core of a CCM (oval symbols) consists of an atmospheric general circulation model (AGCM) that includes calculation of the heating and cooling rates and a detailed chemistry module. They are interactively coupled. Photolysis rates are calculated online or are determined from a lookup table. Arrows indicate the direction of effect. Rectangular boxes denote external impacts. In current CCMs, sea surface temperatures (SSTs) are prescribed based on observations or are adopted from calculations with a climate model. Natural and anthropogenic emissions of gases are considered. Tropospheric and stratospheric aerosol loading (especially after volcanic eruptions) can be taken into account. CCMs often consider the changes of solar radiation caused by the 11-year activity cycle of the Sun.

temperature dependence of both the chemical reaction rates and the transport of chemical species.

The Arctic lower and middle stratosphere tend to be cold and undisturbed during west-wind phases of the equatorial quasi-biennial oscillation (QBO; Section 5.2.2.1), while they are warm and disturbed during QBO east-wind phases (Holton and Tan, 1980; 1982). Further analysis (Labitzke, 1987; Labitzke and van Loon, 1988) showed that this relationship is strong during solar minimum conditions, while during solar maximum years the relationship does not hold. This solar-QBO interaction has remained robust in the observations since its discovery. Equatorial upper stratospheric winds during the early winter appear to be important for the evolution of the Northern Hemisphere winter, especially the timing of stratospheric sudden warmings (Gray et al., 2001a; 2001b; Gray, 2003; Gray et al., 2004).

CLIMATE-OZONE CONNECTIONS

Some modeling studies have confirmed the modulation of the polar night jet and the Brewer-Dobson circulation by the solar cycle (e.g., Matthes et al., 2004). The transfer of the solar signal from the stratosphere to the troposphere is the subject of ongoing research and includes the possibility of the modulation of the Northern Hemisphere Annular Mode (NAM; Section 5.2.2.5) (Kodera, 2002; Matthes et al., 2006) and changes in vertical motion and precipitation in the tropics (e.g., Kodera, 2004; Haigh et al., 2005; Matthes et al., 2006). It is also possible that a “wave-ozone feedback” mechanism communicates the solar signal to the QBO (Cordero and Nathan, 2005), although Mayr et al. (2006) found a solar modulation of the QBO even though there is no wave-ozone feedback in their model.

5.2.2 Dynamics

Although the stratosphere and troposphere are in many ways distinct, the atmosphere is continuous, allowing vertical wave propagation and a variety of other dynamical interactions between these regions. A complete description of atmospheric dynamics requires an understanding of both of these layers. The dynamical coupling of the stratosphere and troposphere is primarily mediated by wave dynamics. A variety of waves originate in the troposphere, propagate upward into the stratosphere and above, and then dissipate, shaping the spatial and temporal structure of the stratospheric flow. This traditional view of a passive stratosphere has more recently given way to a greater appreciation of the stratosphere’s ability to shape not only its own evolution but that of the troposphere as well.

5.2.2.1 ROLE OF WAVES

The climatological temperature structure of the stratosphere, as well as its seasonal cycle and variability, depend crucially on the dynamics of waves that are generated in the troposphere. Wave dynamics can be divided broadly into three processes: generation mechanisms, propagation characteristics, and dissipation (primarily due to wave breaking and thermal damping, with thermal damping important for planetary wave dissipation at high latitudes, outside the surf zones; it is also likely to be important for the dissipation of equatorial waves). In the extratropics, the temperature structure of the stratosphere depends on a balance between diabatic radiative heating and adiabatic heating from induced vertical motion due to planetary wave dissipation (Andrews et al., 1987). Planetary wave breaking in the winter stratosphere (and mesosphere) generally produces a westward force that decelerates the polar

stratospheric jet, resulting in ascent (adiabatic cooling) in the tropics, and descent (adiabatic warming) over the poles (Holton et al., 1995). This response pattern describes a meridional mass circulation that is called the Brewer-Dobson circulation.

The basic climatology of the extratropical stratosphere is broadly understood in terms of wave dynamics together with the seasonal cycle of radiative heating. For example, the easterly winds of the summer stratosphere inhibit upward propagation of planetary waves (Charney and Drazin, 1961) and so the summer stratosphere is much less disturbed than the winter stratosphere. Asymmetries in the continental land mass between the Northern Hemisphere (NH) and Southern Hemisphere (SH) imply asymmetries in the efficiency of planetary wave generation mechanisms. Consequently in winter, planetary wave disturbances in the stratosphere of the NH are significantly larger than those in the SH. In the tropical stratosphere, the dominant form of variability is a quasi-periodic (2-3 year) wave-driven descending zonal mean wind reversal, called the quasi-biennial oscillation (QBO). The peak-to-peak amplitude of the wind QBO is ~55 m/s at 25-30 km (Baldwin and Gray, 2005), while the temperature QBO amplitude is ~8 K. The QBO affects the global stratospheric circulation, and extends to ~20° north and south with an amplitude of about 10 m/s (Dunkerton and Delisi, 1985). It affects a variety of extratropical phenomena including the strength and stability of the wintertime polar vortex, and the distribution of ozone and other gases (see Baldwin et al., 2001 for a review). The QBO is driven by the dissipation of a variety of equatorial waves (Lindzen and Holton, 1968; Dunkerton, 2001) that are primarily forced by deep cumulus convection in the tropics.

5.2.2.2 HOW THE STRATOSPHERE AFFECTS ITS OWN VARIABILITY

Although stratospheric variability has long been viewed as being caused directly by variability in tropospheric wave sources, it is by now widely accepted that the configuration of the stratosphere itself also plays an important role in determining the vertical flux of wave activity from the troposphere. The original theory of Charney and Drazin (1961) states that it is only when the winds are westerly that the longest waves (mainly waves 1, 2, and 3) can propagate vertically. This theory has been extended to account for the strongly inhomogeneous nature of the stratospheric background state and the steep potential vorticity gradients at the polar vortex edge (e.g., Scott et al., 2004). Given a steady source of waves in the troposphere, any changes in the stratospheric background potential vorticity (PV) gradient will change the vertical

wave fluxes, giving rise to the possibility of internally driven variability of the stratosphere, as modeled by Holton and Mass (1976). Similar internal variability has also been demonstrated in more comprehensive AGCMs (see Box 5-1) (e.g., Christiansen, 1999). Modeling studies suggest that realistic stratospheric variability can arise in the absence of tropospheric variability (Scott and Polvani, 2004; 2006).

The modulation of vertical wave flux into the stratosphere by the stratospheric configuration may be related to the extent to which the stratosphere can act as a resonant cavity, involving downward reflection of stationary planetary waves (McIntyre, 1982; Smith, 1989). Further, through these processes, the tropospheric circulation itself is also influenced by the stratospheric configuration. Reflection of stationary planetary wave energy takes place when the polar vortex exceeds a critical threshold in the lower stratosphere, leading to structural changes of the leading tropospheric variability patterns (Perlwitz and Graf, 2001; Castanheira and Graf, 2003; Walter and Graf, 2005).

There exists also an external or barotropic mode whose potential impact on the stratospheric circulation (in terms of its deceleration of the polar night vortex) is significantly larger than that of upward propagating waves. Esler and Scott (2005) demonstrated the relevance of this mode in wavenumber-2 major warmings in which the vortex is split throughout the full depth of the stratosphere.

5.2.2.3 TRANSPORT OF AIR INTO THE STRATOSPHERE

Planetary waves breaking in the stratosphere are also important for the transport of species from the troposphere to and within the stratosphere. The mean circulation of the stratosphere is essentially a “wave-driven pump” (see Holton et al., 1995, for a review) in which stratospheric wave drag moves air poleward and downward over the polar cap. As a consequence, the air in the tropical lower stratosphere rises slowly (0.2 to 0.3 mm/s) and carries ozone-poor air from the troposphere higher into the stratosphere. There, with increasing altitude, photochemical production becomes more effective. The upwelling in the tropics is modulated by the seasonal cycle and the tropical QBO phase (Baldwin et al., 2001). When the QBO is westerly at 40-50 hPa, the ascent rate is lower, there is more time for ozone production, and the tropical ozone column is enhanced. In the subtropics and extratropics, transport of chemical species from the troposphere to the lowermost stratosphere occurs through quasi-isentropic motion associated with synoptic-scale and mesoscale circulations (e.g., baroclinic eddies, frontal circulations). In the same circulations, there is substantial

transport from stratosphere to troposphere. Quantification of this two-way (troposphere-to-stratosphere and stratosphere-to-troposphere) transport has improved significantly over the last few years through modeling and observations. (See, e.g., Stohl et al., 2003 for a review.) However, significant quantitative uncertainty remains over the role of small-scale circulations, e.g., convective systems, in transport from troposphere to stratosphere or vice versa. The transport of air in the tropopause region is discussed in greater detail in Chapter 2, Section 2.4.

5.2.2.4 MODELING AND PARAMETERIZATION OF SMALL-SCALE WAVES

The consideration of wave dynamics in determining the climatology of the stratosphere is very important. Any systematic change in the generation, propagation, or dissipation of waves (both resolved and parameterized) will result in systematic changes in the temperature structure of the stratosphere. The capability to simulate the climatology and space-time changes of stratospheric properties hinges critically on our ability to simulate highly nonlinear wave dynamics in a reliable way. Atmospheric models generally have inadequate horizontal resolution (for baroclinic eddies, interaction with ocean and land surface) and vertical resolution (for the planetary wave propagation characteristics and cross-tropopause transport). Another issue is that deep convection (an important excitation mechanism for waves that propagate into the stratosphere) is a sub-grid-scale process that must be parameterized.

One of the most challenging aspects of modeling the dynamical coupling of the troposphere and stratosphere is the parameterization of unresolved waves (in particular, non-orographic gravity waves) and their feedback on the resolved flow. There are limited observational data to constrain the tropospheric sources and basic middle-atmosphere climatology of gravity waves (e.g., see reviews by Fritts and Alexander, 2003 and Kim et al., 2003). Parameterizations of ever-increasing complexity are being developed to more realistically model the dynamics of these waves, and the free parameters are used to reproduce present-day climate. This raises a credibility issue when these gravity-wave parameterizations are employed for the purpose of climate change simulations (but see Section 5.3.2). With the advent of newer satellite temperature and wind observations of global extent and higher spatial resolution (e.g., Wu, 2004; Eckermann et al., 2006), it is anticipated that current parameterizations of gravity waves will be better constrained and more objectively validated. There are also current efforts to specify gravity wave source spectra in terms of fields calculated by the underlying

CLIMATE-OZONE CONNECTIONS

AGCM, such as frontal zones and convective heating (e.g., Charron and Manzini, 2002; Beres et al., 2005).

5.2.2.5 ANNULAR MODES

Annular modes are hemispheric spatial patterns of climate variability characterized by north-south shifts in mass between polar and lower latitudes (Thompson and Wallace, 2000). Tropospheric signatures of stratospheric variability are often well described by annular mode patterns (e.g., Baldwin and Dunkerton, 2001; Gillett and Thompson, 2003). In both the stratosphere and troposphere, the annular modes explain a larger fraction of variance than any other pattern of climate variability in their respective hemisphere. On month-to-month time scales, annular variability at tropospheric levels is strongly coupled with annular variability at stratospheric levels (Baldwin and Dunkerton, 1999; Thompson and Wallace, 2000). Thus, as noted in Section 5.2.2.6, time series of the annular modes provide a convenient way to describe some aspects of stratosphere-troposphere coupling. The Northern Hemisphere Annular Mode (NAM) near Earth's surface is alternatively known as the Arctic Oscillation (AO; Thompson and Wallace, 1998) and the North Atlantic Oscillation (NAO; Hurrell, 1995). The Southern Hemisphere Annular Mode (SAM) is also referred to as the Antarctic Oscillation and High Latitude Mode.

Recent studies suggest the annular modes reflect feedbacks between the eddies and the zonal flow at middle latitudes (Lorenz and Hartmann, 2001; 2003). Other studies imply the annular modes are expected in any rotating planetary fluid system that conserves momentum and mass, and that has some smoothness property (Gerber and Vallis, 2005). The key dynamics that underlie the annular modes are still under investigation.

5.2.2.6 EFFECTS OF STRATOSPHERIC VARIABILITY ON THE TROPOSPHERE

Observational analysis suggests that stratospheric processes affect surface weather and climate (e.g., Scaife et al., 2005). Figure 5-2 shows composites of indices of the Northern Hemisphere Annular Mode (NAM) during periods when the stratospheric vortex rapidly changes strength. It reveals that within the winter season when the stratospheric flow is westerly, changes to the strength of the northern polar vortex are, on average, accompanied by similarly signed and similarly persistent changes to the tropospheric flow (Baldwin and Dunkerton, 1999; 2001). The illustration would be similar if high-latitude zonal winds ($\sim 60^\circ\text{N}$) were used instead of the annular mode index. The figure thus suggests that changes to the strength

of the polar vortex—especially in the lowermost stratosphere—may affect the tropospheric flow.

Despite the apparent robustness of the above evidence, the principal mechanisms whereby stratospheric variability may influence the tropospheric circulation remain unclear. A complete explanation of the observed coupling likely lies in one or more of the following physical processes:

- 1) Geostrophic and hydrostatic adjustment of the tropospheric flow to anomalous wave drag (Haynes et al., 1991; Thompson et al., 2006) and anomalous diabatic heating at stratospheric levels (Thompson et al., 2006);
- 2) The impact of anomalous shear in the lower stratospheric zonal flow on the momentum flux by baroclinic eddies (Shepherd, 2002; Kushner and Polvani, 2004; Wittman et al., 2004);
- 3) Amplification due to internal tropospheric dynamics (Song and Robinson, 2004);
- 4) The impact of anomalous shear at the tropopause level on vertically propagating waves (Chen and Robinson, 1992; Shindell et al., 1999; Limpasuvan and Hartmann, 2000);
- 5) The reflection of planetary waves (Hartmann et al., 2000; Perlwitz and Harnik, 2004).

Through such mechanisms, long-term changes in temperature and circulation of the stratosphere (e.g., radiative heating anomalies due to a GHG increase or changes to the ozone distribution) may affect surface weather patterns, at least during winter, spring, and early summer.

5.2.3 Tropospheric Composition

Many of the chemical constituents present in the stratosphere have sources that originate in the troposphere. Any changes in the chemical composition of the troposphere can affect the composition of the stratosphere. The chemical constituents are either directly emitted in the troposphere, mostly at or near the surface, or they are oxidation products of emitted species. The predominant source gases for stratospheric hydrogen, halogen, and nonvolcanic sulfur are long-lived species (water vapor, methane (CH_4), nitrous oxide (N_2O), organic halogen gases such as chlorofluorocarbons (CFCs), halons, and carbonyl sulfide (COS)). Surface emissions of short-lived species (sulfur dioxide (SO_2), dimethyl sulfide (DMS)) are also important sources of sulfur to the stratosphere, as are occasional large volcanic eruptions.

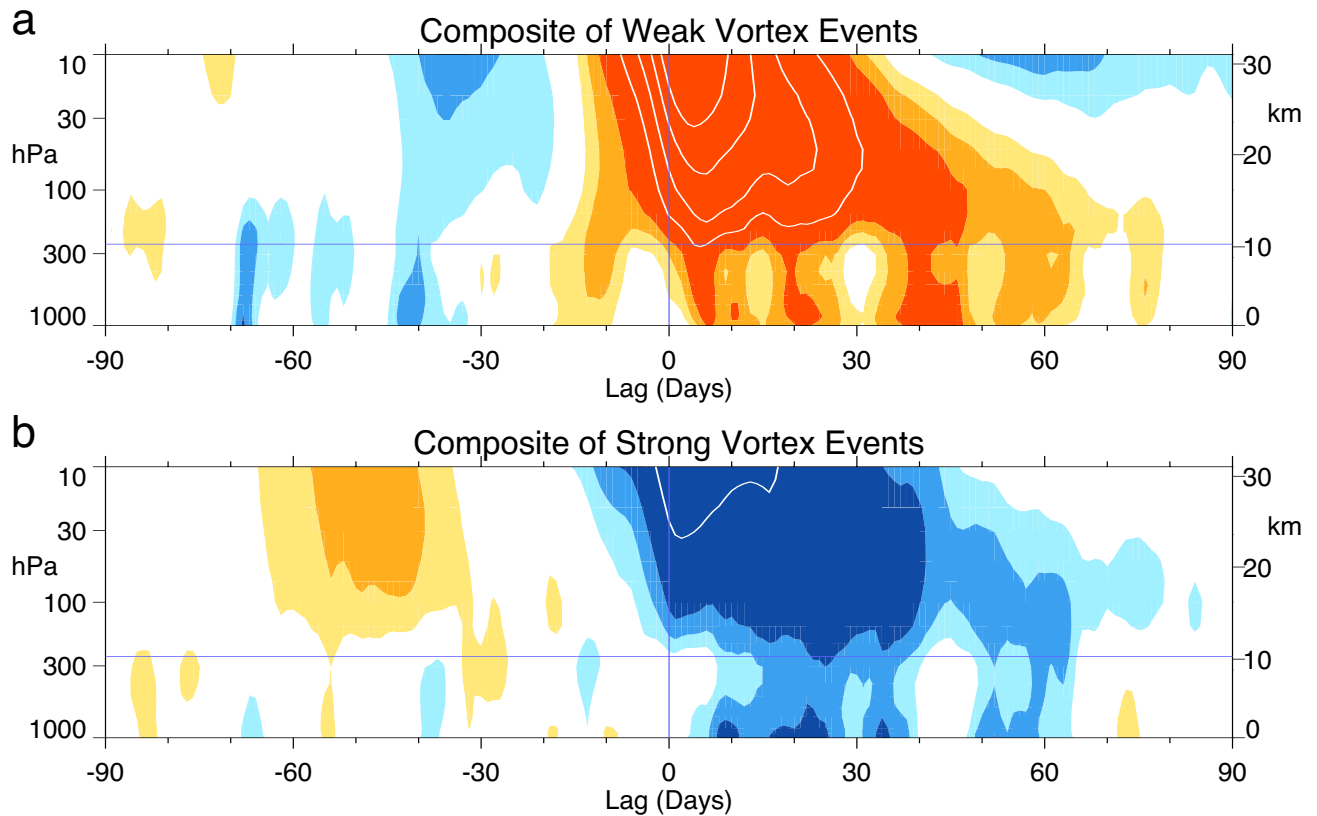


Figure 5-2. Composites of time-height development of the Northern Hemisphere Annular Mode (NAM) for: (a) 22 weak vortex events; and (b) 35 strong vortex events during 1958 to 2006. Updated from Baldwin and Dunkerton (2001). The events are determined by the dates on which the 10 hPa NAM values crossed -3.0 and $+1.5$, respectively. The indices are non-dimensional; the contour interval for the color shading is 0.25, with values between -0.25 and 0.25 unshaded. The white contours begin at ± 1.25 with a contour interval of 0.5. The thin horizontal lines indicate the approximate tropopause. The diagrams illustrate that large anomalies in the strength of the polar vortex at 10 hPa tend to descend to the lowermost stratosphere, where they last, on average, more than two months. After the stratospheric events occur, the tropospheric NAM anomaly is of the same sign as the stratospheric anomaly.

Long-term increases in CH_4 , N_2O , and CFCs brought about by increasing anthropogenic emissions are discussed in Chapter 1. However, with the exception of CFCs and halons, emissions of most stratospheric source gases have a substantial natural component. For instance, natural emissions represent more than a third of the CH_4 source, more than half of the N_2O source (IPCC, 2001), and are the dominant source of carbonyl sulfide (COS) (SPARC, 2006). As natural emissions are very likely to be affected by climate changes and, in particular, changes in precipitation, vegetation, and temperature, it is important to assess their sensitivity to climate changes, taking into account this effect when forecasting their future evolution and their overall impact on ozone recovery. Natural emissions also represent a large source of key short-lived species, such as nitric oxide (NO) emissions from soil and

lightning, or emissions of nonmethane hydrocarbons such as isoprene. Sources, transport, and stratospheric impact of halogenated short-lived species, many of which have predominantly natural origins, are dealt with in Chapter 2. The lifetimes of such short-lived compounds in relation to transport time scales are such that only a fraction of surface emissions reach the stratosphere (see Chapter 2). They may also affect the chemical composition of the troposphere, and hence potentially the lifetimes of other trace gases, through changes in atmospheric hydroxyl radical (OH).

Some progress has been made in estimating the sensitivity of natural sources to various climate parameters. For example, process modeling suggests that CH_4 emissions from wetlands could increase by 20% for a temperature increase of 1 K (Walter and Heimann, 2000). The

CLIMATE-OZONE CONNECTIONS

emissions of short-lived species such as biogenic hydrocarbons also increase with temperature. However, it is difficult to quantify climate-driven changes in natural sources because the temperature is not the only driving factor. Other factors such as water table level, soil moisture, vegetation cover, photosynthetically active radiation, biogenic productivity, or exposure to atmospheric pollutants can play a role, depending on the emitting substrate and the emitted species. Ignoring changes in land use, most natural emissions are expected to increase as Earth's surface warms. The changes that are most relevant to the stratosphere are climate-driven increases in CH₄ and N₂O emissions. An increase in CH₄ would accelerate the ozone recovery whereas an increase in N₂O would delay it (Randeniya et al., 2002; Chipperfield and Feng, 2003).

Climate changes can also alter other key processes in the exchange of chemical constituents between the troposphere and stratosphere. The vertical transport of surface emissions to the tropopause is largely dependent on the intensity of convective activity, and the flux of tropospheric air into the stratosphere is mostly determined by the strength of the upwelling from the troposphere that is linked to the strength of the Brewer-Dobson circulation (see Section 5.2.2.3).

5.2.4 Stratospheric Aerosols

Non-explosive volcanic surface emissions of sulfur species (SO₂, COS) are important sources of stratospheric aerosol loading mainly through tropical stratosphere/troposphere exchange (Notholt et al., 2005). Stratospheric aerosols have a direct radiative impact that decreases the surface temperature, since more shortwave radiation is reflected. Although there has been no significant change in the background (nonvolcanic) stratospheric aerosols for the period 1970 to 2004 (Deshler et al., 2006; see also SPARC, 2006), the non-volcanic aerosol loading could increase in the future if convection increases (Pitari et al., 2002), because convection is a key process that transports the short-lived species SO₂ from the surface to the upper troposphere and lower stratosphere.

Volcanic SO₂ injected into the stratosphere is oxidized to sulfuric acid that condenses and forms aerosols, on which heterogeneous reactions occur. Volcanic eruptions have strong impacts on the lower stratospheric thermal structure because the volcanic aerosols scatter back incoming solar radiation and absorb solar near-infrared and terrestrial infrared radiation (e.g., Stenchikov et al., 1998; Al-Saadi et al., 2001; Rozanov et al., 2002; Timmreck et al., 2003). Heterogeneous chemistry occurring on aerosol surfaces affects ozone concentrations, producing an additional indirect radiative impact depending on the concentration of atmospheric chlorine. In addition,

the modified meridional temperature profile in the stratosphere may result in colder polar vortices in winter (Chapter 3 in WMO, 2003).

The ozone impact of a given volcano depends on the amount of material, in particular sulfur, injected by the volcanic eruption and on whether the material reaches the stratosphere, as well as the phase of the QBO and the latitude of the eruption. The height reached by ejecta depends on the explosivity of the eruption, not on its location. Ejecta from tropical eruptions will be carried upward and poleward by the Brewer-Dobson circulation and, therefore, they will spread throughout much of the stratosphere with a long residence time, whereas ejecta from mid- to high-latitude eruptions will more quickly be returned to the troposphere by the descending branch of the Brewer-Dobson circulation.

The effect of a future major volcanic eruption will depend on chlorine levels. For low-chlorine conditions, heterogeneous chemistry can lead to ozone increases in the stratosphere, whereas for high chlorine conditions, as observed in recent years, volcanic aerosols lead to additional ozone depletion (Tie and Brasseur, 1995). Moreover, volcanic aerosol affects photolysis rates and therefore ozone concentrations (Timmreck et al., 2003).

The results of several CCM simulations (see Box 5-1) are consistent with the Tie and Brasseur study. After the eruption of Mt. Agung in 1963, the total amount of ozone was reduced, particularly in the tropics (see Chapter 3, Figure 3-4). Since the chlorine loading of the atmosphere was low at that time, the solar cycle influences were of particular importance (see Chapter 3, Section 3.4.4). For example, the CCM E39C simulated reasonably well the observed decrease of tropical ozone around 1965, since the influence of the 11-year solar cycle was considered, which was minimal around 1965 (Dameris et al., 2005). Following the major eruptions of El Chichón (1982) and Mt. Pinatubo (1991), when atmospheric chlorine amounts were much higher and solar activity was near maximum, the total ozone significantly decreased in subsequent months in both observations and models, before recovering after two to three years. The simulated globally averaged total ozone decreases for many models in the Eyring et al. (2006) assessment were about 2%, similar to what was observed (cf. Fioletov et al., 2002; WMO, 2003).

In AOGCM and CCM simulations, the temperature perturbations after the eruptions of El Chichón and Mt. Pinatubo are often larger than 1 K (annually averaged) in the lower stratosphere (see Figures 5-3 and 5-11), whereas observations indicate an increase of about 1 K. The temperature impact is important since this will determine to a large extent the water vapor perturbation. In turn, this will

Simulated and Observed Stratospheric Temperature Changes

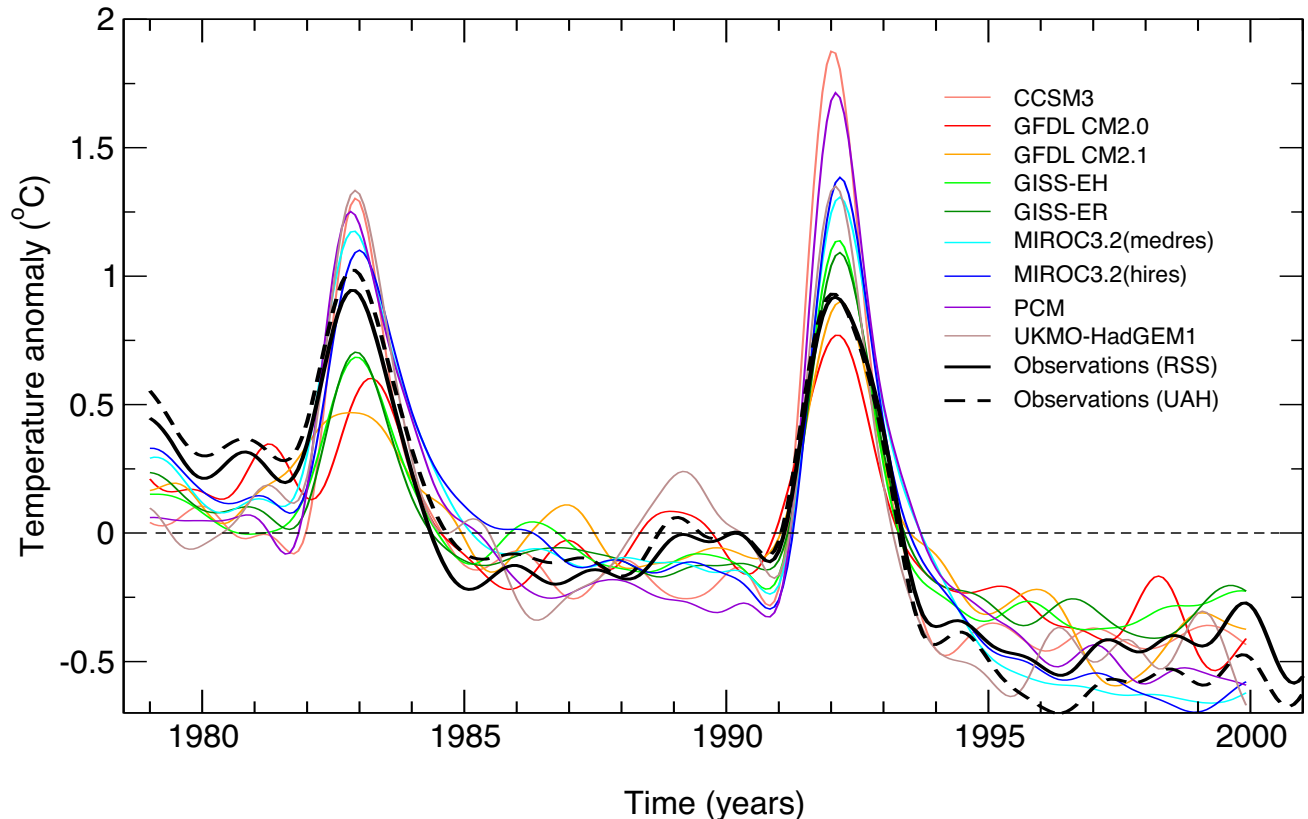


Figure 5-3. Globally averaged temperature anomalies in the lower stratosphere from a range of climate models (Santer et al., 2006) in comparison with Microwave Sounding Unit MSU4 channel temperatures. The MSU4 observations are from two independent analyses by the Remote Sensing Systems (RSS) and the University of Alabama at Huntsville (UAH) groups. See Appendix 5A for information about the models.

influence the ozone chemistry in the lower stratosphere (Section 5.3.5) and lower stratospheric cooling rates (Section 5.2.6). Figure 5-3 shows the globally averaged temperature from a range of tropospheric climate models (Santer et al., 2006; see also Ramaswamy et al., 2006), vertically averaged by the Microwave Sounding Unit MSU4 weighting function, together with MSU4 data. The variations due to volcanic eruptions are clear for several years, with an overall slow cooling. The CCM and climate model studies indicate that the strength of the volcanic signal varies substantially between the models (see also Figures 3-26 and 5-11, and Eyring et al., 2006).

The sulfate aerosols and ash injected into the stratosphere from volcanic eruptions can cause tropospheric cooling (e.g., Hansen et al., 1992; Robock, 2000; Santer et al., 2001; Wigley et al., 2005; Yokohata et al., 2005), although ash particles have a short residence time because

of gravitational settling. The tropospheric cooling would be expected to change the tropospheric circulation, as well as the interaction between the stratosphere and the troposphere (Stenchikov et al., 2002).

Based on the historical volcanic record, a major eruption of similar atmospheric impact to that of Mt. Pinatubo is likely to occur during the next 30 years (Roscoe, 2001). The previous 50-year period, with three such eruptions, appears to be unusual. Much larger eruptions, such as Toba 74,000 years ago, are a remote possibility, with recovery times of a decade (Bekki et al., 1996). Model studies by Rosenfield (2003), assuming a Pinatubo-sized eruption every 10 years from 2010 to 2050, suggest that the long-term recovery of ozone would not be strongly affected by infrequent large volcanic eruptions. The impacts on ozone of all except the largest eruptions would be expected to last only a few years, and not significantly

CLIMATE-OZONE CONNECTIONS

affect long-term ozone recovery, because ozone recovery depends primarily on halogen levels.

5.2.5 Past Changes in Stratospheric Water Vapor

Water vapor is the most important greenhouse gas, and it plays an important role in chemistry-climate interactions. Previous studies reported in WMO (2003) showed that ozone perturbations are amplified in the upper troposphere and lower stratosphere as a result of feedback processes with water vapor. Any increase in stratospheric water vapor could lead to an increase in the level of odd-hydrogen radicals (HO_x), which could affect the nitrogen oxide radicals (NO_x) and chlorine oxide radicals (ClO_x) cycles, leading to ozone depletion (see Section 5.3.5). A change in water vapor concentration could also change the temperature thresholds for polar stratospheric cloud formation over the polar caps (see Section 5.3.5).

Air enters the stratosphere mostly in the tropics, and stratospheric water vapor is primarily controlled by temperatures near the tropical tropopause. The associated processes have been studied in detail over the past few years, for example using trajectory studies (Bonazzola and Haynes, 2004; Fueglistaler et al., 2005). Water vapor is also produced in the stratosphere by the photochemical oxidation of methane, producing approximately two molecules of water vapor per molecule of methane. The increase in the concentration of tropospheric methane since the 1950s (0.55 parts per million by volume (ppmv)) is responsible for part of the increase in stratospheric water vapor over this time period (SPARC, 2000).

Measurements of stratospheric water vapor content are available from ground-based instruments and aircraft observations, plus balloonborne and satellite datasets. The longest continuous dataset is from a single location (Boulder, Colorado, USA), based on balloonborne frost point hygrometer measurements (approximately one per month), beginning in 1980 (Oltmans et al., 2000; see updated data in Figure 5-4). Over the period 1980-2005, a statistically significant linear trend of ~5-10% per decade is observed at all levels between approximately 15 and 26 km. However, although a linear trend can be fitted to this 25-year long record, there is a high degree of variability in the infrequent sampling, and the increases seen are neither continuous nor steady. In particular, stratospheric water vapor concentrations have decreased since 2001. Long-term increases in stratospheric water vapor content are also inferred from a number of other datasets covering the years 1980-2000 (Rosenlof et al., 2001), although the time series are short and the sampling uncertainty is high in many cases.

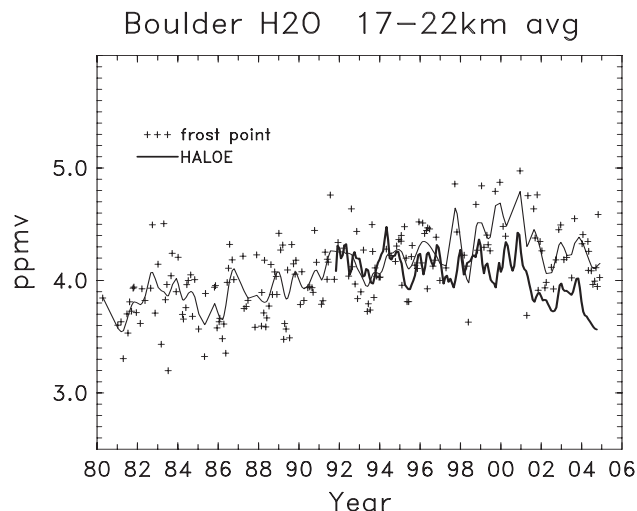


Figure 5-4. Evolution of stratospheric water vapor mixing ratio (in ppmv, averaged over 17-22 km) at Boulder, Colorado (40°N, 105°W), derived from balloonborne frost point hygrometer measurements covering 1980-2005. The thin line shows a smooth fit through the data points, using a running Gaussian window with a half-width of three months. The heavy line shows HALOE satellite water vapor data during 1992-2005 for the same altitude region, using measurements near Boulder (over latitudes 35°N-45°N, and longitudes 80°W-130°W). Note the difference between the two datasets after about 1997. Updated from Randel et al., 2004a.

Recent work has focused on the interannual and long-term evolution of the water vapor distribution using near-global observations from the satellite-based Halogen Occultation Experiment (HALOE). These measurements span more than a decade (late 1991 to 2005). Interannual changes in water vapor derived from HALOE data show excellent agreement with the Polar Ozone and Aerosol Measurement (POAM) satellite data (Randel et al., 2004b) and also with the Stratospheric Aerosol and Gas Experiment II (SAGE II) water vapor data (Thomason et al., 2004; Chiou et al., 2006). An updated comparison of the HALOE measurements with the Boulder balloon data for the period 1992-2005 is shown in Figure 5-4. The Boulder and HALOE data show reasonable agreement for the early part of the record (1992-1996), but the Boulder data are about 5% to 8% higher after 1997. These differences are within the accuracies of both types of observations (reported to be around 10-20% in SPARC, 2000). Year-to-year water vapor changes in each dataset appear to be correlated, and both time series show the persistent decreases after 2001. However, as a result of the differences after 1997, changes

derived from the two datasets over the (short) overlap period 1992-2005 are very different, with net decreases in the HALOE data but not in the Boulder record. These differences seem statistically significant, as Randel et al. (2004b) report a statistical uncertainty of linear fits of the 1992-2002 record of less than $\pm 0.5\%$ /year. The reason for the differences between the balloon and satellite datasets (for the same time period and location) is unclear.

Interannual changes in the HALOE stratospheric water vapor data during 1992-2005 are in quantitative agreement with observed changes in tropical tropopause temperatures for this period (Randel et al., 2004a; Fueglistaler and Haynes, 2005). Tropopause temperature variations associated with the QBO (and to a lesser degree the El Niño-Southern Oscillation, ENSO) are echoed in observed water vapor changes for this period, consistent with the modeling studies of Giorgetta and Bengtsson (1999) and Geller et al. (2002). Furthermore, the persistent decreases in stratospheric water vapor concentrations since 2001 are associated with anomalously low tropopause temperatures (Randel et al., 2004a, 2006; Fueglistaler and Haynes, 2005; see also Figure 5-21). This agreement suggests a reasonable level of understanding for interannual water vapor changes during the HALOE time period (and ability to project future values based on tropical tropopause temperatures). In contrast, the long-term water vapor increases inferred from the Boulder balloon data since 1980 (and from combined datasets beginning in the 1960s; Rosenlof et al., 2001) are difficult to reconcile with observed long-term decreases in tropical tropopause temperatures (e.g., Seidel et al., 2001). Only a fraction of the changes can be attributed to increasing tropospheric methane, as discussed in detail in Fueglistaler and Haynes (2005). Thus, while the HALOE record appears quantitatively well understood, the long-term increases inferred from the Boulder data over 1980-2005 (and combined datasets since the 1960s) are larger than can be explained by observed tropopause temperature changes or past increases in tropospheric methane.

5.2.6 Past Changes in Stratospheric Temperature

Stratospheric temperature changes are closely coupled to ozone changes. Ozone is a key radiatively active constituent in the stratosphere, and it is important to assess the consistency between observed changes in ozone and temperature. Also, the halogen-related ozone destruction rate is generally reduced by lower temperatures in the upper stratosphere, but increased by lower temperatures in the polar lower stratosphere.

Estimates of past temperature changes in the stratosphere have been derived from several different types of data. Most of these datasets were not designed for climate monitoring purposes, and each has strengths and limitations that require careful evaluation and scrutiny. An important advance during the last several years is increased quantification of trend uncertainties, accomplished by comparisons of independent datasets and analyses. Temperature trends can also be derived from meteorological analysis and reanalysis datasets, but evidence suggests these can be influenced by artificial changes related to data inhomogeneity effects (e.g., Santer et al., 2004; Randel et al., 2004a; Birner et al., 2006), and hence may not be reliable in all applications.

Optimal detection and attribution techniques have been widely used to attribute observed changes in surface and tropospheric temperatures to particular external climate influences (Chapter 12 in IPCC, 2001). However, while some detection and attribution studies have identified an anthropogenic influence in variables incorporating stratospheric temperature, such as radiosonde temperature trends in the troposphere and stratosphere (e.g., Tett et al., 2002; Thorne et al., 2002), or tropospheric height (Santer et al., 2003, 2004), none has focused exclusively on stratospheric temperature. One reason may be that the coupled ocean-atmosphere models (AOGCMs; see Box 5-1) required for such studies generally have limited stratospheric resolution, and they underestimate stratospheric variability (Tett et al., 2002). A realistic estimate of internal variability is required in order to distinguish an externally forced response.

A nearly continuous record of stratospheric temperature measurements from satellites is available from the series of operational NOAA satellites beginning in 1979. These are based on the Microwave Sounding Unit (MSU) and Stratospheric Sounding Unit (SSU) instruments, which have flown on ten individual operational satellites over 1979-2005. These data represent mean temperatures for 10- to 15-km thick layers covering the lower to upper stratosphere. The SSU data are available for three fundamental channels (25, 26, and 27), together with several synthetic channels derived by differencing nadir and off-nadir measurements, which provide increased vertical resolution (Nash, 1988). Records of stratospheric temperatures for 1979-2005 are derived by combining data from the individual instruments, adjusted for calibration effects using periods of overlap between adjacent satellites. Effects of orbital drift and decay, and the influence of aliasing atmospheric tides also need to be considered in constructing long-term stratospheric datasets. There are

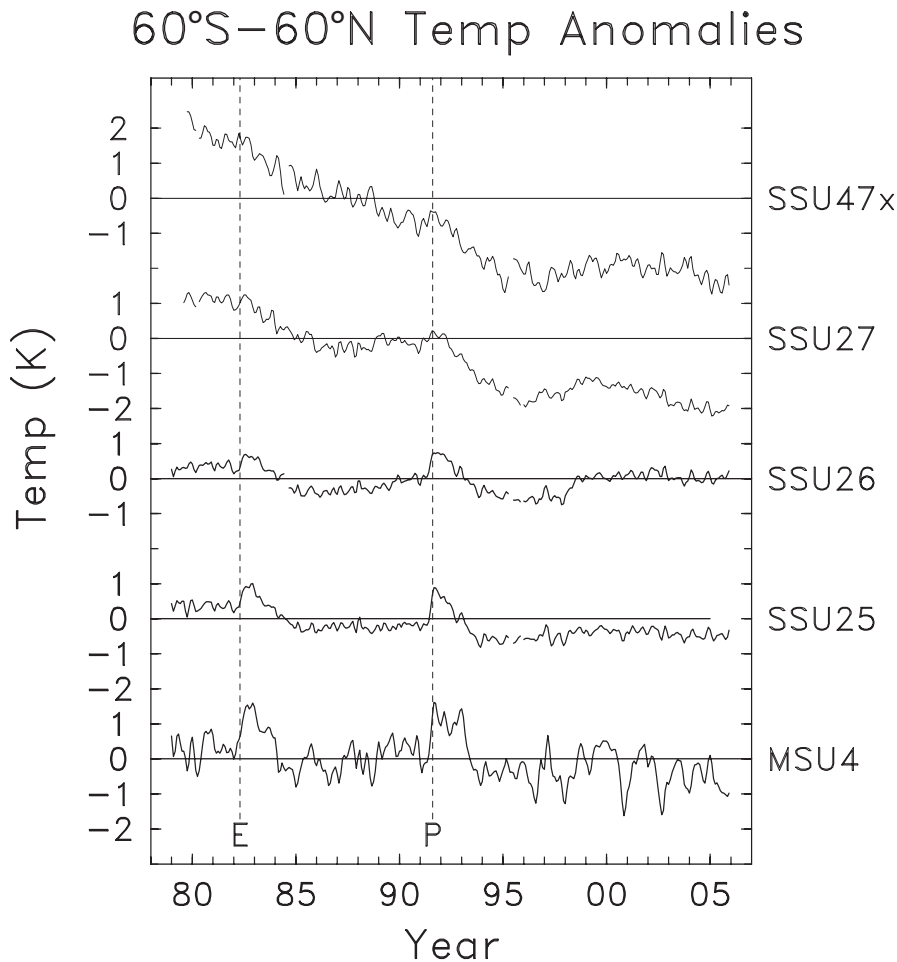


Figure 5-5. Time series of near-global mean (60°N-60°S) temperature anomalies for 1979-2005 derived from satellite radiance measurements. Results are shown for MSU Channel 4 (representing the layer mean temperature over ~13-22 km), and SSU channels 25 (~18-37 km), 26 (~25-44 km), 27 (~34-51 km), and 47x (~44-58 km). Vertical dashed lines mark the occurrence of volcanic eruptions of El Chichón (E) and Mt. Pinatubo (P).

several independent analyses of the MSU Channel 4 data, which covers the lower stratosphere, including results from the University of Alabama at Huntsville (UAH, Christy et al., 2003) and Remote Sensing Systems (RSS, Mears et al., 2003). At present there are two analyses of the combined SSU dataset, with data details discussed in Scaife et al. (2000) and Ramaswamy et al. (2001).

Long-term temperature changes can also be evaluated from historical radiosonde data, for which stratospheric measurements (up to ~25-30 km) are available since approximately 1960. Uncertainties in radiosonde-based temperature trends are associated with spatial sampling (the majority of measurements occur over NH midlatitudes), and more importantly with changes (improvements) in instrumentation over time, which can result in artificial cooling biases (Gaffen, 1994; Luers and Eskridge, 1998). Temperature trends calculated from ensemble radiosonde datasets exhibit strong cooling in the lower stratosphere (Lanzante et al., 2003b; Thompson and Solomon, 2005; Free et al., 2005). However, these

trends are substantially larger than corresponding trends derived from satellite measurements (Seidel et al., 2004) or estimates from current model simulations (Santer et al., 2005), and a recent U.S. Climate Change Science Program Assessment (CCSP, 2006) concludes that the ensemble radiosonde trends are probably influenced by artificial cooling biases.

There is strong evidence for a large and significant cooling in most of the stratosphere since 1980. Figure 5-5 shows near-global average temperature anomalies derived from satellite datasets for 1979-2005, spanning a range of altitudes from the lower to upper stratosphere. The vertical profile of near-global temperature trends during 1979-2005 derived from these satellite data are shown in Figure 5-6, in addition to trends derived from radiosonde data, and a synthesis of model results (taken from Shine et al., 2003). Both the satellite and radiosonde datasets reveal an overall cooling of the stratosphere, with trend values of about 0.5 K/decade in the lower stratosphere, increasing to larger values of about 1 to 2 K/decade in the upper stratosphere. There is reasonable

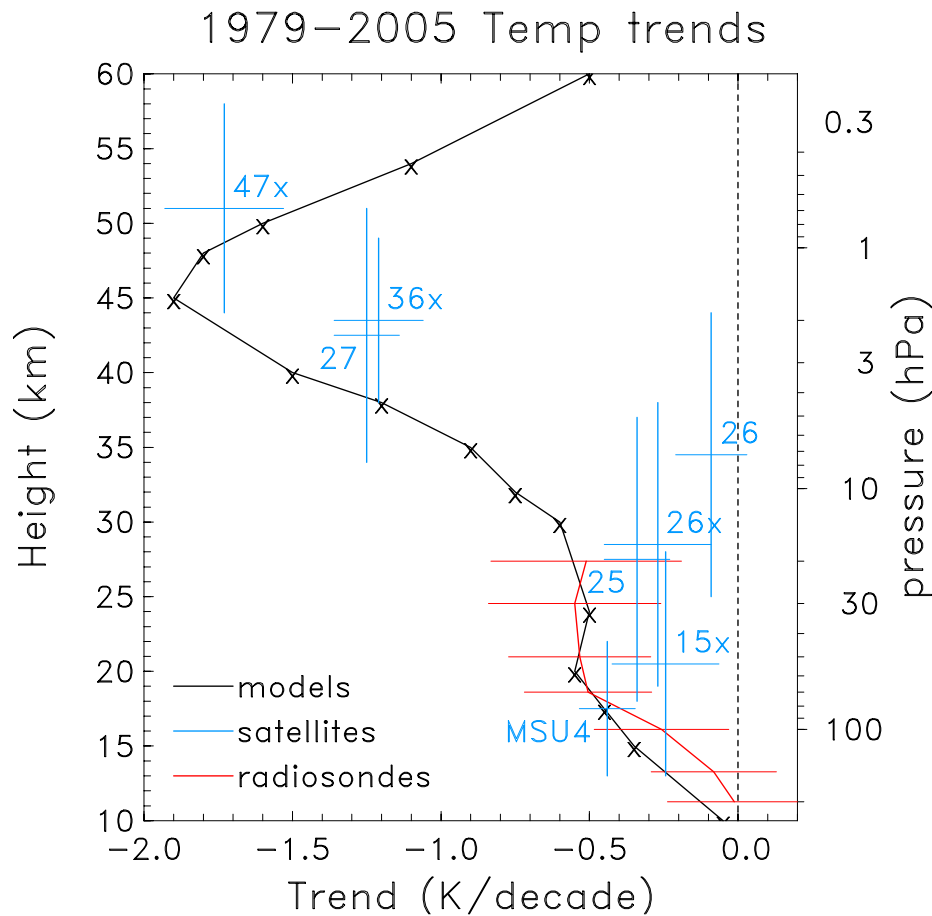


Figure 5-6. Vertical profile of temperature trends derived from satellite and radiosonde data over 60°N-60°S for the period 1979-2005, together with a synthesis of model results taken from Shine et al. (2003). The satellite results are shown for each individual SSU channel (as noted) and MSU Channel 4. For each channel the vertical bar denotes the approximate altitude range sampled by that channel, and the horizontal bar denotes the (two sigma) statistical trend uncertainty. Radiosonde results are shown for individual pressure levels (200-20 hPa), and are derived from a subset of stations described in Lanzante et al. (2003a), updated as described in Randel and Wu (2006). The subset of stations is chosen to omit stations with large artificial cooling biases, in particular stations where MSU4 minus radiosonde trends are greater than 0.3 K/decade (taken from Table 1 of Randel and Wu, 2006). Note that the Shine et al. (2003) results refer to model calculations and observations for the period 1979-1997, whereas the observed trends in the figure are for the longer period 1979-2005.

agreement between the lower stratospheric trends derived from satellite data and radiosondes, although note that the radiosonde results in Figure 5-6 are derived from a subset of one particular homogenized dataset (see Figure 5-6 caption). The radiosonde data suggest there has been significant cooling of the lower stratosphere (70-30 hPa) over most of the globe for 1979-2005, including the tropics.

Temperature trends derived from both the MSU4 (Randel and Wu, 2006) and radiosonde datasets (Thompson and Solomon, 2005; Free et al., 2005; Randel

and Wu, 2006) suggest the cooling of the lower stratosphere spans tropical and extratropical latitudes. However, temperature trends derived from the SSU data (as shown in WMO, 2003) suggest the cooling of the lower stratosphere is restricted to the extratropics. The differences between temperature trends derived from the SSU, MSU4, and radiosonde data are currently under investigation.

The time series in Figure 5-5 show that the observed cooling is not a simple linear trend. A strong imprint of transient warming (for 1-2 years) is observed in the lower

CLIMATE-OZONE CONNECTIONS

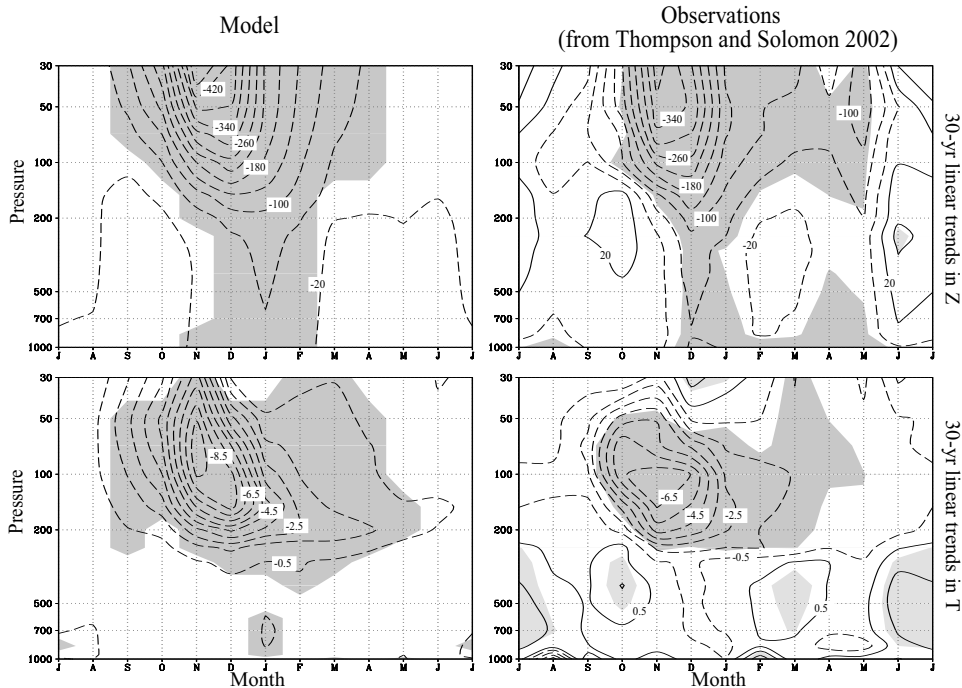


Figure 5-7. Antarctic geopotential height (in m, top) and temperature trends (in K, bottom) by month and pressure level in radiosonde observations over the period 1969-1998 (right) and a simulation of the response to stratospheric ozone depletion (left). Shading indicates regions of significant change based on (left panels) exceedance of one standard deviation of the monthly anomalies and (right panels) a two-sample t-test at the 5% level. From Gillett and Thompson, 2003.

and middle stratosphere following the volcanic eruptions of El Chichón (1982) and Mt. Pinatubo (1991). In the lower stratosphere, the long-term cooling manifests itself as more of a step-like change following the volcanic warming events (Pawson et al., 1998; Seidel and Lanzante, 2004). The overall lower stratospheric cooling is primarily a response to ozone decreases (Shine et al., 2003; Langematz et al., 2003), with a possible but much less certain contribution from changes in stratospheric water vapor. Ramaswamy et al. (2006) suggest that the step-like time series behavior is due to a combination of volcanic, solar cycle, and ozone influences. There is a substantial flattening of these trends evident in Figure 5-5 after approximately 1995; the latter aspect agrees with small global trends in the upper stratosphere and lower mesosphere observed in HALOE data for 1992-2004 (Remsberg et al., 2005). Although some flattening might be expected in response to changes in the ozone trends, the strength of this behavior is curious in light of continued increases in well-mixed greenhouse gases during this decade.

5.2.7 Impact of Ozone Changes on Surface Climate

5.2.7.1 SOUTHERN HEMISPHERE

The largest stratospheric ozone depletion is observed in the austral spring in the Antarctic stratosphere, and therefore it is here that one might expect any effect of stratospheric ozone depletion on tropospheric

climate to be largest. While the largest stratospheric temperature and geopotential height trends over the Antarctic have been observed in November, coincident in space with the maximum ozone depletion, significant decreases in geopotential height also extend to the troposphere 1-2 months later (Thompson and Solomon, 2002) (Figure 5-7).

Several modeling studies have examined the tropospheric response to prescribed changes in stratospheric ozone. Two studies using atmospheric models with prescribed sea surface temperatures demonstrated that a tropospheric response similar to the positive phase of the SAM is simulated in the austral summer in response to prescribed changes in stratospheric ozone (Kindem and Christiansen, 2001; Sexton, 2001). Using a model with high vertical resolution in the stratosphere and a mixed-layer ocean, Gillett and Thompson (2003) simulated a significant tropospheric geopotential height response to prescribed stratospheric ozone changes (Figure 5-7) with no greenhouse gas (GHG) changes. The simulated and observed geopotential height and temperature changes agreed well, both in magnitude and in seasonality, supporting the hypothesis that the observed trends were largely induced by stratospheric ozone depletion.

Transient simulations with coupled ocean-atmosphere models (AOGCMs) also indicate that ozone depletion has played an important role in inducing SAM trends, particularly in the summer (Marshall et al., 2004; Shindell and Schmidt, 2004; Arblaster and Meehl, 2006),

although all three studies found that GHG changes have played at least as large a role in inducing trends in the annual mean SAM.

The observed trend toward the positive phase of the SAM in December to May has been associated with a surface cooling of the Antarctic interior of ~1 K, and a warming of the Antarctic Peninsula, the Scotia Sea, and the southern tip of South America (Thompson and Solomon, 2002) (Figure 5-8). A similar pattern of warming

and cooling has been simulated in response to stratospheric ozone depletion (Gillett and Thompson, 2003) and combined stratospheric ozone depletion and GHG increases (Shindell and Schmidt, 2004; Arblaster and Meehl, 2006) (Figure 5-8). Thompson and Solomon (2002) also identified an associated strengthening of the westerlies over the Southern Ocean, corresponding to a poleward shift of the storm track, which is also simulated in response to stratospheric ozone depletion (Gillett and Thompson, 2003;

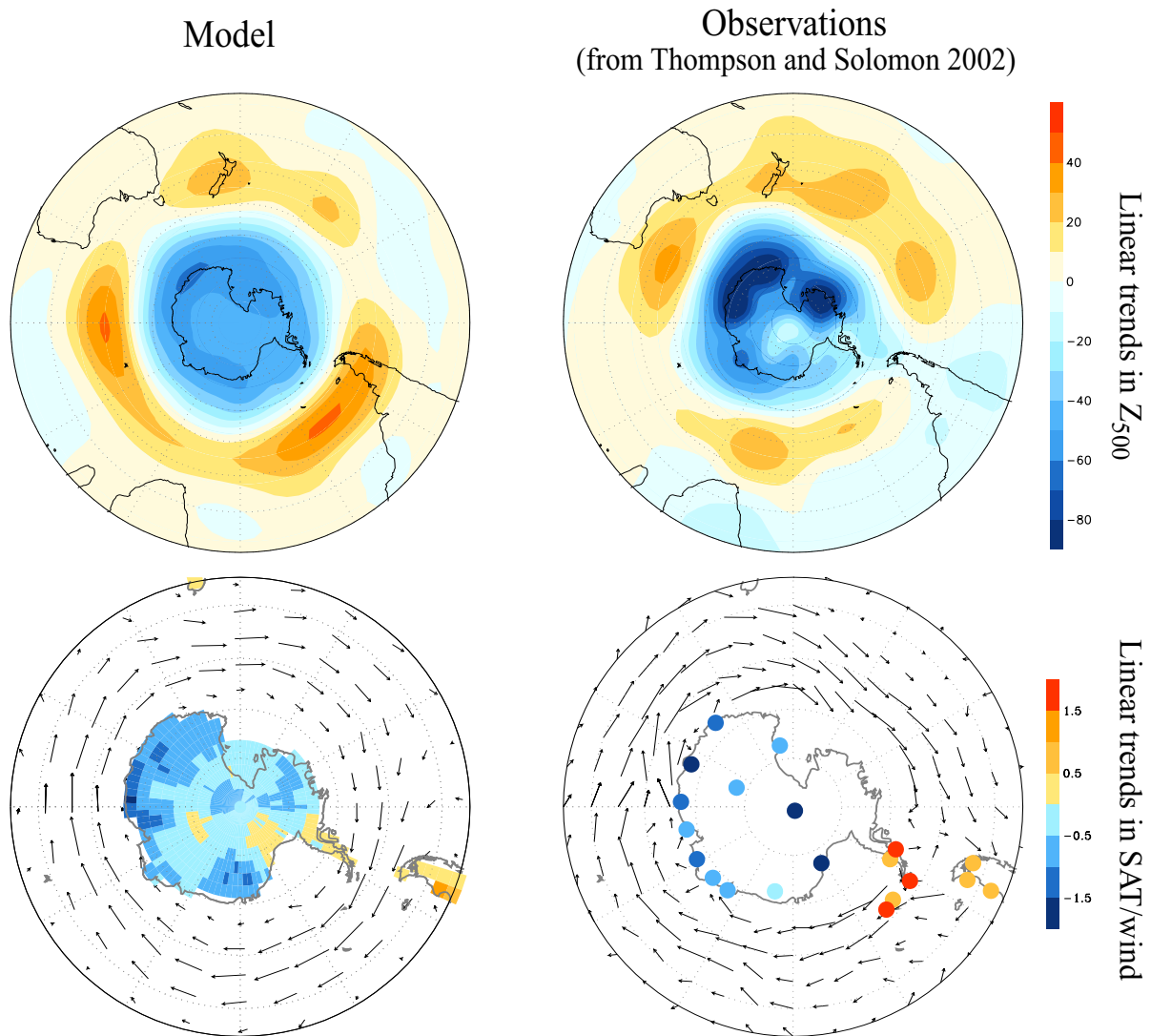


Figure 5-8. Simulated (left column) and observed (right column) changes in (upper row) 500 hPa geopotential height (in m) and (lower row) near-surface temperature (in K) and winds. Observed changes (Thompson and Solomon, 2002) are 22-year linear trends in 500 hPa geopotential height and 925 hPa winds (1979 to 2000), and 32-year linear trends in surface temperature (1969 to 2000) averaged over December to May. Simulated changes are differences between the perturbed and control integrations in 500 hPa geopotential height, 950 hPa winds, and land surface temperature averaged over December to February. The longest wind vector corresponds to ~4 m/s. From Gillett and Thompson, 2003.

CLIMATE-OZONE CONNECTIONS

Shindell and Schmidt, 2004) (see also Figure 5-8). Simulated and observed wind changes of ~1 m/s extend to 30°S (Gillett and Thompson, 2003).

Stratospheric ozone depletion likely influences tropospheric climate through both radiative and dynamical processes. Idealized model simulations indicate that a perturbation to the diabatic heating in the stratosphere gives an annular-mode response in sea level pressure over intraseasonal time scales (Polvani and Kushner, 2002; Kushner and Polvani, 2004; see also Section 5.2.2.6). Recent results suggest that the tropospheric response to stratospheric perturbations may result directly from wave driving and radiative forcing changes in the stratosphere (Thompson et al., 2006; see Section 5.2.2.6), although this direct forcing effect cannot explain the latitudinal structure of the tropospheric response. Antarctic stratospheric ozone depletion acts as a direct radiative cooling influence at the surface. Indeed, an early study of the response to stratospheric ozone depletion with a radiative-convective model found a surface cooling over Antarctica in response to stratospheric ozone depletion (Lal et al., 1987).

Maximum stratospheric ozone depletion close to the tropopause occurs in December to January, more than a month after the maximum ozone depletion at 70 hPa, due to the downward transport of ozone-depleted air (Solomon et al., 2005). Since surface temperature is particularly sensitive to changes in ozone concentration close to the tropopause (Forster and Shine, 1997), this suggests that surface cooling is radiatively induced, and that the apparent lag between stratospheric and tropospheric responses is due to the downward transport of ozone-depleted air toward the tropopause, rather than any dynamical effect.

Most studies suggest that Antarctic ozone depletion is likely to peak sometime in the current decade, and that a recovery is likely to follow over the next 50 years (Chapter 6). Therefore, over the coming decades, increases in stratospheric ozone should drive a decrease in the SAM index toward values seen before ozone depletion. However, increasing GHGs will likely have the opposite effect, contributing an increase in the SAM index (Shindell and Schmidt, 2004; Arblaster and Meehl, 2006). The magnitudes of the future ozone and GHG effects on the SAM are therefore uncertain.

5.2.7.2 NORTHERN HEMISPHERE

Stratospheric ozone depletion has also occurred in the Northern Hemisphere, where it has led to a smaller cooling of the Arctic polar vortex, maximizing in the spring, although model studies indicate that only part of the cooling observed in the Northern Hemisphere stratosphere can be explained by ozone depletion (Section 3.4.3.1 in WMO,

2003). Some studies have suggested that ozone depletion has contributed to the observed trend toward the positive phase of the NAO or NAM (Graf et al., 1998; Volodin and Galin, 1999; Hartmann et al., 2000). Ozone was found to contribute a small trend toward the positive phase of the NAM in model simulations, albeit one rather smaller than that due to GHGs, or indeed that observed (Graf et al., 1998; Shindell et al., 2001). However, while the largest response to stratospheric ozone depletion is simulated in the spring (Graf et al., 1998), the largest trends have been observed in the winter months (Thompson et al., 2000), when no significant trends are simulated in response to ozone depletion (Gillett et al., 2003; Gillett, 2005). Overall, therefore, based on theoretical considerations and some modeling studies, it can be concluded that Arctic ozone depletion has likely contributed to the weak positive trend in the NAM in the spring, but that it cannot explain the observed winter trends.

5.3 EFFECTS OF ANTHROPOGENIC CLIMATE CHANGE AND OF EMISSIONS ON STRATOSPHERIC OZONE

5.3.1 Stratospheric Temperature Changes Due to Shifts in Radiative Forcing

Long-term changes in radiative forcing over the next few decades will continue to impact global mean temperatures in both the troposphere and stratosphere. Over the past three decades, increases in well-mixed greenhouse gas (WMGHG) concentrations and declines in stratospheric ozone have been the primary forcing mechanisms affecting stratospheric climate.

Global concentrations of WMGHGs will continue to rise in the next half century, although significant uncertainties remain as to the exact rate of increase. These changes will act, on average, to cool the stratosphere (see Section 5.2.1), but there can still be a seasonal warming, particularly at high latitudes, due to changes in planetary wave activity. Therefore, the assessment of the future evolution of polar temperatures is uncertain. Future changes in stratospheric water vapor are also difficult to predict, in part because the changes observed over the last four decades are still not fully understood (e.g., Randel et al., 2004b, 2006; see also Section 5.2.5). While declines in stratospheric ozone also act to cool the stratosphere, within this decade global ozone levels will likely begin to rise (Chapter 6). Higher ozone levels will increase stratospheric ozone heating, which will at least partially offset the cooling due to increases in WMGHG concentrations. Because ozone concentrations are so sensitive to the background temperature field, understanding the complex

interaction between changing constituent concentrations and temperature requires an evaluation of the coupling between chemistry, radiation, and atmospheric dynamics.

The primary method used for quantifying the interaction between changing chemistry and dynamics is the Chemistry-Climate Model (CCM). With advances in CCMs, the nonlinear coupled evolution of chemistry and dynamics can be studied. One of the continuing challenges for climate models (AOGCMs, coupled ocean-atmosphere general circulation models) is predicting future changes in tropospheric and stratospheric wave dynamics, which in turn affect the structure and evolution of lower and upper atmospheric temperature (see Section 5.2.2). Improvements in CCMs (Eyring et al., 2006; see also Section 6.6) are providing valuable insight into how temperatures will evolve in the future.

Model simulations for doubled CO₂ conditions with and without interactive ozone chemistry show a substantial temperature decrease throughout most of the middle atmosphere, with a maximum cooling of 10-12 K near the stratopause (Jonsson et al., 2004; Sigmond et al., 2004; Fomichev et al., 2006; see Figure 5-13a). In these calculations, stratospheric ozone increases are associated with lower temperatures, which partially modulate the CO₂-induced cooling through enhanced ozone heating. While simulations using CCMs demonstrate how the inclusion of interactive chemistry alters model meteorology (Austin and Butchart, 2003; Manzini et al., 2003; Tian and Chipperfield, 2005), more fundamental dynamical processes such as the parameterization of gravity waves and propagation characteristics of planetary waves remain significant modeling challenges (see also Section 5.2.2.4).

AOGCMs (i.e., AGCM coupled with an ocean model) whose output will be used in the Intergovernmental Panel on Climate Change (IPCC) Fourth Assessment Report (AR4; IPCC, in preparation for 2007) represent the most advanced and comprehensive set of climate simulations so far produced. To better represent the many physical processes responsible for climate variability and change, enhanced horizontal and vertical resolution has been used in these models compared with earlier IPCC Assessments. While the AOGCMs used for the IPCC were not specifically designed for stratospheric simulations, it is becoming increasingly apparent that accurate simulations of the stratosphere are important in determining the evolution of the surface climate, as well as other aspects of climate change. It is for this reason that the assumptions that have been chosen in the IPCC AOGCM simulations for the 21st century (i.e., future greenhouse gas (GHG) concentrations are only specified by different scenarios from the Special Report on Emissions Scenarios (IPCC, 2000) that differ primarily in

the emissions of WMGHGs) constitute a restriction for an assessment of climate change within the next few decades. In the high (A2) scenario, concentrations of CO₂ increase from today's value (~380 ppmv) to approximately 850 ppmv by 2100, while the low (B1) scenario reaches 550 ppmv by 2100 (IPCC, 2001). In these AOGCM simulations, ozone concentrations are prescribed and not interactively computed during the 21st century, which is an obvious restriction and has an impact on the assessment of the future development of lower stratospheric temperature (see below).

Figure 5-9 shows a time series of global-mean temperature anomalies between 2000 and 2100 at 50 hPa from fifteen AOGCMs adopting the A2 emission scenario used for the IPCC AR4. See Appendix 5A for information concerning the specific AOGCMs. While all simulations show 50 hPa global temperatures declining over the 21st century, the range of predictions for temperature change varies from -0.5 to -3.5 K by 2100. Differences in model ozone concentrations over the 21st century are likely responsible for some of the range in model predictions, while variations in model dynamics, the limited vertical extent of many of the AOGCMs, and differences in radiation schemes are also likely contributors.

The relative uncertainty in model predictions of future stratospheric temperature is further illustrated in Figure 5-10, which shows the globally averaged temperature trend computed during the 21st century using the models submitted to the IPCC AR4 for low (B1) and high (A2) emission scenarios. In the troposphere, temperatures rise during the next century, ranging between 0.2 K/decade (low) to 0.5 K/decade (high) for the different emission scenarios. In the stratosphere, the rate of cooling is also strongly dependent on the emission scenario, ranging from 0.07 ± 0.20 K/decade (low) to 0.18 ± 0.20 K/decade (high) at 50 hPa and 0.38 ± 0.09 K/decade (low) to 0.72 ± 0.47 K/decade (high) at 10 hPa. However, it should be reemphasized that in the present set of IPCC AOGCM simulations, the ozone forcing in the 21st century varies from constant ozone to a slow recovery by 2050, and thus contributes to the large model-to-model variability (Hare et al., 2004).

A similar analysis of global-mean temperature trends from CCMs (Eyring et al., 2006) that consider interactive ozone feedback (see Box 5-1) generally shows less model-to-model variability compared with the AOGCM results submitted to the IPCC AR4. See Chapter 6, Table 6-4 for information concerning the specific CCMs. Figure 5-11 (bottom panel) shows that global temperature trends at 50 hPa from CCMs are in reasonable agreement with ERA-40 (European Centre for Medium-Range Weather Forecasts (ECMWF) 40-year Reanalysis) and radiosonde data (Radiosonde

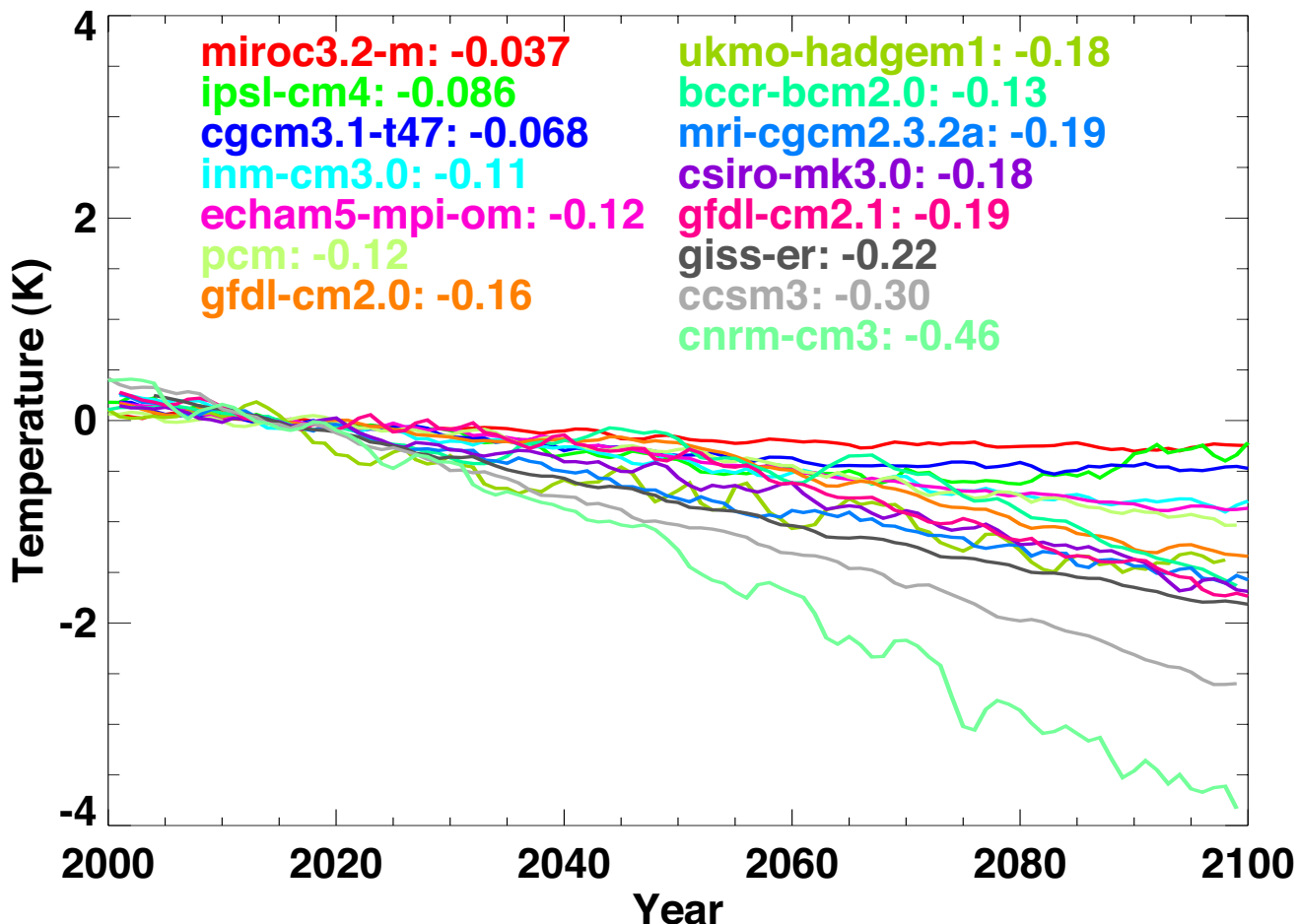


Figure 5-9. Evolution of global-mean temperature anomaly at 50 hPa between 2000 and 2100 as estimated from AOGCMs for the A2 emission scenario. The temperature trend in K/decade is given next to the name of each participating model. Anomalies are computed with respect to temperatures between 2010 and 2020. For clarity, models are labeled in order from weakest to strongest temperature variation. Information about the AOGCMs is given in Appendix 5A.

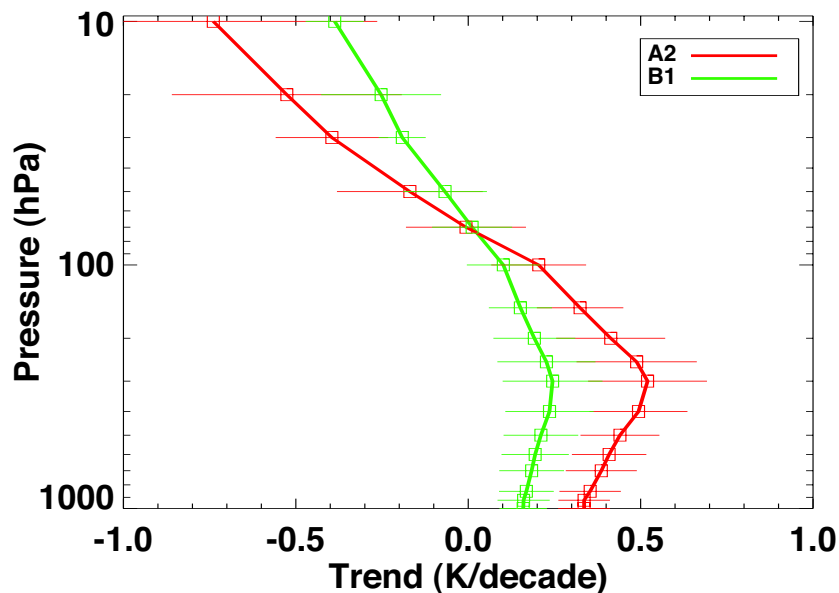


Figure 5-10. Global and annual mean 21st century temperature trends from AOGCMs using A2 (high) and B1 (low) emission scenarios. The boxes indicate the average trend computed for all models, while the thin horizontal lines indicate the range of model-calculated trends. Information about the AOGCMs is given in Appendix 5A.

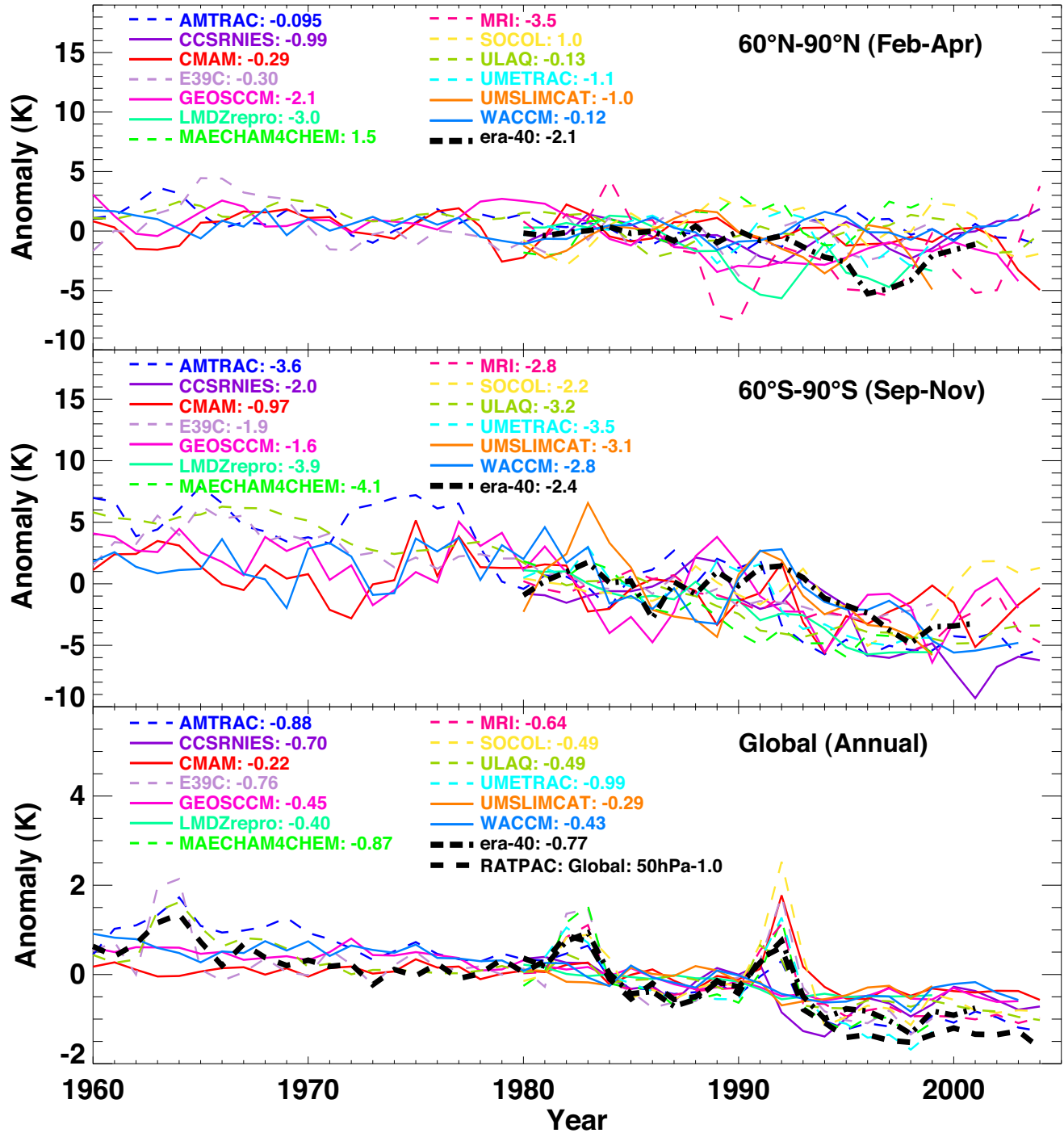


Figure 5-11. Time series of temperature anomalies for Arctic spring (top), Antarctic spring (middle), and the annual global mean (bottom) at 50 hPa derived from the REF1 (20th century climate) CCM simulations and from observations (i.e., ECMWF 40-year reanalysis, ERA-40, and Radiosonde Atmospheric Temperature Products for Assessing Climate, RATPAC). The temperature anomalies are calculated with respect to a mean reference period between 1980 and 1989. A linear temperature trend in K/decade is calculated for each model using data between 1980 and 1999. AMTRAC, MAECHAM4CHEM, MRI, UMETRAC, SOCOL, ULAQ, and E39C are shown with dashed lines, all other CCMs with solid lines. The temperature trend is given next to the name of each participating model (from Eyring et al., 2006). See Table 6-4 and Appendix 6A of Chapter 6 for information about the CCMs and the model runs.

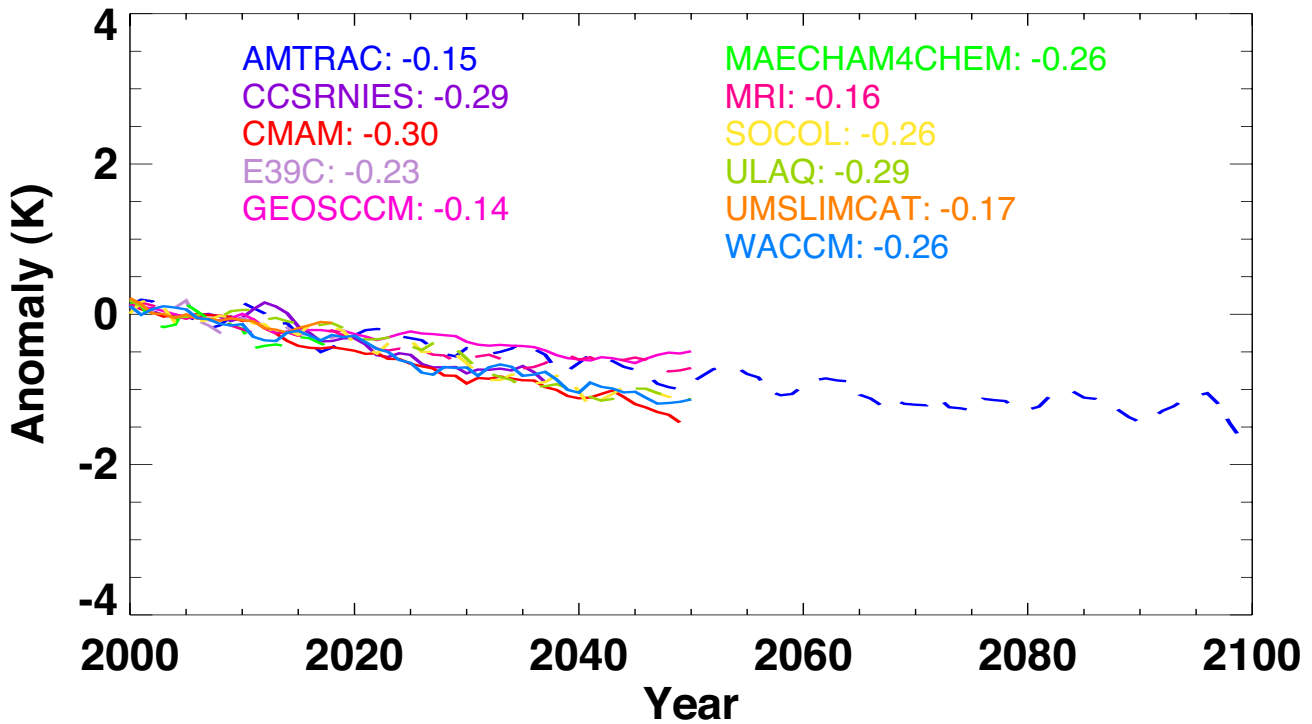


Figure 5-12. Time series of global-mean annual temperature anomalies at 50 hPa from the REF2 (21st century climate, A1B scenario; IPCC, 2001) CCM simulations (see Chapter 6, Appendix 6A). The temperature anomalies are calculated with respect to a mean reference period between 2000 and 2010. AMTRAC, E39C, MAECHAM4CHEM, MRI, SOCOL, and ULAQ are shown with dashed lines, all others CCMs with solid lines. A linear temperature trend in K/decade is calculated for each model using data after 2000 and is shown next to the name of each participating model. See Chapter 6, Table 6-4 and Appendix 6A for information about the CCMs and the model runs.

Atmospheric Temperature Products for Assessing Climate, RATPAC; Free et al., 2005) and display an obvious cooling from 1980 to present day. The model temperature trends range from -0.22 K/decade to -0.99 K/decade (average = -0.64 K/decade), with 7 out of 13 CCMs showing statistically significant trends, compared

with the ERA-40 (-0.77 K/decade; not significant) and RATPAC (-1.0 K/decade; significant) data. Corresponding AOGCM results show model temperature trends ranging from -0.03 to -0.97 (average = -0.38 K/decade). Perturbations by volcanic eruptions are well captured in many of the CCMs, but generally the temperature response is over-predicted (see Section 5.2.4; Figure 5-3). A similar over-prediction of the warming effect at 50 hPa from volcanic aerosols was also found with the AOGCMs. The evolution of lower stratospheric (50 hPa) springtime temperatures in the polar regions (Figure 5-11, top and middle panel) indicates a much greater inter-annual variability, which is caused by the specific impact of wave dynamics (Section 5.2.2.1; see also Chapter 4, Section 4.1.1.1). This is another reason for larger uncertainties in the assessment of the future evolution of stratospheric springtime temperatures in these geographical regions.

Table 5-1. Mean linear temperature trend in K/decade calculated from different types of models and for different emission scenarios using model data after year 2000. See text for detailed description.

Pressure Level	Emission Scenario (Model Employed)		
	B1 (AOGCM)	A1B (CCM)	A2 (AOGCM)
50 hPa	-0.07 ± 0.20	-0.23 ± 0.09	-0.18 ± 0.20
10 hPa	-0.38 ± 0.09	-0.63 ± 0.23	-0.72 ± 0.47

Figure 5-12 shows that there is good agreement between the CCM results showing a global cooling trend at 50 hPa through the first half of the 21st century. The

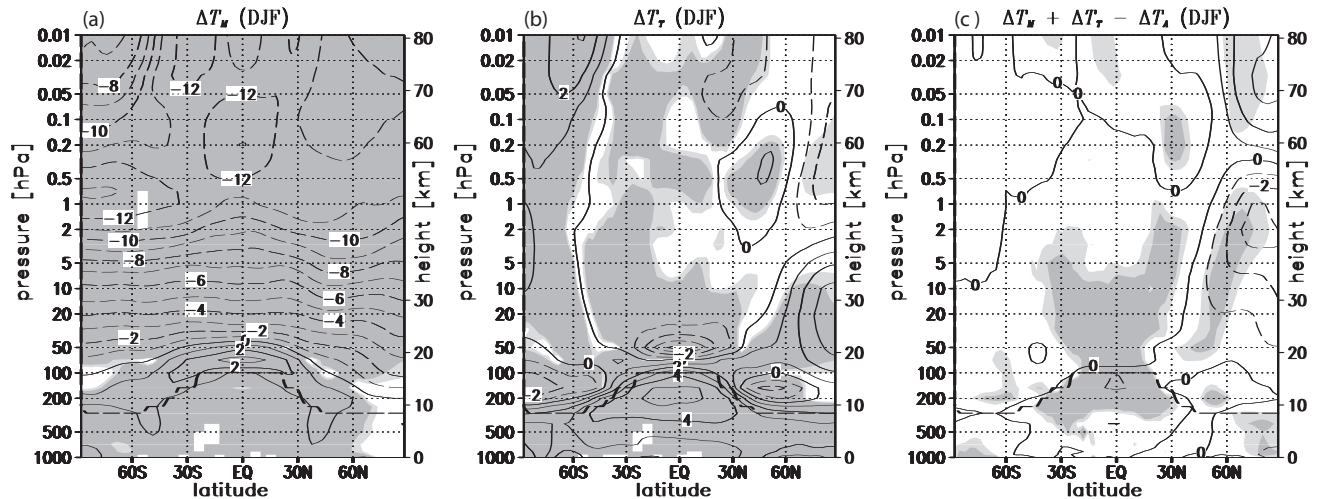


Figure 5-13. Changes in the middle atmosphere resulting from different doubling CO_2 model runs for the months of December-January-February: (a) The change in the zonally averaged temperature due to a doubling of CO_2 in the middle atmosphere, ΔT_M ; (b) the change due to a doubling of CO_2 in the troposphere, ΔT_T ; and (c) the degree of non-additivity, i.e., the sum of the temperature changes due to a doubling of CO_2 separately in middle atmosphere and troposphere, minus the temperature change resulting from a doubling of CO_2 in all the atmosphere ($\Delta T_M + \Delta T_T - \Delta T_A$). Light (dark) shading denotes significance at 95% (99%) level of the changes in (a) and (b) and of the non-additivity in (c). The contour interval is 1 K. The thick dashed line denotes the position of the tropopause. From Sigmond et al., 2004.

CCMs adopted a medium (A1B) emission scenario used for the IPCC AR4, which reaches 720 ppmv by 2100. Considering the CCM results up to the year 2050, the cooling trend ranges from 0.14 to 0.30 K/decade. In the lower stratosphere, the temperature trends derived from the CCM simulations using the medium (A1B) emission scenario are larger compared with the AOGCM results which are related to the high (A2) emission scenario (cp. Table 5-1). At 10 hPa, where ozone changes are expected to be weak, AOGCM and CCM simulations are in line, i.e., the calculated trends derived from the AOGCM A2 simulations are stronger than those derived from the CCM A1B simulations (see Table 5-1). The fact that the different CCM results are more tightly constrained may be due to the smaller range in the prescribed forcing (see Chapter 6, Appendix 6A). Both results from AOGCMs and CCMs point to the changing nature of the stratosphere and troposphere and the important role that emission of WMGHGs has in the prediction of future temperature in the stratosphere.

5.3.2 Stratospheric Temperature Changes Due to Additional Effects

Future changes in radiative forcing will have both a direct in-situ effect on stratospheric temperatures (Section 5.3.1) and an indirect effect resulting from changes in the

wave forcing from the troposphere. For the stratosphere, to a first approximation, the effects of in-situ radiative changes and those of changes in wave forcing from the troposphere are additive and therefore can be assessed separately (Sigmond et al., 2004; Fomichev et al., 2006). Figure 5-13 illustrates the response of the middle atmosphere (10-80 km) to a doubling of CO_2 in the troposphere and middle atmosphere separately, as well as together (Sigmond et al., 2004). Anthropogenic climate change is likely to have an impact on sea surface temperatures (SSTs), land-sea temperature differences, tropospheric jets, and synoptic scale activity, which in turn are likely to have an impact on the planetary wave forcing originating in the troposphere, as well as their regional effects in the lower stratosphere. Climate change can also affect the propagation of planetary waves into the stratosphere (Rind et al., 2005a; 2005b; Scott and Polvani, 2004; Scott et al., 2004). Changes in planetary wave forcing and propagation in the polar winter are a major source of uncertainty for predicting future levels of Arctic ozone loss (Austin et al., 2003). CCM (see Box 5-1) results used for WMO (2003) did not agree on the sign of the trend in the planetary wave flux from the troposphere. Recently, Fomichev et al. (2006) found that the response in the polar winter stratosphere to a doubling of CO_2 in the first 15 years of a 30-year simulation differed from the response in the last 15 years, which also supports earlier findings (e.g.,

CLIMATE-OZONE CONNECTIONS

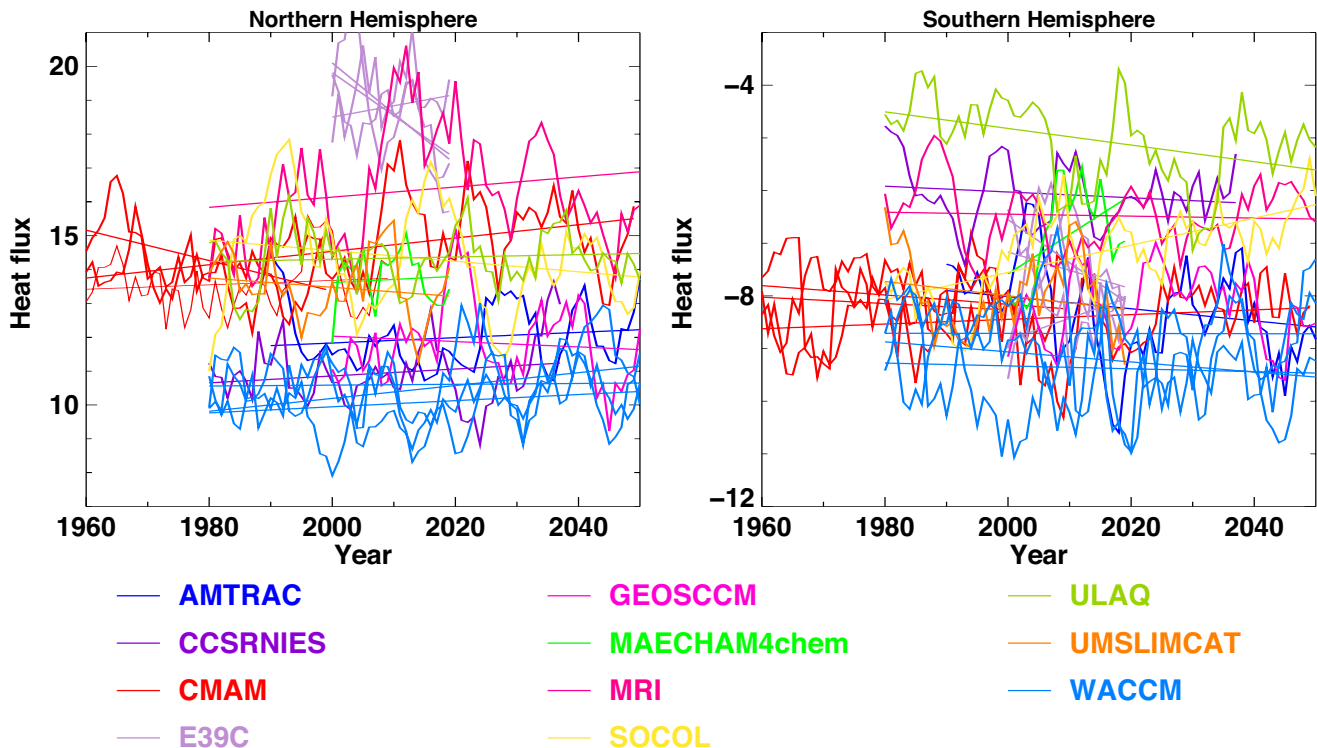


Figure 5-14. Evolution of the heat flux (K m/s) at 100 hPa as derived from CCM calculations. The analysis is based on model data derived from the REF2 and SCN2 simulations (see Chapter 6, Appendix 6A). Left panel: Heat flux averaged over 40°N to 80°N in January and February. Right panel: Heat flux averaged over 40°S to 80°S in July and August. Results are shown for each year of the simulations but have been smoothed with a 5-year running mean. The straight lines represent the least squares linear fit for the individual model runs. The heat flux at 100 hPa provides a measure of the wave flux propagating from the troposphere to the stratosphere. A negative heat flux in the SH corresponds to an upward planetary wave flux.

Butchart et al., 2000) that on a decadal time scale, the dynamics of the polar winter stratosphere are unpredictable due to internal variability.

Since WMO (2003), a number of transient CCM simulations have been run into the 21st century using the same climate forcing and halogen loadings (see Chapter 6, Table 6-4 and Appendix 6A). Eyring et al. (2006) assessed the CCMs used for these simulations and found that temperature biases in the northern winter in the polar lower stratosphere were quite small, and most of the models exhibited the correct temperature sensitivity to variations in the wave forcing from the troposphere. These are both notable improvements relative to the CCMs used by Austin et al. (2003). In contrast, there was little improvement in the Southern Hemisphere, with most of the CCMs still predicting Antarctic cold biases in spring, and the polar vortex breaking down much later than observed. Again, these latest CCM simulations do not provide any consensus as to what will happen to the planetary wave forcing from the troposphere in a future cli-

mate (see Figure 5-14), despite each model using the same amounts of greenhouse gases and halogens.

The reasons why the models continue to fail to provide a consensus are unclear. In part it could be due to model deficiencies, especially in the SH where many of the models are unable to reproduce the correct polar temperature sensitivity to the wave forcing from the troposphere. On the other hand, as argued in WMO (2003, Chapter 3), it could reflect true atmospheric behavior: in a truly chaotic system, planetary wave forcing from the troposphere may not be inherently predictable, and so models are giving a range of results reflecting that unpredictability. Clarification is strongly required because the assessment of the evolution of the ozone layer depends on the ability of CCMs to predict wave changes.

The most important SST factor affecting the troposphere and the stratosphere is tropical SST gradients, as found during El Niño-Southern Oscillation (ENSO) events. Anomalous tropical SST gradients are also known to have an impact on planetary wave forcing. The strato-

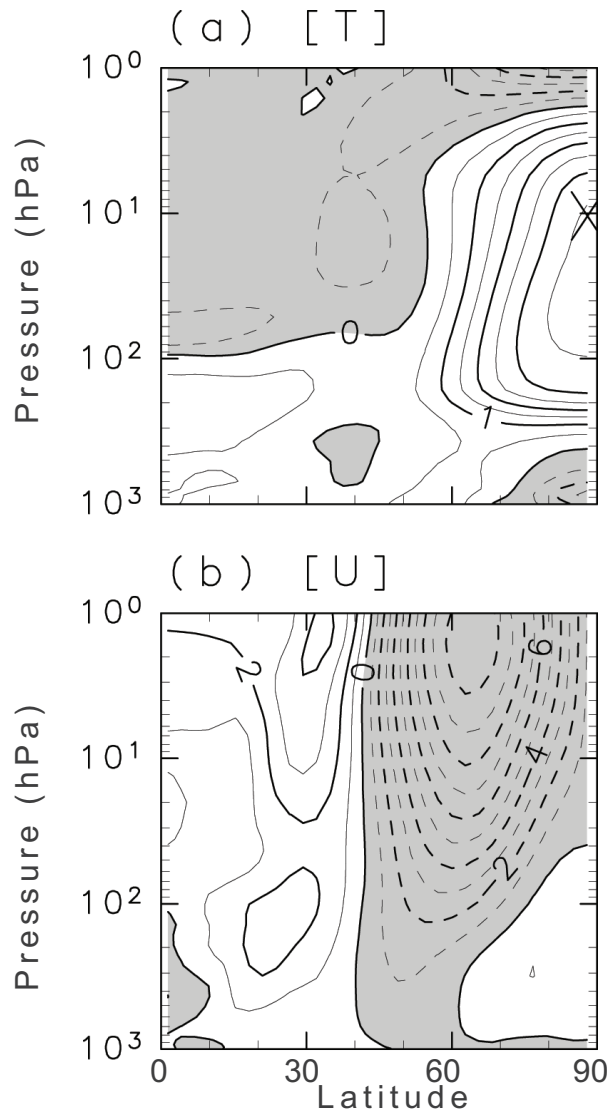


Figure 5-15. Climatological differences between WACCM (Whole Atmosphere Community Climate Model) simulations forced with high and low SSTs in the eastern tropical Pacific: (a) zonal mean temperature [T] in K and (b) zonal mean zonal wind [U] in m/s. Both panels display results for the Northern Hemisphere, with the equator on the left and the North Pole on the right. From Taguchi and Hartmann, 2006.

spheric polar vortex tends to be weaker than average during warm ENSO years, when SSTs are anomalously warm in the eastern tropical Pacific (van Loon and Labitzke, 1987), while cold ENSO years are associated with suppressed incidences of stratospheric sudden warmings (Limpasuvan et al., 2005). Similar relationships have been noted in several numerical simulations (Hamilton, 1993; Sassi et al., 2004; Manzini et al., 2006). Moreover,

there are indications of increased incidences of sudden stratospheric warmings in CCM simulations run with high SST anomalies in the eastern tropical Pacific (Taguchi and Hartmann, 2006; see Figure 5-15). Hoerling et al. (2001; 2004) and Hurrell et al. (2004) argued that changes in Indian Ocean SSTs have a demonstrable impact on the Northern Hemisphere Annular Mode/North Atlantic Oscillation (NAO/NAM) on decadal time scales, but the extent to which these changes extend to stratospheric levels remains unclear.

Outside the polar regions in winter, changes in the tropospheric forcing are also expected to have an impact on lower stratospheric temperatures throughout the year. There are indications from model assessments that anthropogenic climate change will increase the upwelling across the tropical tropopause and downwelling in the extratropics (see Sections 5.3.3 and 5.3.7). The associated adiabatic heating will then lead to a cooling of the tropical lower stratosphere and warmer extratropics in all months (Figure 5-16), but it is more pronounced during the boreal winter and spring, which is consistent with the asymmetry in the SST change between the NH and SH in the adopted model (Fomichev et al., 2006). Other climate change simulations (Butchart et al., 2006) also indicate that, on average, the increase in planetary wave driving is greater during the northern winter than during the southern winter.

All CCMs and AOGCMs used to predict stratospheric temperature changes (see Section 5.3.1) parameterize the effects of small-scale gravity waves. The more sophisticated of these schemes parameterize the vertical propagation and breaking of the waves in terms of the large-scale flow, and therefore are able to respond to climate perturbations in the stratosphere resulting from radiative or planetary wave forcing. Moreover, research by Shaw and Shepherd (2007) suggests that, provided the parameterizations are implemented to conserve momentum, the climate response will be robust to differences in the gravity wave source spectrum, background flow, gravity wave-breaking criterion, and model upper boundary. McLandress and Scinocca (2005) also showed that the response is not very dependent on the choice of gravity wave drag parameterization, at least among those schemes that have been developed to represent the propagation and breaking. It is not clear what proportion of the change in gravity wave forcing will result from the indirect effect of climate change modifying the propagation and breaking of the waves, and how much will result directly from a change in the source. The greatest uncertainty is in knowing how the source spectrum will evolve in a changing climate. Unfortunately, the spectrum is rather poorly constrained by observations for the present climate, and it will be difficult to quantify the effects of

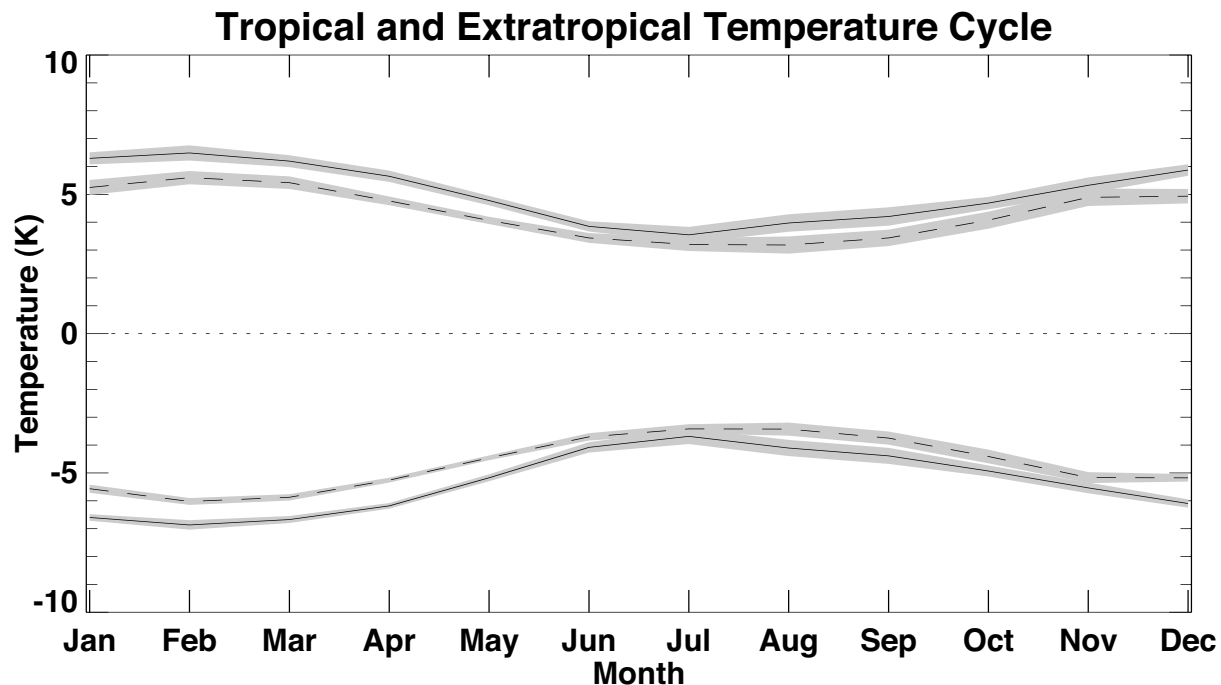


Figure 5-16. Annual cycle of the tropical (30°S - 30°N ; negative curves) and extratropical (positive curves) mean temperature, with global mean subtracted, at 50 hPa. The dashed curve results from a model simulation in which the atmospheric CO_2 was doubled, but the SSTs were not adjusted for the doubled CO_2 conditions. The solid curve is from a simulation with both the CO_2 doubling and adjusted SSTs, and therefore includes an additional effect on the temperatures due to changes in wave forcing from the troposphere. From Fomichev et al., 2006.

changes in gravity wave forcing on the stratospheric temperatures without further progress toward specifying sources in terms of other flow parameters to allow for climate feedbacks.

5.3.3 Troposphere-Stratosphere Exchange and the Brewer-Dobson Circulation

The net mass exchange between the troposphere and stratosphere is associated with the large-scale Brewer-Dobson circulation (Holton et al., 1995; Shepherd, 2002), with a net upward flux in the tropics balanced by a net downward flux in the extratropics. However, near the tropopause itself, the picture is more complex, with two-way mixing across the extratropical tropopause at and below synoptic scales, and vertical mixing in the tropical-tropopause layer (TTL) resulting from convective processes (see Section 5.3.4). Nonetheless, above the lowermost extratropical stratosphere and at the top of the TTL, the exchange is more one-way with, in particular, air slowly rising into the stratosphere above the TTL. Model studies indicate that climate change will impact the mass exchange across the tropopause. Rind et al.

(2001) estimated a 30% increase in the mass flux due to a doubling of atmospheric CO_2 amounts, and Butchart and Scaife (2001) estimated that the net upward mass flux above the TTL would increase by about 3% per decade due to climate change. In both of these studies, the changes in the mass flux resulted from more vigorous wave propagation from the troposphere into the stratosphere. Modeling studies of tropospheric ozone (Collins et al., 2003; Zeng and Pyle, 2003; Sudo et al., 2003) also found that climate change caused a comparable percentage increase in the extratropical stratosphere-to-troposphere ozone flux.

For a doubled CO_2 concentration, all 14 climate-change model simulations in Butchart et al. (2006) resulted in an increase in the annual mean troposphere-to-stratosphere mass exchange rate (Figure 5-17), with a mean trend of $11 \text{ Gg s}^{-1} \text{ year}^{-1}$, or about 2% per decade. The predicted increase occurred throughout the year but was, on average, larger during the boreal winter than during the austral winter. The Butchart et al. study was unable to conclude whether stratospheric ozone changes or ozone feedbacks had a significant impact on the underlying trend in the mass exchange rate. Other simulations

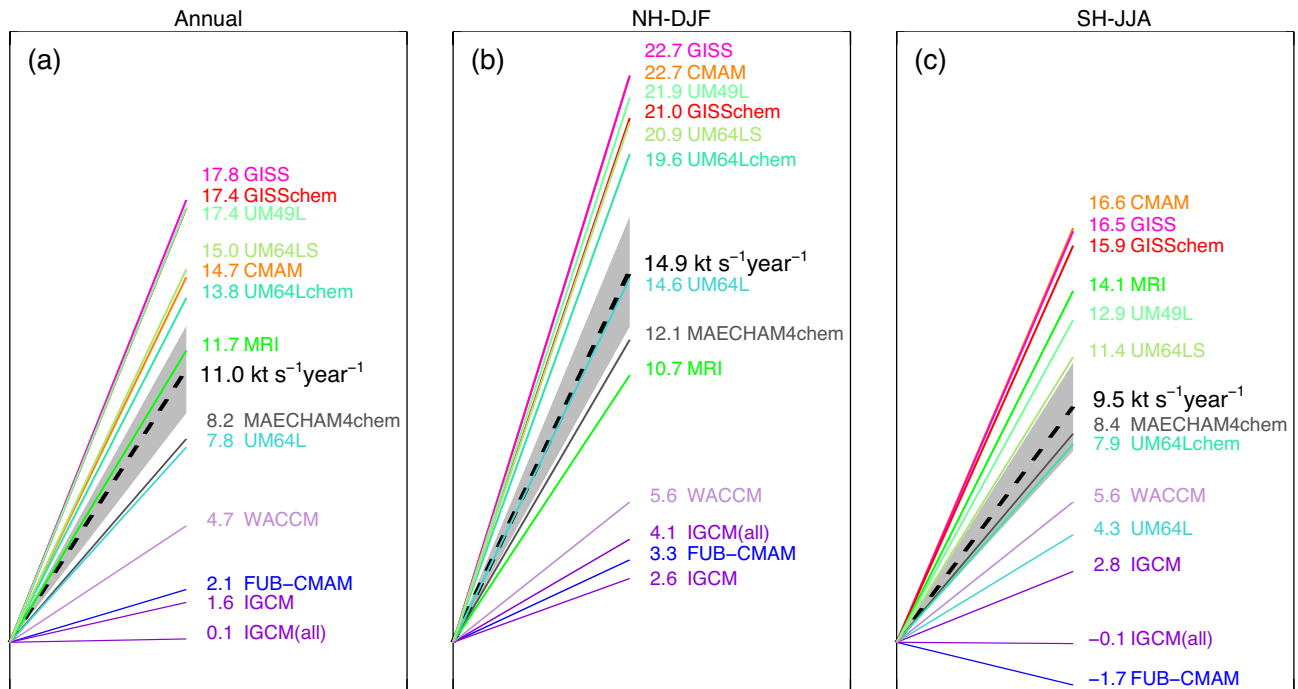


Figure 5-17. Schematic representation of the trends in troposphere-to-stratosphere mass exchange rate computed in a set of 14 CCMs and climate models that consider the complete stratosphere (from Butchart et al., 2006). The trends ($\text{Gg s}^{-1} \text{ year}^{-1}$) are given by the slope of the lines. For the transient simulations, trends were calculated from a least squares fit to the mass flux data. For the time-slice simulations (see Box 5-1) the difference in flux was converted to a mean mass flux trend, assuming a doubling time of 70 years for CO_2 . The dashed line is the multi-model mean; the standard error is given by the gray shading.

(e.g., Austin et al., 2006) suggest that the trend in tropical upwelling is not constant. Periods of enhanced upwelling coincide with periods of significant ozone depletion.

The calculation of tropical upwelling (or of mean age of air¹; see below) from measurements or assimilated datasets is challenging, and it is not possible to calculate reliable trends. Calculations of age of air using a transport model and meteorological fields (Schoeberl et al., 2003; Meijer et al., 2004; Scheele et al., 2005) gave values that were lower than those determined using observations of long-lived tracers (e.g., Boering et al., 1996; Andrews et al., 2001; Schoeberl et al., 2005). Similar results have been obtained recently from a suite of CCMs (Eyring et al., 2006; see Chapter 6).

Tropical upwelling is inversely related to model age of air (Austin and Li, 2006), so that the age of air changes as the stratospheric climate changes. As noted for the tropical upwelling, the age of air does not change steadily

(Figures 5-18 and 5-19). In both CCMs AMTRAC (e.g., Austin et al., 2006) and WACCM (e.g., Beres et al., 2005), age of air decreased significantly from about 1975 to 2000, consistent with an increase in tropical upwelling, which in AMTRAC was identified as due in part to ozone depletion (Austin et al., 2006). As shown in Figure 5-19, WACCM also indicates that age of air remains constant for conditions of fixed GHG concentrations and sea surface temperatures (SSTs) (see also Section 5.3.7), indicating that changes in GHG concentrations and SSTs are major influences for age of air changes in the future. The overall decrease of age of air and increase in tropical upwelling on climate time scales implies a more rapid removal of the long-lived CFCs from the entire atmosphere (Butchart and Scaife, 2001), as well as source species such as CH_4 and N_2O . Once enhanced CH_4 concentrations reached the stratosphere, enhanced CH_4 oxidation would occur, leading to a faster increase in water

¹ Age of air: The length of time that a stratospheric air mass has been out of contact with the well-mixed troposphere. The content of a unit element of air at a particular location and particular time of year in the stratosphere can be thought of as a mixture of different air parcels that have taken different routes from the tropopause to arrive at that location. The mean age of air at a specific location is defined as the average transit times of the elements since their last contact with the tropopause.

Age of Air 20°N-20°S, 1.3 hPa

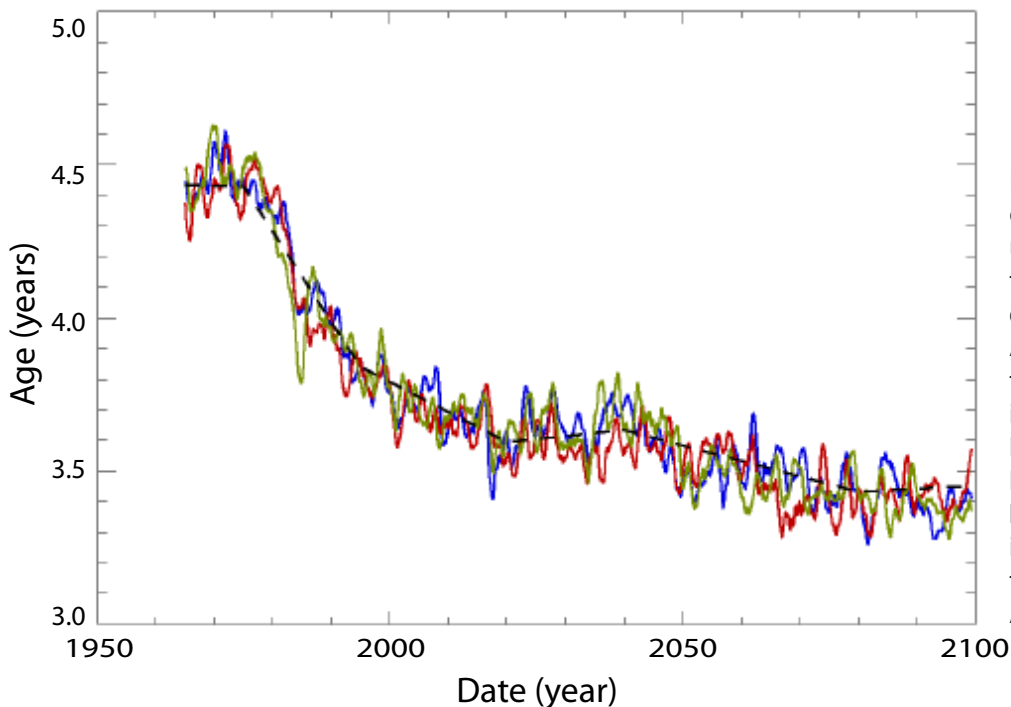


Figure 5-18. Mean age of air in the tropical upper stratosphere for the period 1960-2100 computed from the CCM AMTRAC. The three different colored curves indicate individual simulations. A piecewise linear curve (black broken line) is included to illustrate changes in trends. Modified from Austin and Li, 2006.

Age of Air 22°N-22°S, 1.24 hPa

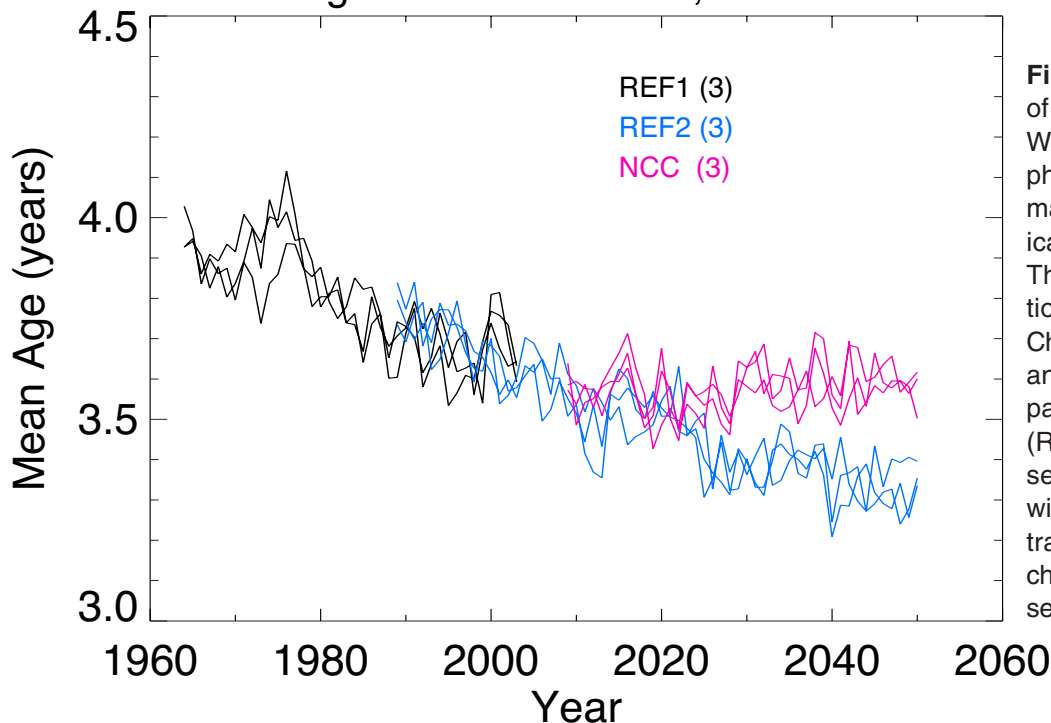


Figure 5-19. Mean age of air for the CCM WACCM (Whole Atmosphere Community Climate Model) in the tropical upper stratosphere. The individual simulations are described in Chapter 6 (Appendix 6A) and cover the recent past (REF1), the future (REF2), and an ensemble of simulations with fixed GHG concentrations (“no climate change” scenario (NCC); see also Section 5.3.7).

vapor amounts than would be anticipated on the basis of the tropospheric CH_4 concentrations alone.

5.3.4 Changes in the Tropical and Extratropical Tropopause Layer

5.3.4.1 THE TROPICAL TROPOPAUSE LAYER (TTL)

The TTL (Sherwood and Dessler, 2001) is typically defined as the body of air extending from the level of the temperature lapse rate minimum at 11-13 km (Gettelman and Forster, 2002) to the level of highest convective overshoot, slightly above the cold point tropopause (CPT) at 16-17 km (see Chapter 2, Section 2.4.1 for other definitions). This encompasses the level of zero net radiative heating (z_0) that marks the transition from radiative cooling to radiative heating, divides the TTL into the lower and upper TTL (Section 2.4.1), and depends on the presence of clouds (Corti et al., 2005). Below z_0 , the cooling air sinks back into the troposphere, whereas above z_0 the warming air rises and eventually enters the stratosphere. The chemical state of this air depends on its residence time in the TTL (Folkens et al., 1999; Thuburn and Craig, 2002; Bonazzola and Haynes, 2004; Fueglistaler et al., 2004). In addition, the minimum temperature experienced by this air is crucial for dehydration along the transport pathway in the TTL, and thus for stratospheric humidity (see Sections 5.2.5 and 5.3.5).

The TTL has undergone changes within the last few decades that are not well known or understood, and our predictive capabilities remain extremely limited. There is no merged reference dataset of long-term global temperature observations for this height region.

The TTL is sandwiched between a warming troposphere and a cooling stratosphere, which makes it difficult to produce a theoretical estimate of the response of the CPT and stratospheric humidity. A simple conceptual picture is shown in Figure 5-20. If one assumes a convectively controlled troposphere with a constant lapse rate, then tropospheric warming raises and warms the tropopause (cold point temperature increasing from T_1 to T_2). A cooling of the stratosphere further raises the tropopause but leads to a cooling (from T_2 to T_3). It seems likely that the tropospheric warming should be the dominant effect, because the enhanced infrared cooling by enhanced greenhouse gas concentrations is weak due to the very low temperatures close to the tropopause (e.g., Clough and Iacono, 1995). The observed temperature trends just above the tropical tropopause correspond to a cooling of less than 0.4 K/decade but are not statistically significant (Chapter 4 in WMO, 2003). The general con-

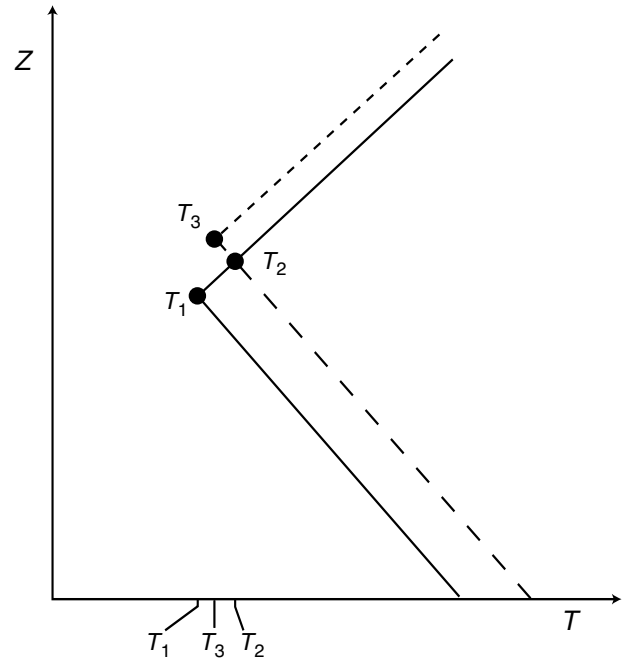


Figure 5-20. Simplified sketch of the sensitivity of the tropopause temperature and height with regard to changes of temperature in the stratosphere and troposphere. Solid lines: reference profile with cold point T_1 . Long-dashed line with solid line: perturbed profile reflecting tropospheric warming with cold point T_2 . Long-dashed line with short-dashed line: perturbed profile reflecting tropospheric warming and stratospheric cooling with cold point T_3 . After Shepherd, 2002.

cept behind Figure 5-20 has been corroborated by AGCM time-slice (Shepherd, 2002) and transient simulations (Santer et al., 2003) (see Box 5-1).

The evolution of TTL temperatures is further complicated by the fact that there is a tropospheric amplification of surface warming (Santer et al., 2005). Conversely, a strengthening of the Brewer-Dobson circulation, as suggested by model climate studies with enhanced CO_2 (Butchart and Scaife, 2001; Rind et al., 2002a, b; Sigmond et al., 2004; Eichelberger and Hartmann, 2005), would imply a lowering of TTL temperatures.

Seidel et al. (2001) obtained an increase in CPT height of about 40 meters and a decrease in pressure of about 1 hPa during 1978-1997. Both Seidel et al. (2001) and Zhou et al. (2001) have also noted a decrease of tropical tropopause temperatures by about 1 K during this period, resulting in a decrease in the saturation volume mixing ratio of water of about 0.5 ppmv during 1978-1997. These temperatures are therefore at odds with tropospheric warming dominating the response of the CPT. Rather, they

CLIMATE-OZONE CONNECTIONS

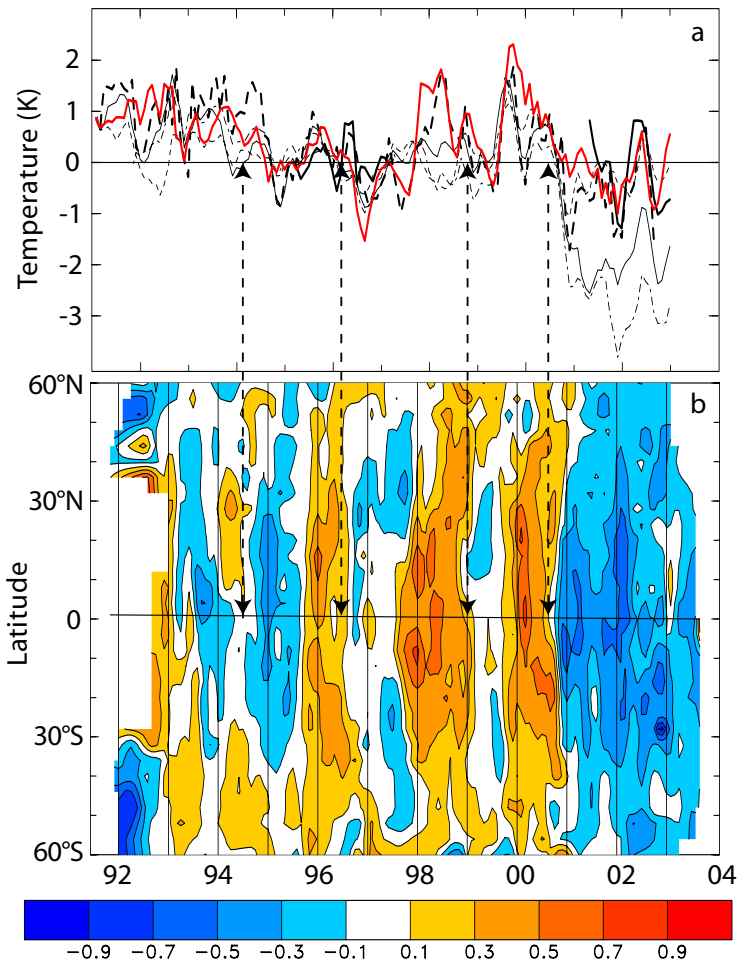


Figure 5-21. (a) Time series of deseasonalized 100 hPa temperature anomalies over 10°N-10°S, showing results from six different datasets (red = radiosondes, thick black = GPS, and various model results). (b) Latitude-time cross sections at 82 hPa of deseasonalized anomalies in $\text{H}_2\text{O} + 2 \times \text{CH}_4$ from HALOE measurements. Contours are $\pm 0.1, 0.3$, etc., ppmv. Dashed vertical lines show the onsets of various cold phases ascribed to the quasi-biennial oscillation and El Niño-Southern Oscillation. From Randel et al., 2004a.

suggest that the CPT is being largely controlled by increases in the Brewer-Dobson circulation and by increased convection as suggested by Zhou et al. (2001). Zhou et al. (2004) have also shown how the QBO and El Niño-Southern Oscillation effects produce extremely high and low tropical CPT temperatures.

Figure 5-21a indicates a very small negative trend of tropical temperatures on the 100 hPa level over the past decade, which merges into an enhanced negative evolution during 2001-03. The reasons for the most recent development are not clear at present. Figure 5-21b shows stratospheric total water content. Large anomalies are centered in the tropics and are in phase with the 100 hPa tropical temperatures. The low 2001-03 water vapor anomaly covers nearly the entire globe. The observed strong seasonal and interannual T- H_2O correlations suggest stratospheric total water content to be strongly controlled by temperatures between the 100 hPa level and the CPT, which is in agreement with recent trajectory calculations (Hatsushika and Yamazaki, 2003; Bonazzola and Haynes,

2004; Fueglistaler et al., 2005; Fueglistaler and Haynes, 2005).

Changes in the TTL may also affect the abundance of many other species in the stratosphere. This may concern short-lived chemical species, such as biogenic bromine compounds that may be carried to the stratosphere via deep convection followed by transport through the TTL (see Chapter 2, Section 2.4.1). Changes in deep convection may further affect the transport of longer-lived species produced by biomass burning, such as methyl bromide (Andreae and Merlet, 2001). Finally, species may be transported in particulate form across the tropical tropopause, e.g., organic sulfur-containing species (Notholt et al., 2005). Little is known about these processes, and even less is known about climate-induced changes.

In summary, given the uncertainties in our understanding of mechanisms in the TTL and of their previous changes, predictions of future changes in TTL morphology, processes, or transport are rendered difficult. A future atmosphere with increasing greenhouse gas load-

ings is expected to develop a warmer troposphere with enhanced deep convection. But for the reasons mentioned above, it remains speculative that this will be reflected in a warmer tropopause, higher water mixing ratios, and as a consequence, a moister stratosphere with less rapid recovery of ozone. The past decades suggest the dominance of other processes, possibly related to changes in the Brewer-Dobson circulation, which may give rise to surprises.

5.3.4.2 THE EXTRATROPICAL TROPOPAUSE LAYER (ExTL)

As described in Section 2.4.2 of Chapter 2, the ExTL is a layer of air adjacent to the local extratropical (thermal) tropopause, which has been interpreted as the result of irreversible mixing of tropospheric air into the lowermost stratosphere (Hoor et al., 2004; Hegglin et al., 2005) or as the result of two-way stratosphere-troposphere exchanges (Pan et al., 2004; Bischoff et al., 2006).

The origin of ozone in the ExTL changes markedly with season, with photochemical production dominating in summer and transport from the stratosphere dominating in winter and spring. A general upward trend of the extratropical tropopause height has been identified and has been related to ozone column changes (Steinbrecht et al., 1998; Varotsos et al., 2004). This long-term change provides a sensitive indicator of human effects on climate (Santer et al., 2004) and may be related to changes such as are sketched in Figure 5-20. However, it is presently not clear how these changes have affected, or will affect, the dominant transport pathways of air between the troposphere and the stratosphere on the synoptic scale or mesoscale.

Possible future changes in midlatitude circulation—increased strength of Brewer-Dobson circulation (e.g., Butchart and Scaife, 2001), changes in synoptic eddies (e.g., Schneider, 2004), changes in midlatitude convection (e.g., IPCC, 2001)—are all likely to change ozone concentration in the upper troposphere and lower stratosphere. However, limitations of our knowledge regarding the ExTL prevent any firm predictions on the future of the ExTL. In particular, the relative contribution of isentropic (quasi-horizontal) and convective (vertical) transport of tropospheric air into the lowermost stratosphere is not well established, though there is evidence that vertical mixing (both convectively and radiatively driven) might have a significant influence on the large-scale trace gas distributions in the lowermost stratosphere (Hegglin et al., 2005). If the frequency or intensity of midlatitudinal deep convection were to change in a future warmer climate, this could affect the lowermost stratosphere and, thus, the midlatitudinal ozone layer. Simulations of the 20th century in

the IPCC climate models (AOGCMs) generally show a decrease in the total number of extratropical storms in both hemispheres, but an increase in the number of the most intense storms (Lambert and Fyfe, 2006). Predictions of implications for ExTL dynamics and chemistry will require further investigations.

5.3.5 Impact of Future Water Vapor Changes on Ozone Chemistry

It is difficult to assess the magnitude of recent changes to stratospheric water vapor concentrations (Section 5.2.5), and future changes are uncertain. Water vapor concentrations may remain similar to current values, or possibly increase. For example, most of the CCM future simulations (i.e., REF2; see Chapter 6, Appendix 6A) show increasing stratospheric water vapor concentrations in the stratosphere. In this section, the implications for ozone of possible future increases in water vapor concentrations are discussed.

A positive trend in stratospheric water vapor concentrations would affect stratospheric ozone production and loss chemistry. Increases in water vapor would cause increases in hydrogen oxide (HO_x) radicals, affecting ozone loss processes. HO_x chemistry is the primary ozone loss process in the lower stratosphere (Wennberg et al., 1994; 1998), except over the polar caps. In addition, balloon constituent data, in conjunction with a photochemical box model, have highlighted the important role that HO_x plays in the stratosphere and lower mesosphere (Osterman et al., 1997; Jucks et al., 1998).

Evans et al. (1998) examined the effect of increased water vapor concentrations on ozone; they found that increased humidity slightly increased ozone in the middle stratosphere, and decreased ozone in the upper stratosphere. The decrease in upper stratospheric ozone was primarily from increased loss by the HO_x catalytic cycles. Dvortsov and Solomon (2001) modeled past and future changes in greenhouse gas concentrations and atmospheric chlorine and bromine loading. The model was forced to have an annual stratospheric H_2O increase of 1% per year. The water vapor trend in the model intensified the Northern Hemisphere midlatitude ozone trends, primarily due to increased ozone loss in the lower stratosphere from enhanced HO_x , and subsequent HO_x -amplified ClO_x ozone loss. The study suggests that a 1% per year stratospheric humidity trend during this century would enhance ozone loss via the HO_x catalytic cycles and delay the ozone recovery by approximately 10 years. Shindell (2001), using a CCM, also showed that including a similar future trend in water vapor may delay the ozone recovery time by approximately 15 years.

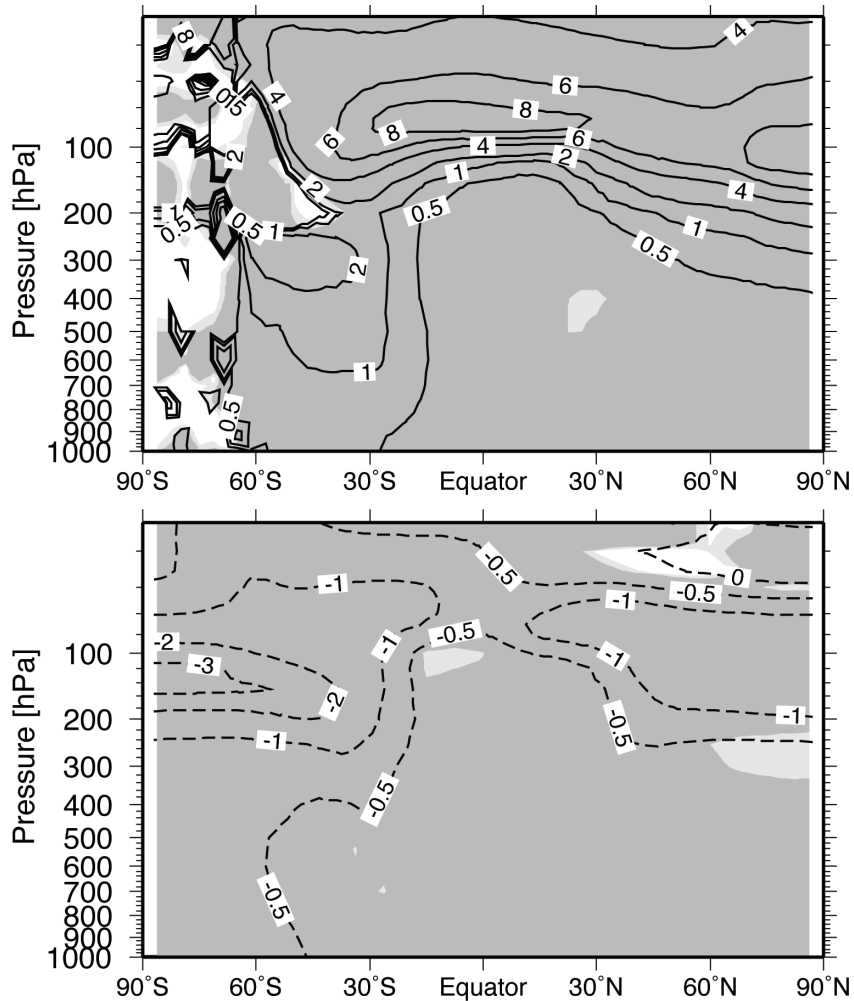


Figure 5-22. Impact of 1 ppmv water vapor perturbation above a baseline simulation in the CCM E39C. The top panel shows the percentage change in zonally and monthly averaged local OH. The bottom panel shows the percentage change in zonally and monthly averaged local O₃. Light (dark) shading indicates regions in which differences are statistically significant at the 95% (99%) level (t-test). From Stenke and Grewe, 2005.

The CCM study of Stenke and Grewe (2005) found that an increase of 1 ppmv in stratospheric water vapor would result in a 5-10% hydroxyl radical (OH) increase in the tropical lower stratosphere between 100 and 30 hPa (Figure 5-22, top panel). In the model, the OH increase caused an increase in the HO_x ozone destruction cycle of about 6%. Ozone in the lower stratosphere decreased by 1-3% (Figure 5-22, bottom panel), reducing the column by less than 1% in nonpolar latitudes (Figure 5-23).

Increases in water vapor concentration can also affect polar ozone depletion on polar stratospheric clouds (PSCs). Enhanced water vapor concentrations would increase the critical temperature below which heterogeneous reaction on liquid aerosols become important (Kirk-Davidoff et al., 1999). Tabazadeh et al. (2000) estimated that the enhancement of PSC formation for an addition of 1 ppmv water vapor is approximately the same as the PSC enhancement from a 1 K radiative cooling. Stenke and Grewe (2005) concluded that increased humidity will enhance heterogeneous ozone depletion in the Antarctic spring due to a longer PSC- existence period (Figure 5-23).

5.3.6 Impact of Temperature Changes on Ozone Chemistry

The assessment of ozone chemistry’s sensitivity to changes in temperature in the atmosphere is complicated by the concomitant changes that occur in the dynamics, transport, and radiation as the temperature changes. In addition, the chemical state of the atmosphere will change as the concentration of trace species change and ozone-depleting substances (ODSs) decrease over the coming decades. This in turn will alter the sensitivity of the stratospheric chemical system to temperature changes.

5.3.6.1 UPPER STRATOSPHERE

There is a relatively solid understanding of the sensitivity of ozone chemistry in the upper stratosphere to changes in temperature. In this region the chemical system is generally under photochemical control and is constrained by gas-phase reaction cycles that are well understood. The largest stratospheric cooling associated with

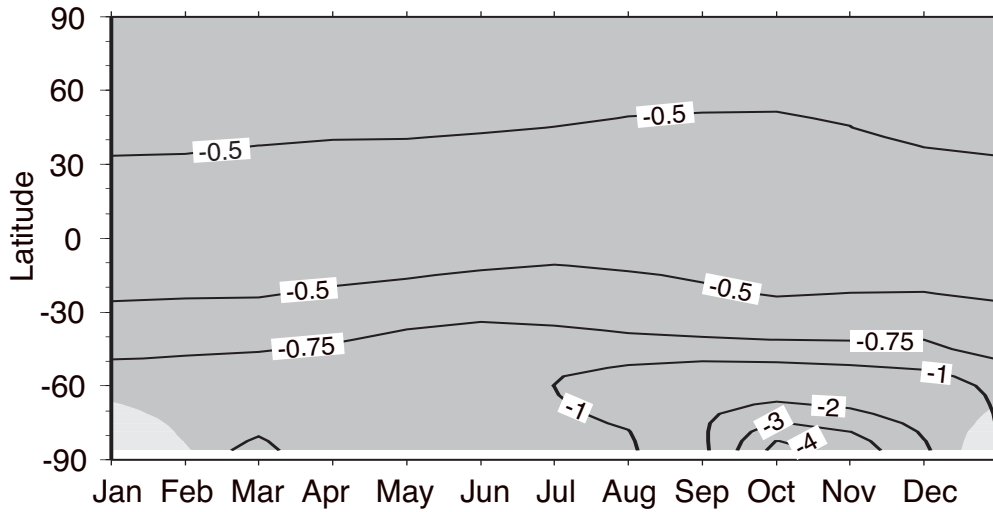


Figure 5-23. Impact of 1 ppmv water vapor perturbation above baseline simulation in the CCM E39C. This figure shows the percentage change in zonally averaged total column ozone. Light (dark) shading indicates regions in which differences are statistically significant at the 95% (99%) level (t-test). From Stenke and Grewe, 2005.

increased greenhouse gas concentrations (see Sections 5.2.6 and 5.3.1) has been observed in the upper stratosphere and mesosphere. The dominant ozone loss cycles in the upper stratosphere (NO_x , ClO_x , and HO_x) are expected to slow with decreasing temperatures (e.g., Haigh and Pyle, 1982). CCM simulations for doubled- CO_2 conditions presented by Jonsson et al. (2004) indicated an increase of 15-20% in the ozone mixing ratios in the upper stratosphere associated with a 10-12 K temperature decrease (see Section 5.3.1). In the lower mesosphere, the ozone increase is primarily due to the negative temperature dependence of the $\text{O} + \text{O}_2 + \text{M} \rightarrow \text{O}_3 + \text{M}$ reaction. The situation is more complex in the upper stratosphere, with different loss cycles having greater influence on ozone concentrations at different altitude ranges (50-60 km: HO_x ; 45-50 km: all cycles; below 45 km: NO_x). The slower loss rates are controlled by the temperature dependence of the reaction rate constants and by the reduction in the abundance of atomic oxygen (change in O_x partitioning). The rate-limiting reactions for all the loss cycles are proportional to the atomic oxygen number density. The atomic oxygen number density, in turn, is strongly determined by the reaction $\text{O} + \text{O}_2 + \text{M} \rightarrow \text{O}_3 + \text{M}$ (Jonsson et al., 2004).

5.3.6.2 POLAR LOWER STRATOSPHERE

In the springtime polar lower stratosphere, the gas-phase loss cycles described above play a similar role in determining the ozone concentration. Any decrease in temperature is expected to slow the rate of ozone loss (Zeng and Pyle, 2003). Counteracting this effect, chlorine- and bromine-containing reservoir species are activated via heterogeneous processes on cloud and cold aerosol particles, leading to markedly increased ClO_x

and BrO_x concentrations. This in turn leads to significant ozone loss via ClO_x and BrO_x catalytic cycles in the presence of sunlight. The rate of chlorine and bromine activation on the surface of cloud and aerosol particles is strongly temperature dependent, increasing sharply below approximately 195 K.

For the current polar lower stratosphere with elevated ODS concentrations, halogen activation, and consequent ozone losses at lower temperatures, offset any effect of ozone increases through reduction in NO_x and HO_x gas-phase ozone loss. This is clear from comparisons of the Antarctic and Arctic spring ozone concentrations (see Chapter 4). The Antarctic stratosphere routinely experiences temperatures below the threshold for heterogeneous halogen activation during the winter and early spring, with the consequent significant loss of ozone. The Arctic lower stratosphere, on the other hand, is highly variable and lies close to the halogen activation threshold. This means that a significant change in Arctic stratospheric temperatures would strongly influence springtime ozone concentrations in this region.

Arctic Spring

Chapter 4 discusses the compact linear relationship between chemical ozone loss in the Arctic winter and the vortex-averaged volume of air that is below the PSC threshold temperature (V_{PSC}) introduced by Rex et al. (2004). They deduce a linear relationship of approximately 15 DU of additional chemical ozone loss per Kelvin of cooling of the lower stratosphere, on the basis of ozonesonde soundings. This result is supported by a similar study by Tilmes et al. (2004). The V_{PSC} , as defined by Rex et al. (2004), is essentially a temperature metric and thus the relationship they derive indicates the temperature

CLIMATE-OZONE CONNECTIONS

sensitivity of chemical Arctic ozone loss, but other factors (e.g., vortex isolation) are also coupled to vortex temperature and influence the chemical ozone loss over the Arctic vortex period.

The ozone loss vs. V_{PSC} linear relationship determined by Rex et al. (2004) is compact and robust for recent winters. This is surprising given the highly nonlinear nature of some processes within the system being described. Their relationship was derived by averaging over the Arctic vortex for the period mid-December to the end of March, which concatenates a number of complex nonlinear processes (microphysical details of PSC formation, denitrification and dehydration, and chemical activation on PSC surfaces).

It should be noted that the ozone loss vs. V_{PSC} relationship is valid for current conditions of elevated ODSs. As concentrations of ODSs in the stratosphere decrease through the early part of this century, it is likely that the ozone loss vs. V_{PSC} relationship will change. Also, vortex conditions (e.g., size) may change, so it is unclear whether the ozone loss vs. V_{PSC} relationship has any use as a predictive tool.

Antarctic Spring

In contrast to the Arctic polar vortex, the extent of ozone loss within the Antarctic polar vortex during winter and spring is primarily dictated by the amount of stratospheric halogen present.

A major predictor for ozone mass deficit over the Antarctic vortex period for the years 1979 to 2003 is the lagged equivalent effective stratospheric chlorine (EESC); it explains 82% of the variance in the ozone mass deficit (Huck et al., 2005). The 100 hPa polar temperatures modulate the interannual variability in the ozone mass deficit anomaly. The Antarctic ozone hole size is primarily sensitive to EESC and secondarily to temperatures near the edge of the vortex (collar temperature) (Newman et al., 2004). Changes in sulfate aerosol particle surface area and surface reactivity were used to explain the correlation between the residual ozone hole size and collar temperature. Using the residuals from a quadratic fit of the ozone hole size to the EESC amounts, they estimated that a 1 K decrease in collar temperature leads to an increase in size of the late September ozone hole of 1.1 million km².

Both Huck et al. (2005) and Newman et al. (2004) used regression analysis based on data from recent (1979-2003) years to derive empirical models of Antarctic ozone loss. The models can only be expected to remain valid for descriptions of near-future ozone losses when stratospheric conditions remain broadly similar to the 1979-2003 period used to construct the models. Both models' ozone hole indices will become less meaningful as meas-

ures of Antarctic ozone levels as the ozone hole begins to close from the middle of this century.

5.3.7 Impact of Climate Change on Ozone Recovery

As discussed in the previous sections, the long-term evolution of stratospheric ozone concentrations depends not only on changes of many stratospheric constituents (including ozone-depleting substances (ODSs), greenhouse gases (GHGs), water vapor, and aerosols), but also on changes in the climate of the troposphere and stratosphere caused by natural variability and anthropogenic forcing. While it is expected that the reduction of ODSs in the next years to decades will lead to an increase in ozone, this increase could be affected by changes in temperature (Section 5.3.6) and in chemical composition and transport (Sections 5.3.3 through 5.3.5). This section discusses results of sensitivity studies that use CCMs to elucidate how climate change could affect formation and destruction of future stratospheric ozone.

Recent Assessment reports (Section 12.2.1.3 in WMO, 1999; Section 4.8 in WMO, 2003) presented results derived from an ensemble of two-dimensional (2-D) models (see Box 5-1) that calculated the evolution of total ozone through the year 2050. For some models, near-global mean (60°N-60°S) column ozone remained up to 1% below 1980 levels even in 2050, while for others the ozone column amounts in 2050 were 3.5% higher than in 1980. Several of the 2-D models did not include the impact of greenhouse gas-induced stratospheric cooling on ozone. Temperatures affect ozone by changing the reaction rates that determine O_x abundance, primarily in the middle and upper stratosphere. Moreover, in the polar lower stratosphere, in addition to gas-phase photochemistry, chlorine and bromine reservoir species are activated via heterogeneous processes on cloud and cold aerosol particles (see Section 5.3.6). For example, in the 2-D models of Rosenfield et al. (2002) and Chipperfield and Feng (2003), ozone recovers to 1980 values 10-20 years earlier in many latitudes and seasons, due to the inclusion of the stratospheric cooling effect from enhanced GHG concentrations (e.g., Figure 6-11 of Chapter 6).

The aforementioned 2-D model studies illustrate that the future evolution of ozone is sensitive to changes in both chemical constituents *and* climate. Although a few 2-D models include some of the effects of changes in dynamics, they do not consider any variability in tropospheric wave forcing due to climate change and the impact this may have on the stratosphere (see Sections 5.2.2 and 5.3.2). Another weak point of 2-D models is that they are simply not useful for investigations of polar regions (WMO, 2003). Nowadays CCMs offer a more complete possibility to fur-

ther investigate the impact of climate change on ozone, since these models do consider interactions and feedbacks of radiative, dynamical, and chemical processes. Recently a number of CCMs (see Chapter 6, Table 6-4) have been used to simulate the past and future evolution of ozone (see Chapter 6, Appendix 6A). The following discussion highlights some results of additional CCM sensitivity studies (using the “no climate change” scenario, NCC) that enable a more detailed investigation of the impact of fixed greenhouse gas concentrations on the recovery of the stratospheric ozone layer. The results derived from these model sensitivity studies provide useful and supplementary information to better understand the expected evolution of the ozone layer in the 21st century (Chapter 6).

Three CCMs (E39C, ULAQ, WACCM) were employed to carry out long-term sensitivity simulations (through 2050), wherein concentrations of well-mixed greenhouse gases (CO₂, CH₄, and N₂O) are held constant after a given date (E39C: 1980; ULAQ: 1970; WACCM: 2000), whereas the evolution of halocarbon is based on the “Ab” scenario from WMO (2003). Additionally, in E39C and ULAQ, the sea surface temperatures (SSTs) were prescribed according to observations of the years 1970 to 1979. This SST dataset was used again for every succeeding decade in the model simulation (E39C: 1980 to 2020; ULAQ: 1960 to 2050). The methods used to prescribe SSTs in the NCC simulations are a bit simplified, but reasonable for this kind of sensitivity study. In reality, the thermal inertia of the oceans must be considered. A mixed-layer ocean model needs approximately 20 to 30 years to reach a new equilibrium, and a deep-ocean model even several hundred years (e.g., Hansen et al., 2005). For this kind of sensitivity study, the neglect of this effect is expected to be of small significance. Nonetheless, this effect was considered in the WACCM NCC simulations using SSTs from a coupled ocean-atmosphere model (AOGCM) that was run in support of the most recent IPCC Assessment (IPCC CCSM/CAM3). The CCSM/CAM3 simulation was run with IPCC emissions for 2000 held constant from 2000 to 2100, i.e., the same GHG scenario as adopted for the NCC simulations.

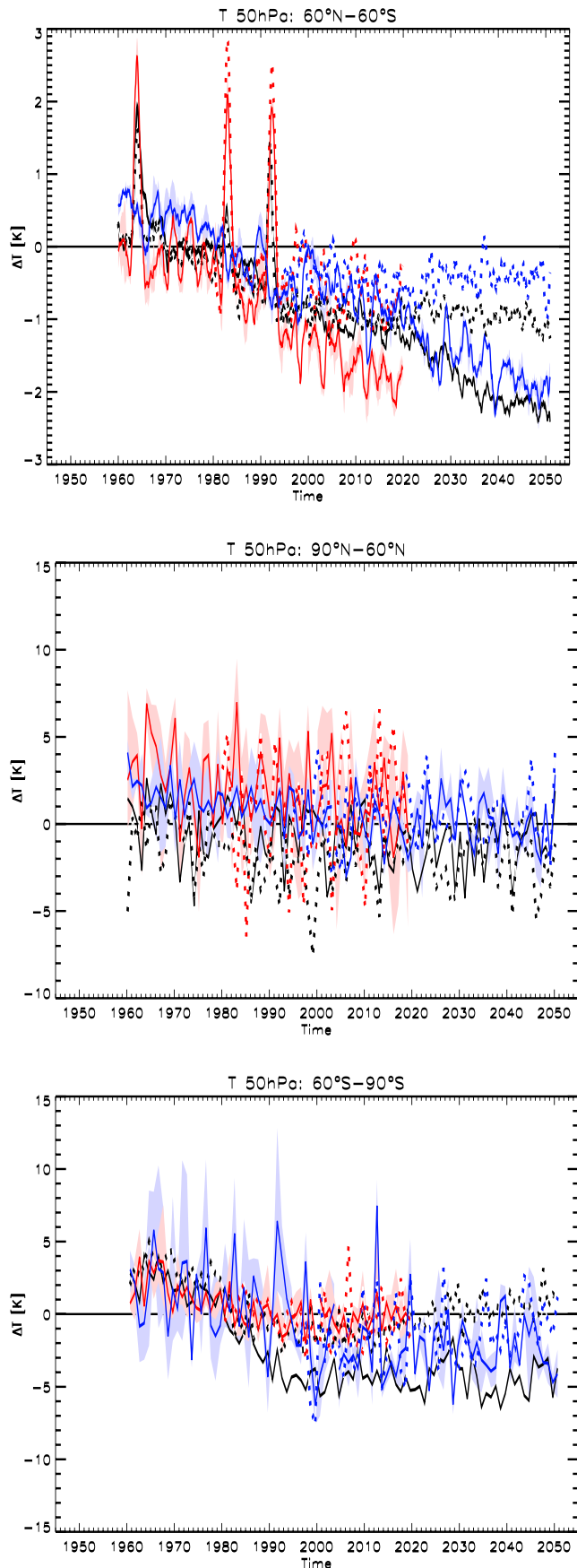
In all three CCMs, ozone and water vapor are prognostic variables, i.e., the radiative feedback of ozone and water vapor changes is considered. A direct comparison of results from the NCC simulations with results from reference simulations (prescribing past and expected future changes, i.e., REF1 and REF2/SCN2; see Chapter 6, Appendix 6A) allows a qualitative estimation of the future impact of climate change on ozone. Figure 5-24 (top) displays the evolution of the near-global (60°N-60°S) mean temperature deviations of the lower stratosphere at 50 hPa. The results derived from the reference simulations

show an obvious cooling trend because of increasing GHG concentrations (see Section 5.3.1). Nearly zero trends are calculated by all three CCMs when fixed GHG concentrations are assumed. It takes about 20 years before a difference is apparent between curves derived from the reference and the sensitivity simulations. This statement is not valid for mean temperatures (at 50 hPa) over the Northern Hemisphere polar region (i.e., 60°-90°N, Figure 5-24 middle panel), which does not show statistically significant differences between the reference and the sensitivity simulations. The picture is unclear for the Southern Hemisphere polar region (i.e., 60°-90°S, Figure 5-24 bottom panel). E39C shows no obvious differences between the two simulations, whereas WACCM results indicate slightly higher and ULAQ much higher temperatures in the NCC simulations.

Investigations of the CCM results do not indicate a clear impact of climate (temperature) change on metrics like minimum ozone column values in the polar stratosphere or “maximum ozone hole area,” either in the Northern Hemisphere or the Southern Hemisphere (not shown). These metrics are evidently insensitive to temperature changes of less than about 1 K. But the results shown in Figure 5-25 demonstrate that the recovery of near-global mean (60°N-60°S) column ozone is accelerated in a changing climate: since the global stratosphere is under photochemical control (constrained by gas-phase reaction cycles), the ozone loss cycles in the stratosphere (primarily O_x) slow down with decreasing temperature. When climate change is included, ULAQ and WACCM show a return to the 1980 global ozone amount approximately 10 to 15 years earlier than without climate change. This is in agreement with former estimates derived from 2-D model studies (see above). The results derived from the CCM E39C are not as clear in this sense, but here it must be considered that in contrast to ULAQ and WACCM, E39C has a low uppermost layer which is centered at 10 hPa, and therefore neglects the impact of dynamical and photochemical effects on ozone in the upper part of the stratosphere. In any case, the E39C simulations were not long enough for the difference between NCC and REF simulations to become apparent.

Results derived from ULAQ and WACCM show that by 2050, the middle to upper stratosphere is 5-10 K colder in the reference runs than in corresponding NCC simulations (not shown). As a result of this cooling, ozone mixing ratios in the middle and upper stratosphere are higher in the reference cases than in NCC (up to 15% below the stratopause). The most important impact is through the effect of temperature on the ozone loss rate. Below 10 hPa, all three CCMs show a consistent behavior. These results indicate a delay in the recovery of ozone in

CLIMATE-OZONE CONNECTIONS



the Antarctic lower stratosphere (not shown) due to “intensified” heterogeneous chemistry that is caused by reduced temperatures in the lower polar stratosphere. The changes are not statistically significant in the Arctic lower stratosphere. Interestingly, all models very clearly show less ozone in the tropical lower stratosphere in the reference simulations, which may point to an enhanced updraft in the tropics (intensified Brewer-Dobson circulation) in the reference simulations.

Qualitatively, the evolution of column ozone and lower stratospheric temperatures (50 hPa) in the polar regions (60°-90°) is very similar in the reference and NCC simulations (Figure 5-26). The results seem to indicate that the net impact of changes of well-mixed greenhouse gas concentrations and SSTs on total ozone is perhaps slightly larger in the Arctic stratosphere than in the Antarctic stratosphere. Differences in ozone column between results derived from reference simulations and NCC are not apparent in the polar SH. In the polar NH, the WACCM model indicates that after the year 2020, the ozone column is systematically larger in the reference simulations. So, lower temperatures in the ozone loss regions of high latitudes have the opposite effect of lower temperatures in the ozone production region in the tropics. Notwithstanding, it may be that in the NH the transport of air with enhanced ozone mixing ratios to high latitudes by an intensified Brewer-Dobson circulation dominates the effect of enhanced chlorine/bromine catalysis of ozone destruction in the polar region. The fact that it takes at least until 2020 for a noticeable difference to emerge between the reference simulations and NCC in the NH may be consistent with this conjecture.

Figure 5-24. Time series of zonally averaged near-global (top panel, 60°N-60°S) temperature deviations at 50 hPa between 1960 and 2050 relative to the year 1980 (in K). Data have been smoothed with a 13-month running mean. Respective time series are shown for the northern polar region (middle panel, 60°N-90°N) and the southern polar region (lower panel, 60°S-90°S). Here, data have been considered only for springtime months, i.e., 3-month mean values of February, March, and April in the NH, and August, September, and October in the SH. For each model, i.e., E39C (red lines), ULAQ (black lines), and WACCM (blue lines), the solid curves show results derived from the reference simulations (REF). Since WACCM and E39C have performed ensemble simulations, the envelope of results is shown for each model. The dotted curves indicate the results derived from the “no climate change runs” (NCC).

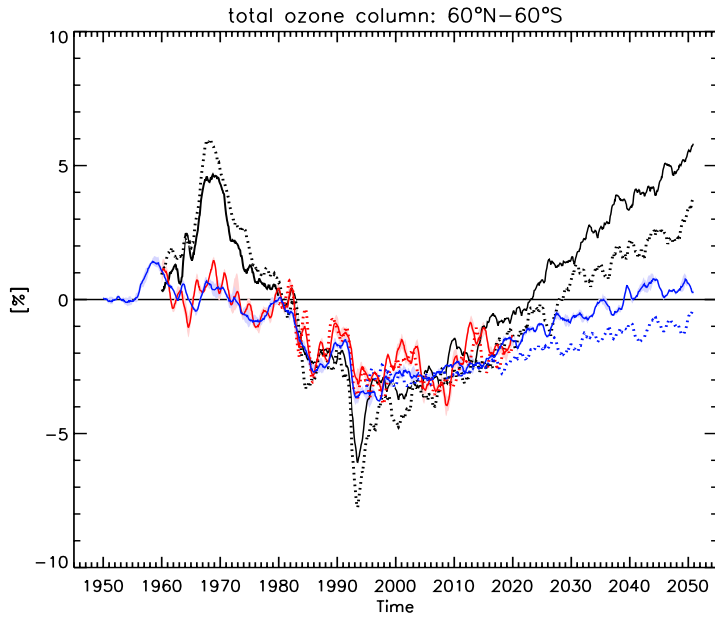


Figure 5-25. Time series of zonally averaged near-global (60°N-60°S) total ozone deviations between 1960 and 2050 with regard to the year 1980 (in %). For each model, i.e., E39C (red lines), ULAQ (black lines), and WACCM (blue lines), the solid curves show results derived from the reference simulations (REF). Since WACCM and E39C have performed ensemble simulations, the envelope of results is shown for each model. The dotted curves indicate the results derived from the “no climate change runs” (NCC). All data are smoothed with a 13-month running mean.

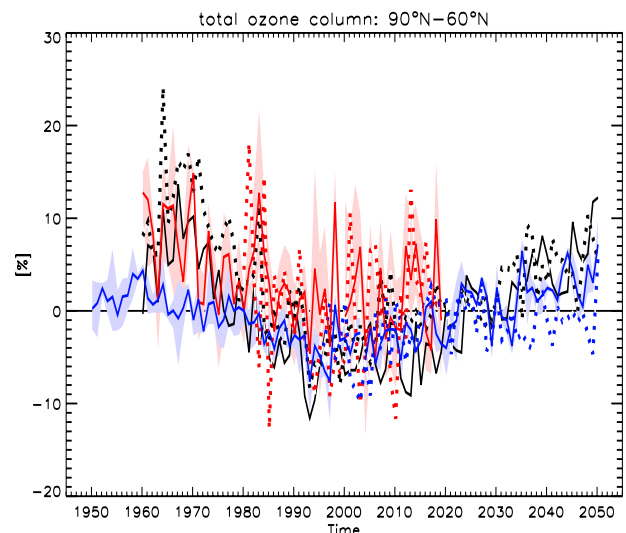
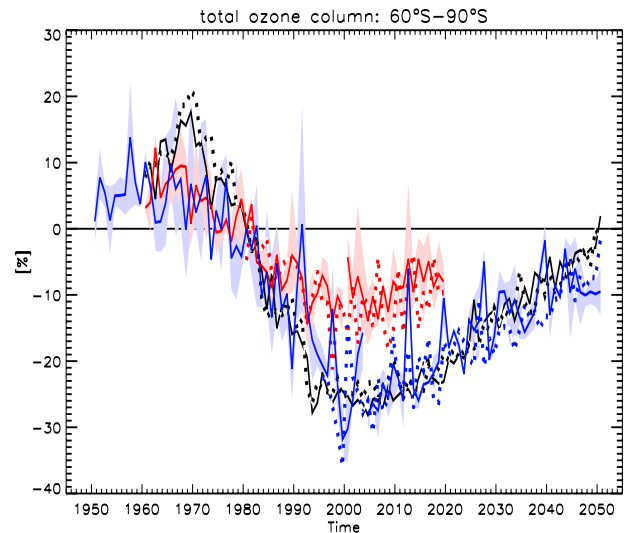


Figure 5-26. Time series of zonally averaged total ozone deviations at southern polar latitudes (top panel, 60°S-90°S) and northern polar latitudes (lower panel, 60°N-90°N) between 1960 and 2050 with regard to the year 1980 (in %). For each model, i.e., E39C (red lines), ULAQ (black lines), and WACCM (blue lines), the solid curves show results derived from the reference simulations (REF). Since WACCM and E39C have performed ensemble simulations, the envelope of results is shown for each model. The dotted curves indicate the results derived from the “no climate change runs” (NCC). Data have been considered only for springtime months, i.e., 3-month mean values of February, March, and April in the NH, and August, September, and October in the SH.

REFERENCES

- Al-Saadi, J.A., R.B. Pierce, T.D. Fairlie, M.M. Kleb, R.S. Eckman, W.L. Grose, M. Natarajan, and J.R. Olson, Response of middle atmosphere chemistry and dynamics to volcanically elevated sulfate aerosol: Three-dimensional coupled model simulations, *J. Geophys. Res.*, 106 (D21), 27255-27275, doi: 10.1029/2000JD000185, 2001.
- Andreae, M.O., and P. Merlet, Emission of trace gases and aerosols from biomass burning, *Global Biogeochem. Cycles*, 15 (4), 955-966, 2001.
- Andrews, A.E., K.A. Boering, B.C. Daube, S.C. Wofsy, M. Loewenstein, H. Jost, J.R. Podolske, C.R. Webster, R.L. Herman, D.C. Scott, G.J. Flesch, E.J. Moyer, J.W. Elkins, G.S. Dutton, D.F. Hurst, F.L. Moore, E.A. Ray, P.A. Romashkin, and S.E. Strahan, Mean ages of stratospheric air derived from in situ observations of CO₂, CH₄, and N₂O, *J. Geophys. Res.*, 106 (D23), 32295-32314, 2001.
- Andrews, D.G., J.R. Holton, and C.B. Leovy, *Middle Atmosphere Dynamics*, Academic Press, 489 pp., Orlando, Fla., 1987.
- Arblaster, J.M., and G.A. Meehl, Contributions of external forcings to Southern Annular Mode trends, *J. Clim.*, 19 (12), 2896-2905, doi: 10.1175/JCL13774.1, 2006.
- Austin, J., and N. Butchart, Coupled chemistry-climate model simulations for the period 1980 to 2020: Ozone depletion and the start of ozone recovery, *Quart. J. Roy. Meteorol. Soc.*, 129 (595), 3225-3249, 2003.
- Austin, J., and F. Li, On the relationship between the strength of the Brewer-Dobson circulation and the age of stratospheric air, *Geophys. Res. Lett.*, 33, L17807, doi: 10.1029/2006GL026867, 2006.
- Austin, J., D. Shindell, S.R. Beagley, C. Brühl, M. Dameris, E. Manzini, T. Nagashima, P. Newman, S. Pawson, G. Pitari, E. Rozanov, C. Schnadt, and T.G. Shepherd, Uncertainties and assessments of chemistry-climate models of the stratosphere, *Atmos. Chem. Phys.*, 3 (1), 1-27, 2003.
- Austin, J., J. Wilson, F. Li, and H. Vömel, Evolution of water vapor and age of air in coupled chemistry climate model simulations of the stratosphere, *J. Atmos. Sci.*, 33, L17807, doi:10.1029/2006GL026867, 2006.
- Baldwin, M.P., and T.J. Dunkerton, Propagation of the Arctic Oscillation from the stratosphere to the troposphere, *J. Geophys. Res.*, 104 (D24), 30937-30946, doi: 10.1029/1999JD900445, 1999.
- Baldwin, M.P., and T.J. Dunkerton, Stratospheric harbingers of anomalous weather regimes, *Science*, 244 (5542), 581-584, 2001.
- Baldwin, M.P., and L.J. Gray, Tropical stratospheric zonal winds in ECMWF ERA-40 reanalysis, rocketsonde data, and rawinsonde data, *Geophys. Res. Lett.*, 32 (9), L09806, doi: 10.1029/2004GL022328, 2005.
- Baldwin, M.P., L.J. Gray, T.J. Dunkerton, K. Hamilton, P.H. Haynes, W.J. Randel, J.R. Holton, M.J. Alexander, I. Hirota, T. Horinouchi, D.B.A. Jones, J.S. Kinnerson, C. Marquardt, K. Sato, and M. Takahashi, The Quasi-Biennial Oscillation, *Rev. Geophys.*, 39 (2), 179-229, 2001.
- Bekki, S., J.A. Pyle, W. Zhong, R. Toumi, J.D. Haigh, and D.M. Pyle, The role of microphysical and chemical processes in prolonging the climate forcing of the Toba eruption, *Geophys. Res. Lett.*, 23 (19), 2669-2672, 1996.
- Beres, J.H., R.R. Garcia, B.A. Boville, and F. Sassi, Implementation of a gravity wave source spectrum parameterization dependent on the properties of convection in the Whole Atmosphere Community Climate Model (WACCM), *J. Geophys. Res.*, 110, D10108, doi: 10.1029/2004JD005504, 2005.
- Birner, T., D. Sankey, and T.G. Shepherd, The tropopause inversion layer in models and analyses, *Geophys. Res. Lett.*, 33, L14804, doi: 10.1029/2006GL026549, 2006.
- Bischoff, S.A., P.O. Canziani, A.E. Yuchechechen, The tropopause at southern extratropical latitudes: Argentine operational rawinsonde climatology, *Int. J. Climatol.*, doi:10.1002/joc.1385, in press, 2006.
- Boering, K.A., S.C. Wofsy, B.C. Daube, H.R. Schneider, M. Loewenstein, and J.R. Podolske, Stratospheric mean ages and transport rates from observations of CO₂ and N₂O, *Science*, 274 (5291), 1340-1343, 1996.
- Bonazzola, M., and P.H. Haynes, A trajectory-based study of the tropical tropopause region, *J. Geophys. Res.*, 109, D20112, doi: 10.1029/2003JD004356, 2004.
- Butchart, N., and A.A. Scaife, Removal of chlorofluorocarbons by increased mass exchange between the stratosphere and the troposphere in a changing climate, *Nature*, 410 (6830), 799-802, 2001.
- Butchart, N., J. Austin, J.R. Knight, A.A. Scaife, and M.L. Gallani, The response of the stratospheric climate to projected changes in the concentrations of well-mixed greenhouse gases from 1992 to 2051, *J. Clim.*, 13 (13), 2142-2159, 2000.
- Butchart, N., A.A. Scaife, M. Bourqui, J. de Grandpre, S.H.E. Hare, J. Kettleborough, U. Langematz, E. Manzini, F. Sassi, K. Shibata, D. Shindell, and M. Sigmund, Simulations of anthropogenic change in the strength of the Brewer-Dobson circulation,

- Clim. Dyn.*, 27 (7-8), 727-741, doi:10.1007/s00382-006-0162-4, 2006.
- Castanheira, J.M., and H.-F. Graf, North Pacific-North Atlantic relationships under stratospheric control?, *J. Geophys. Res.*, 108 (D1), 4036, doi: 10.1029/2002JD002754, 2003.
- CCSP (U.S. Climate Change Science Program), *Temperature Trends in the Lower Atmosphere: Steps for Understanding and Reconciling Differences*, edited by T.R. Karl, S.J. Hassol, C.D. Miller, and W.L. Murray, A Report by the Climate Change Science Program and the Subcommittee on Global Change Research, 164 pp., Washington, D.C., 2006.
- Charney, J.G., and P.G. Drazin, Propagation of planetary-scale disturbances from the lower into the upper atmosphere, *J. Geophys. Res.*, 66 (1), 83-109, 1961.
- Charron, M., and E. Manzini, Gravity waves from fronts: Parameterization and middle atmosphere response in a general circulation model, *J. Atmos. Sci.*, 59 (5), 923-941, 2002.
- Chen, P., and W.A. Robinson, Propagation of planetary waves between the troposphere and stratosphere, *J. Atmos. Sci.*, 49 (24), 2533-2545, 1992.
- Chiou, E.W., L.W. Thomason, and W.P. Chu, Variability of stratospheric water vapor inferred from SAGE II, HALOE and Boulder (Colorado) balloon measurements, *J. Clim.*, 19 (16), 4121-4133, doi: 10.1175/JCL13841.1, 2006.
- Chipperfield, M.P., and W. Feng, Comment on: Stratospheric Ozone Depletion at northern mid-latitudes in the 21st century: The importance of future concentrations of greenhouse gases nitrous oxide and methane, *Geophys. Res. Lett.*, 30 (7), 1389, doi: 10.1029/2002GL016353, 2003.
- Christiansen, B., Stratospheric vacillations in a general circulation model, *J. Atmos. Sci.*, 56 (12), 1858-1872, 1999.
- Christy, J.R., R.W. Spencer, W.B. Norris, W.D. Braswell, and D.E. Parker, Error estimates of version 5.0 of MSU-AMSU bulk atmospheric temperatures, *J. Atmos. Oceanic Technol.*, 20 (5), 613-629, 2003.
- Clough, S.A., and M.J. Iacono, Line-by-line calculation of atmospheric fluxes and cooling rates 2. Application to carbon dioxide, ozone, methane, nitrous oxide and the halocarbons, *J. Geophys. Res.*, 100 (D8), 16519-16535, 1995.
- Collins, W.D., P.J. Rasch, B.A. Boville, J.R. McCaa, D.L. Williamson, J.T. Kiehl, B. Briegleb, C. Bitz, S.-J. Lin, M. Zhang, and Y. Dai, *Description of the NCAR Community Atmosphere Model (CAM3.0)*, Technical Note TN-464+STR, National Center for Atmospheric Research, 214 pp., Boulder, Colo., 2004.
- Collins, W.J., R.G. Derwent, B. Garnier, C.E. Johnson, M.G. Sanderson, and D.S. Stevenson, Effect of stratosphere-troposphere exchange on the future tropospheric ozone trend, *J. Geophys. Res.*, 108 (D12), 8528, doi: 10.1029/2002JD002617, 2003.
- Cordero, E.C., and T.R. Nathan, A new pathway for communicating the 11-year solar cycle signal to the QBO, *Geophys. Res. Lett.*, 32, L18805, doi: 10.1029/2005GL023696, 2005.
- Corti, T., B.P. Luo, T. Peter, H. Vömel, and Q. Fu, Mean radiative energy balance and vertical mass fluxes in the equatorial upper troposphere and lower stratosphere, *Geophys. Res. Lett.*, 32 (6), L06802, doi: 10.1029/2004GL021889, 2005.
- Dameris, M., V. Grewe, M. Ponater, R. Deckert, V. Eyring, F. Mager, S. Matthes, C. Schnadt, A. Stenke, B. Steil, C. Brühl, and M.A. Giorgetta, Long-term changes and variability in a transient simulation with a chemistry-climate model employing realistic forcing, *Atmos. Chem. Phys.*, 5, 2121-2145, 2005.
- Déqué, M., C. Dreveton, A. Braun, and D. Cariolle, The ARPEGE/IFS atmosphere model: A contribution to the French community climate modeling, *Clim. Dyn.*, 10, 249-266, 1994.
- Deshler, T., R. Anderson-Sprecher, H. Jäger, J. Barnes, D.J. Hofmann, B. Clemesha, D. Simonich, M. Osborn, R.G. Grainger, and S. Godin-Beekmann, Trends in nonvolcanic component of stratospheric aerosol over the period 1971-2004, *J. Geophys. Res.*, 111, D01201, doi: 10.1029/2005JD006089, 2006.
- Dunkerton, T.J., Quasi-biennial and sub-biennial variations of stratospheric trace constituents derived from HALOE observations, *J. Atmos. Sci.*, 58 (1), 7-25, 2001.
- Dunkerton, T.J., and D.P. Delisi, Climatology of the equatorial lower stratosphere, *J. Atmos. Sci.*, 42 (4), 376-396, 1985.
- Dvortsov, V.L., and S. Solomon, Response of the stratospheric temperatures and ozone to past and future increases in stratospheric humidity, *J. Geophys. Res.*, 106 (D7), 7505-7514, 2001.
- Eckermann, S.D., D.L. Wu, J.D. Doyle, J.F. Burris, T.J. McGee, C.A. Hostetler, L. Coy, B.N. Lawrence, A. Stephens, J.P. McCormack, and T.F. Hogan, Imaging gravity waves in lower stratospheric AMSU-A radiances, Part 2: Validation case study, *Atmos. Chem. Phys.*, 6, 3343-3362, 2006.
- Eichelberger, S.J., and D.L. Hartmann, Changes in the strength of the Brewer-Dobson circulation in a simple AGCM, *Geophys. Res. Lett.*, 32, L15807, doi: 10.1029/2005GL022924, 2005.
- Esler, J.G., and R.K. Scott, Excitation of transient Rossby

CLIMATE-OZONE CONNECTIONS

- waves on the stratospheric polar vortex and the barotropic sudden warming, *J. Atmos. Sci.*, *62* (10), 3661-3682, 2005.
- Evans, S.J., R. Toumi, J.E. Harries, M.P. Chipperfield, and J.M. Russell III, Trends in stratospheric humidity and the sensitivity of ozone to these trends, *J. Geophys. Res.*, *103* (D8), 8715-8725, 1998.
- Eyring, V., N. Butchart, D.W. Waugh, H. Akiyoshi, J. Austin, S. Bekki, G.E. Bodeker, B.A. Boville, C. Brühl, M.P. Chipperfield, E. Cordero, M. Dameris, M. Deushi, V.E. Fioletov, S.M. Frith, R.R. Garcia, A. Gettelman, M.A. Giorgetta, V. Grewe, L. Jourdain, D.E. Kinnison, E. Mancini, E. Manzini, M. Marchand, D.R. Marsh, T. Nagashima, P.A. Newman, S. Pawson, G. Pitari, D.A. Plummer, E. Rozanov, M. Schraner, T.G. Shepherd, K. Shibata, R.S. Stolarski, H. Struthers, W. Tian, and M. Yoshiki, Assessment of temperature, trace species, and ozone in chemistry-climate model simulations of the recent past, *J. Geophys. Res.*, *111* (D22308), doi: 10.1029/2006JD007327, 2006.
- Fioletov, V.E., G.E. Bodeker, A.J. Miller, R.D. McPeters, and R. Stolarski, Global and zonal total ozone variations estimated from ground-based and satellite measurements: 1964-2000, *J. Geophys. Res.*, *107* (D22), 4647, doi: 10.1029/2001JD001350, 2002.
- Flato, G.M., The Third Generation Coupled Global Climate Model (CGCM3) (and included links to the description of the AGCM3 atmospheric model), <http://www.cccma.bc.ec.gc.ca/models/cgcm2.shtml>, 2005.
- Folkins, I., M. Loewenstein, J. Podolske, S.J. Oltmans, and M. Proffitt, A barrier to vertical mixing at 14 km in the tropics: Evidence from ozonesondes and aircraft measurements, *J. Geophys. Res.*, *104* (D18), 22095-22102, 1999.
- Fomichev, V.I., A.I. Jonsson, J. de Grandpré, S.R. Beagley, C. McLandress, K. Semeniuk, and T.G. Shepherd, Response of the middle atmosphere to CO₂ doubling: Results from the Canadian Middle Atmosphere Model, *J. Clim.*, in press, 2006.
- Forster, P.M. de F., and K.P. Shine, Radiative forcing and temperature trends from stratospheric ozone changes, *J. Geophys. Res.*, *102* (D9), 10841-10855, 1997.
- Forster, P.M. de F., and K.P. Shine, Stratospheric water vapour changes as a possible contributor to observed stratospheric cooling, *Geophys. Res. Lett.*, *26* (21), 3309-3312, 1999.
- Free, M., D.J. Seidel, J.K. Angell, J. Lanzante, I. Dure, and T.C. Peterson, Radiosonde Atmospheric Temperature Products for Assessing Climate (RATPAC): A new data set of large-area anomaly time series, *J. Geophys. Res.*, *110*, D22101, doi: 10.1029/2005JD006169, 2005.
- Fritts, D.C., and M.J. Alexander, Gravity wave dynamics and effects in the middle atmosphere, *Rev. Geophys.*, *41* (1), 1003, doi: 10.1029/2001RG000106, 2003.
- Fueglistaler, S., and P.H. Haynes, Control of interannual and longer-term variability of stratospheric water vapor, *J. Geophys. Res.*, *110*, D24108, doi: 10.1029/2005JD006019, 2005.
- Fueglistaler, S., H. Wernli, and T. Peter, Tropical troposphere-to-stratosphere transport inferred from trajectory calculations, *J. Geophys. Res.*, *109*, D03108, doi: 10.1029/2003JD004069, 2004.
- Fueglistaler, S., M. Bonazzola, P.H. Haynes, and T. Peter, Stratospheric water vapor predicted from the Lagrangian temperature history of air entering the stratosphere in the tropics, *J. Geophys. Res.*, *110*, D08107, doi: 10.1029/2004JD005516, 2005.
- Gaffen, D.J., Temporal inhomogeneities in radiosonde temperature records, *J. Geophys. Res.*, *99* (D2), 3667-3676, 1994.
- Galin, V. Ya., E.M. Volodin, and S.P. Smyshliaev, Atmospheric general circulation model of INM RAS with ozone dynamics, *Russian Meteorol. Hydro.*, *5*, 13-22, 2003.
- Geller, M.A., X.L. Zhou, and M.H. Zhang, Simulations of the interannual variability of stratospheric water vapor, *J. Atmos. Sci.*, *59* (6), 1076-1085, 2002.
- Gerber, E.P., and G.K. Vallis, A stochastic model for the spatial structure of annular patterns of variability and the North Atlantic oscillation, *J. Clim.*, *18* (12), 2102-2118, 2005.
- Gettelman, A., and P.M. de F. Forster, A climatology of the tropical tropopause layer, *J. Meteorol. Soc. Japan*, *80* (4B), 911-924, 2002.
- Gillett, N.P., Northern Hemisphere circulation, *Nature*, *437* (7058), 496, doi: 10.1038/437496a, 2005.
- Gillett, N.P., and D.W.J. Thompson, Simulation of recent Southern Hemisphere climate change, *Science*, *302* (5643), 273-275, 2003.
- Gillett, N.P., M.R. Allen, and K.D. Williams, Modelling the atmospheric response to doubled CO₂ and depleted stratospheric ozone using a stratosphere-resolving coupled GCM, *Quart. J. Roy. Meteorol. Soc.*, *129* (589), 947-966, 2003.
- Giorgetta, M.A., and L. Bengtsson, The potential role of the quasi-biennial oscillation in the stratosphere-troposphere exchange as found in water vapour in general circulation model experiments, *J. Geophys. Res.*, *104* (D6), 6003-6019, 1999.
- Gordon, H.B., L.D. Rotstayn, J.L. McGregor, M.R.

- Dix, E.A. Kowalezyk, S.P. O'Farrell, L.J. Waterman, A.C. Hirst, S.G. Wilson, M.A. Collier, I.G. Watterson, and T.I. Elliott, *The CSIRO Mk3 Climate System Model, CSIRO Atmospheric Research Technical Paper No. 60*, 130 pp., Aspendale, Victoria, Australia, 2002, (http://www.dar.csiro.au/publications/gordon_2002a.pdf).
- Graf, H.-F., I. Kirchner, and J. Perlwitz, Changing lower stratospheric circulation: The role of ozone and greenhouse gases, *J. Geophys. Res.*, *103* (D10), 11251-11261, 1998.
- Gray, L.J., The influence of the equatorial upper stratosphere on stratospheric sudden warmings, *Geophys. Res. Lett.*, *30* (4), 1166, doi: 10.1029/2002GL016430, 2003.
- Gray, L.J., E.F. Drysdale, T.J. Dunkerton, and B.N. Lawrence, Model studies of the interannual variability of the northern hemisphere stratospheric winter circulation: the role of the Quasi Biennial Oscillation, *Quart. J. Roy. Meteorol. Soc.*, *127* (578), 1413-1432, 2001a.
- Gray, L.J., S.J. Phipps, T.J. Dunkerton, M.P. Baldwin, E.F. Drysdale, and M.R. Allen, A data study of the influence of the equatorial upper stratosphere on northern hemisphere stratospheric sudden warmings, *Quart. J. Roy. Meteorol. Soc.*, *127* (576), 1985-2003, 2001b.
- Gray, L.J., S. Crooks, C. Pascoe, S. Sparrow, and M. Palmer, Solar and QBO influences on the timing of stratospheric sudden warmings, *J. Atmos. Sci.*, *61* (23), 2777-2796, 2004.
- Haigh, J.D., The role of stratospheric ozone in modulating the solar radiative forcing of climate, *Nature*, *370* (6490), 544-546, 1994.
- Haigh, J.D., and J.A. Pyle, Ozone perturbation experiments in a two-dimensional circulation model, *Quart. J. Roy. Meteorol. Soc.*, *108*, 551-574, 1982.
- Haigh, J.D., M. Blackburn, and R. Day, The response of tropospheric circulation to perturbations in lower-stratospheric temperature, *J. Clim.*, *18* (17), 3672-3685, 2005.
- Hamilton, K., An examination of observed Southern Oscillation effects in the Northern Hemisphere stratosphere, *J. Atmos. Sci.*, *50* (20), 3468-3473, 1993.
- Hansen, J., A. Lacis, R. Ruedy, and M. Sato, Potential climate impact of Mount Pinatubo eruption, *Geophys. Res. Lett.*, *19* (2), 215-218, doi: 10.1029/91GL02788, 1992.
- Hansen, J., M. Sato, R. Ruedy, L. Nazarenko, A. Lacis, G.A. Schmidt, G. Russell, I. Aleinov, M. Bauer, S. Bauer, N. Bell, B. Cairns, V. Canuto, M. Chandler, Y. Cheng, A. Del Genio, G. Faluvegi, E. Fleming, A. Friend, T. Hall, C. Jackman, M. Kelley, N. Kiang, D. Koch, J. Lean, J. Lerner, K. Lo, S. Menon, R. Miller, P. Minnis, T. Novakov, V. Oinas, Ja. Perlwitz, Ju. Perlwitz, D. Rind, A. Romanou, D. Shindell, P. Stone, S. Sun, N. Tausnev, D. Thresher, B. Wielicki, T. Wong, M. Yao, and S. Zhang, Efficacy of climate forcings, *J. Geophys. Res.*, *110*, D18104, doi: 10.1029/2005JD005776, 2005.
- Hare, S.H.E., L.J. Gray, W.A. Lahoz, A. O'Neill, and L. Steenman-Clark, Can stratospheric temperature trends be attributed to ozone depletion?, *J. Geophys. Res.*, *109*, D05111, doi: 10.1029/2003JD003897, 2004.
- Hartmann, D.L., J.M. Wallace, V. Limpasuvan, D.W.J. Thompson, and J.R. Holton, Can ozone depletion and global warming interact to produce rapid climate change?, *Proc. Natl. Acad. Sci.*, *97* (4), 1412-1417, 2000.
- Hatsushika, H., and K. Yamazaki, Stratospheric drain over Indonesia and dehydration within the tropical tropopause layer diagnosed by air parcel trajectories, *J. Geophys. Res.*, *108* (D19), 4610, doi: 10.1029/2002JD002986, 2003.
- Haynes, P.H., C.J. Marks, M.E. McIntyre, T.G. Shepherd, and K.P. Shine, On the "downward control" of extratropical diabatic circulations by eddy-induced mean zonal forces, *J. Atmos. Sci.*, *48* (4), 651-678, 1991.
- Hegglin, M.I., D. Brunner, T. Peter, J. Staehelin, V. Wirth, P. Hoor, and H. Fischer, Determination of eddy diffusivity in the lowermost stratosphere, *Geophys. Res. Lett.*, *32*, L13812, doi:10.1029/2005GL022495, 2005.
- Hoerling, M.P., J.W. Hurrell, and T. Xu, Tropical origins for recent North Atlantic climate change, *Science*, *292* (5514), 90-92, 2001.
- Hoerling, M.P., J.W. Hurrell, T. Xu, G.T. Bates, and A.S. Phillips, Twentieth century North Atlantic climate change. Part II: Understanding the effect of Indian Ocean warming, *Clim. Dyn.*, *23* (3-4), 391-405, 2004.
- Holton, J.R., and C. Mass, Stratospheric vacillation cycles, *J. Atmos. Sci.*, *33* (11), 2218-2225, 1976.
- Holton, J.R., and H.-C. Tan, The influence of the equatorial quasi-biennial oscillation on the global circulation at 50 mb, *J. Atmos. Sci.*, *37* (10), 2200-2208, 1980.
- Holton, J.R., and H.-C. Tan, The quasi-biennial oscillation in the Northern Hemisphere lower stratosphere, *J. Meteorol. Soc. Japan*, *60*, 140-148, 1982.
- Holton, J.R., P.H. Haynes, M.E. McIntyre, A.R. Douglass, R.B. Rood, and L. Pfister, Stratosphere-troposphere

CLIMATE-OZONE CONNECTIONS

- exchange, *Rev. Geophys.*, 33 (4), 403-440, 1995.
- Hoor, P., C. Gurk, D. Brunner, M.I. Hegglin, H. Wernli, and H. Fischer, Seasonality and extent of extratropical TST derived from in-situ CO measurements during SPURT, *Atmos. Chem. Phys.*, 4, 1427-1442, 2004.
- Hourdin, F., I. Musat, S. Bony, P. Braconnot, F. Codron, J.-L. Dufresne, L. Fairhead, M.-A. Filiberti, P. Friedlingstein, J.-Y. Grandpeix, G. Krinner, P. LeVan, Z.-X. Li, and F. Lott, The LMDZ4 general circulation model: Climate performance and sensitivity to parameterized physics with emphasis on tropical convection, *Clim. Dyn.*, 27 (7-8), 787-813, doi:10.1007/s00382-006-0158-0, 2006.
- Huck, P.E., A.J. McDonald, G.E. Bodeker, and H. Struthers, Interannual variability in Antarctic ozone depletion controlled by planetary waves and polar temperatures, *Geophys. Res. Lett.*, 32, L13819, doi: 10.1029/2005GL022943, 2005.
- Hurrell, J.W., Decadal trend in the North Atlantic Oscillation: Regional temperatures and precipitation, *Science*, 269 (5224), 676-679, 1995.
- Hurrell, J.W., M.P. Hoerling, A.S. Phillips, and T. Xu, Twentieth century North Atlantic climate change. Part I: assessing determinism, *Clim. Dyn.*, 23 (3-4), 371-389, 2004.
- IPCC (Intergovernmental Panel on Climate Change), *Emissions Scenarios. A Special Report of Working Group III of the Intergovernmental Panel on Climate Change*, edited by N. Nakicenovic and R. Swart, 570 pp., Cambridge University Press, Cambridge, U.K., and New York, N.Y., 2000.
- IPCC (Intergovernmental Panel on Climate Change), *Climate Change 2001: The Scientific Basis: Contribution of Working Group I to the Third Assessment Report of the Intergovernmental Panel on Climate Change*, edited by J.T. Houghton, Y. Ding, D.J. Griggs, M. Noguer, P.J. van der Linden, X. Dai, K. Maskell, and C.A. Johnson, 881 pp., Cambridge University Press, Cambridge, U.K., 2001.
- IPCC/TEAP (Intergovernmental Panel on Climate Change/Technology and Economic Assessment Panel), *IPCC/TEAP Special Report on Safeguarding the Ozone Layer and the Global Climate System: Issues Related to Hydrofluorocarbons and Perfluorocarbons*. Prepared by Working Group I and III of the IPCC, and the TEAP. Edited by B. Metz, L. Kuijpers, S. Solomon, S.O. Andersen, O. Davidson, J. Pons, D. de Jager, T. Kestin, M. Manning, and L.A. Meyers, 488 pp., Cambridge University Press, Cambridge, U.K. and New York, NY, USA, 2005.
- IPCC (Intergovernmental Panel on Climate Change), *Climate Change 2007: The Physical Science Basis*, in preparation, 2007.
- Jonsson, A.I., J. de Grandpré, V.I. Fomichev, J.C. McConnell, and S.R. Beagley, Doubled CO₂-induced cooling in the middle atmosphere: Photochemical analysis of the ozone radiative feedback, *J. Geophys. Res.*, 109, D24103, doi: 10.1029/2004JD005093, 2004.
- Jucks, K.W., D.G. Johnson, K.V. Chance, W.A. Traub, J.J. Margitan, G.B. Osterman, R.J. Salawitch, and Y. Sasano, Observations of OH, HO₂, H₂O, and O₃ in the upper stratosphere: Implications for HO_x photochemistry, *Geophys. Res. Lett.*, 25 (21), 3935-3938, 1998.
- K-1 Model Developers, *K-1 Coupled Model (MIROC) Description. K-1 Technical Report 1*, edited by H. Hasumi and S. Emori, 34 pp., Center for Climate System Research, University of Tokyo, Tokyo, Japan, 2004, (<http://www.ccsr.u-tokyo.ac.jp/kyosei/hasumi/MIROC/tech-repo.pdf>).
- Kiehl, J.T., J.J. Hack, G. Bonan, B.A. Boville, D. Williamson, and P. Rasch, The National Center for Atmospheric Research Community Climate Model: CCM3, *J. Clim.*, 11, 1131-1149, 1998.
- Kim, Y.-J., S.D. Eckermann, and H.-Y. Chun, An overview of the past, present and future of gravity-wave drag parameterization for numerical climate and weather prediction models, *Atmos. Ocean*, 41 (1), 65-98, 2003.
- Kindem, I.T., and B. Christiansen, Tropospheric response to stratospheric ozone loss, *Geophys. Res. Lett.*, 28 (8), 1547-1550, 2001.
- Kirk-Davidoff, D.B., E.J. Hints, J.G. Anderson, and D.W. Keith, The effect of climate change on ozone depletion through changes in stratospheric water vapour, *Nature*, 402 (6760), 399-401, 1999.
- Kodera, K., Solar cycle modulation of the North Atlantic Oscillation: Implication in the spatial structure of the NAO, *Geophys. Res. Lett.*, 29 (8), 1218, doi: 10.1029/2001GL014557, 2002.
- Kodera, K., Solar influence on the Indian Ocean Monsoon through dynamical processes, *Geophys. Res. Lett.*, 31, L24209, doi: 10.1029/2004GL020928, 2004.
- Kodera, K., and Y. Kuroda, Dynamical response to the solar cycle, *J. Geophys. Res.*, 107 (D24), 4749, doi: 10.1029/2002JD002224, 2002.
- Kushner, P.J., and L.M. Polvani, Stratosphere-troposphere coupling in a relatively simple AGCM: The role of eddies, *J. Clim.*, 17 (3), 629-639, 2004.
- Labitzke, K., Sunspots, the QBO and the stratospheric temperature in the north polar region, *Geophys. Res.*

- Lett.*, 14 (5), 535-537, 1987.
- Labitzke, K., and H. van Loon, Associations between the 11-year solar cycle, the QBO, and the atmosphere, Part I: Troposphere and stratosphere in the Northern Hemisphere in winter, *J. Atmos. Terr. Phys.*, 50, 197-206, 1988.
- Lal, M., A.K. Jain, and M.C. Sinha, Possible climatic implications of depletion of Antarctic ozone, *Tellus*, 39B, 326-328, 1987.
- Lambert, S.J., and J.C. Fyfe, Changes in winter cyclone frequencies and strengths simulated in enhanced greenhouse warming experiments: Results from the models participating in the IPCC diagnostic exercise, *Clim. Dyn.*, 26 (7-8), 713-728, doi: 10.1007/s00382-006-0110-3, 2006.
- Langematz, U., M. Kunze, K. Krüger, K. Labitzke, and G.L. Roff, Thermal and dynamical changes of the stratosphere since 1979 and their link to ozone and CO₂ changes, *J. Geophys. Res.*, 108 (D1), 4027, doi: 10.1029/2002JD002069, 2003.
- Lanzante, J.R., S.A. Klein, and D.J. Seidel, Temporal homogenization of monthly radiosonde temperature data. Part I: Methodology, *J. Clim.*, 16 (2), 224-240, 2003a.
- Lanzante, J.R., S.A. Klein, and D.J. Seidel, Temporal homogenization of monthly radiosonde temperature data. Part II: Trends, sensitivities, and MSU comparisons, *J. Clim.*, 16 (2), 241-262, 2003b.
- Limpasuvan, V., and D.L. Hartmann, Wave-maintained annular modes of climate variability, *J. Clim.*, 13 (24), 4414-4429, 2000.
- Limpasuvan, V., D.L. Hartmann, D.W.J. Thompson, K. Jeev, and Y.L. Yung, Stratosphere-troposphere evolution during polar vortex intensification, *J. Geophys. Res.*, 110, D24101, doi: 10.1029/2005JD006302, 2005.
- Lindzen, R.S., and J.R. Holton, A theory of the Quasi-Biennial Oscillation, *J. Atmos. Sci.*, 25 (6), 1095-1107, 1968.
- Lorenz, D.J., and D.L. Hartmann, Eddy-zonal flow feedback in the Southern Hemisphere, *J. Atmos. Sci.*, 58 (21), 3312-3327, 2001.
- Lorenz, D.J., and D.L. Hartmann, Eddy-zonal flow feedback in the Northern Hemisphere winter, *J. Clim.*, 16 (8), 1212-1227, 2003.
- Luers, J.K., and R.E. Eskridge, Use of radiosonde temperature data in climate studies, *J. Clim.*, 11 (5), 1002-1019, 1998.
- Manzini, E., B. Steil, C. Brühl, M.A. Giorgetta, and K. Krüger, A new interactive chemistry climate model: 2. Sensitivity of the middle atmosphere to ozone depletion and increase in greenhouse gases and implications for recent stratospheric cooling, *J. Geophys. Res.*, 108 (D14), 4429, doi: 10.1029/2002JD002977, 2003.
- Manzini, E., M.A. Giorgetta, M. Esch, L. Kornblueh, and E. Roeckner, The influence of sea surface temperatures on the Northern winter stratosphere: Ensemble simulations with the MAECHAM5 model, *J. Clim.*, 19, 3863-3881, 2006.
- Marshall, G.J., P.A. Stott, J. Turner, W.M. Connolley, J.C. King, and T.A. Lachlan-Cope, Causes of exceptional atmospheric circulation changes in the Southern Hemisphere, *Geophys. Res. Lett.*, 31, L14205, doi: 10.1029/2004GL019952, 2004.
- Martin, G.M., C. Dearden, C. Greeves, T. Hinton, P. Inness, P. James, V.D. Pope, M.A. Ringer, R.A. Stratton, and G.Y. Yang, *Evaluation of the Atmospheric Performance of HadGAM/GEM1*. Hadley Centre Technical Note No. 54, Hadley Centre for Climate Prediction and Research/Met Office, Exeter, U.K., 2004, (<http://www.metoffice.gov.uk/research/hadleycentre/pubs/HCTN/index.html>).
- Matthes, K., U. Langematz, L.L. Gray, K. Kodera, and K. Labitzke, Improved 11-year solar signal in the Freie Universität Berlin Climate Middle Atmosphere Model (FUB-CMAM), *J. Geophys. Res.*, 109, D06101, doi: 10.1029/2003JD004012, 2004.
- Matthes, K., Y. Kuroda, K. Kodera, and U. Langematz, Transfer of the solar signal from the stratosphere to the troposphere: Northern winter, *J. Geophys. Res.*, 111, D06108, doi: 10.1029/2005JD006283, 2006.
- Mayr, H.G., J.G. Mengel, C.L. Wolff, and H.S. Porter, QBO as potential amplifier of solar cycle influence, *Geophys. Res. Lett.*, 33, L05812, doi: 10.1029/2005GL025650, 2006.
- McIntyre, M.E., How well do we understand the dynamics of stratospheric warmings?, *J. Meteorol. Soc. Japan*, 60 (1), 37-65, 1982.
- McLandress, C., and J.F. Scinocca, The GCM response to current parameterizations of nonorographic gravity wave drag, *J. Atmos. Sci.*, 62 (7), 2394-2413, 2005.
- Mears, C.A., M.C. Schabel, and F.J. Wentz, A reanalysis of the MSU Channel 2 tropospheric temperature record, *J. Clim.*, 16 (22), 3650-3664, 2003.
- Meijer, E.W., B. Bregman, A. Segers, and P.F.J. van Velthoven, The influence of data assimilation on the age of air calculated with a global chemistry-transport model using ECMWF wind fields, *Geophys. Res. Lett.*, 31, L23114, doi: 10.1029/2004GL021158, 2004.
- Nash, J., Extension of explicit radiance observations by the Stratospheric Sounding Unit into the lower

CLIMATE-OZONE CONNECTIONS

- stratosphere and lower mesosphere, *Quart. J. Roy. Meteorol. Soc.*, *114*, 1153-1171, 1988.
- Newman, P.A., S.R. Kawa, and E.R. Nash, On the size of the Antarctic ozone hole, *Geophys. Res. Lett.*, *31*, L21104, doi: 10.1029/2004GL020596, 2004.
- Notholt, J., B.P. Luo, S. Fueglistaler, D. Weisenstein, M. Rex, M.G. Lawrence, H. Bingemer, I. Wohltmann, T. Corti, T. Warneke, R. von Kuhlmann, and T. Peter, Influence of tropospheric SO₂ emissions on particle formation and the stratospheric humidity, *Geophys. Res. Lett.*, *32*, L07810, doi: 10.1029/2004GL022159, 2005.
- Oltmans, S.J., H. Vömel, D.J. Hofmann, K.H. Rosenlof, and D. Kley, The increase in stratospheric water vapor from balloonborne frostpoint hygrometer measurements at Washington D.C., and Boulder, Colorado, *Geophys. Res. Lett.*, *27* (21), 3453-3456, 2000.
- Osterman, G.B., R.J. Salawitch, B. Sen, G.C. Toon, R.A. Stachnik, H.M. Pickett, J.J. Margitan, J.-F. Blavier, and D.B. Peterson, Balloon-borne measurements of stratospheric radicals and their precursors: Implications for the production and loss of ozone, *Geophys. Res. Lett.*, *24* (9), 1107-1110, 1997.
- Pan, L.L., W.J. Randel, B.L. Gary, M.J. Mahoney, and E.J. Hints, Definitions and sharpness of the extratropical tropopause: A trace gas perspective, *J. Geophys. Res.*, *109*, D23103, doi: 10.1029/2004JD004982, 2004.
- Pawson, S., K. Labitzke, and S. Leder, Stepwise changes in stratospheric temperature, *Geophys. Res. Lett.*, *25* (12), 2157-2160, 1998.
- Perlwitz, J., and H.-F. Graf, Troposphere-stratosphere dynamic coupling under strong and weak polar vortex conditions, *Geophys. Res. Lett.*, *28* (2), 271-274, doi: 10.1029/2000GL012405, 2001.
- Perlwitz, J., and N. Harnik, Downward coupling between the stratosphere and troposphere: The relative roles of wave and zonal mean processes, *J. Clim.*, *17* (24), 4902-4909, 2004.
- Pitari, G., E. Mancini, V. Rizi, and D.T. Shindell, Impact of future climate and emission changes on stratospheric aerosols and ozone, *J. Atmos. Sci.*, *59* (3), 414-440, 2002.
- Polvani, L.M., and P.J. Kushner, Tropospheric response to stratospheric perturbations in a relatively simple general circulation model, *Geophys. Res. Lett.*, *29* (7), 1114, doi: 10.1029/2001GL014284, 2002.
- Ramaswamy, V., M.-L. Chanin, J. Angell, J. Barnett, D. Gaffen, M. Gelman, P. Keckhut, Y. Koshelkov, K. Labitzke, J.-J.R. Lin, A. O'Neill, J. Nash, W. Randel, R. Rood, K. Shine, M. Shiotani, and R. Swinbank, Stratospheric temperature trends: Observations and model simulations, *Rev. Geophys.*, *39* (1), 71-122, 2001.
- Ramaswamy, V., M.D. Schwarzkopf, W.J. Randel, B.D. Santer, B.J. Soden, and G.L. Stenchikov, Anthropogenic and natural influences in the evolution of lower stratospheric cooling, *Science*, *311* (5764), 1138-1141, doi: 10.1126/science.1122587, 2006.
- Randel, W.J., and F. Wu, Biases in stratospheric and tropospheric temperature trends derived from historical radiosonde data, *J. Clim.*, *19*, 2094-2104, 2006.
- Randel, W.J., F. Wu, S.J. Oltmans, K. Rosenlof, and G.E. Nedoluha, Interannual changes of stratospheric water vapor and correlations with tropical tropopause temperatures, *J. Atmos. Sci.*, *61* (17), 2133-2148, 2004a.
- Randel, W., P. Udelhofen, E. Fleming, M. Geller, M. Gelman, K. Hamilton, D. Karoly, D. Ortland, S. Pawson, R. Swinbank, F. Wu, M. Baldwin, M. Chanin, P. Keckhut, K. Labitzke, E. Remsberg, A. Simmons, and D. Wu, The SPARC intercomparison of middle-atmosphere climatologies, *J. Clim.*, *17* (5), 986-1003, 2004b.
- Randel, W.J., F. Wu, H. Vömel, G.E. Nedoluha, and P. Forster, Decreases in stratospheric water vapor after 2001: Links to changes in the tropical tropopause and the Brewer-Dobson circulation, *J. Geophys. Res.*, *111*, D12312, doi: 10.1029/2005JD006744, 2006.
- Randeniya, L.K., P.F. Vohralik, and I.C. Plumb, Stratospheric ozone depletion at northern mid latitudes in the 21st century: The importance of future concentrations of greenhouse gases nitrous oxide and methane, *Geophys. Res. Lett.*, *29* (4), 1051, doi: 10.1029/2001GL014295, 2002.
- Remsberg, E.E., and L.E. Deaver, Interannual, solar cycle, and trend terms in middle atmospheric temperature time series from HALOE, *J. Geophys. Res.*, *110*, D06106, doi: 10.1029/2004JD004905, 2005.
- Rex, M., R.J. Salawitch, P. von der Gathen, N.R.P. Harris, M.P. Chipperfield, and B. Naujokat, Arctic ozone loss and climate change, *Geophys. Res. Lett.*, *31*, L04116, doi: 10.1029/2003GL018844, 2004.
- Rind, D., J. Lerner, and C. McLinden, Changes of tracer distributions in the doubled CO₂ climate, *J. Geophys. Res.*, *106* (D22), 28061-28080, doi: 10.1029/2001JD000439, 2001.
- Rind, D., J. Lerner, J. Perlwitz, C. McLinden, and M. Prather, Sensitivity of tracer transports and stratospheric ozone to sea surface temperature patterns in the doubled CO₂ climate, *J. Geophys. Res.*, *107* (D24), 4800, doi: 10.1029/2002JD002483, 2002a.
- Rind, D., P. Lonergan, N.K. Balachandran, and D. Shindell,

- 2 x CO₂ and solar variability influences on the troposphere through wave-mean flow interactions, *J. Meteorol. Soc. Japan*, 80 (4B), 863-876, 2002b.
- Rind, D., J. Perlwitz, and P. Lonergan, AO/NAO response to climate change: 1. Respective influences of stratospheric and tropospheric climate changes, *J. Geophys. Res.*, 110, D12107, doi: 10.1029/2004JD005103, 2005a.
- Rind, D., J. Perlwitz, P. Lonergan, and J. Lerner, AO/NAO response to climate change: 2. Relative importance of low- and high-latitude temperature changes, *J. Geophys. Res.*, 110, D12108, doi: 10.1029/2004JD005686, 2005b.
- Robock, A., Volcanic eruptions and climate, *Rev. Geophys.*, 38 (2), 191-219, 2000.
- Roeckner, E., G. Bäuml, L. Bonaventur, R. Brokopf, M. Esch, M. Giorgetta, S. Hagemann, I. Kirchner, L. Kornbluh, E. Manzini, A. Rhodin, U. Schlese, U. Schulzweida, and A. Tompkins, *The Atmospheric General Circulation Model ECHAM5: Part I, Model Description. Max Planck Institute for Meteorology Report 349*, 127 pp., Max Planck Institute for Meteorology, Bundesstrasse, Hamburg, Germany, 2003.
- Roscoe, H.K., The risk of large volcanic eruptions and the impact of this risk on future ozone depletion, *Nat. Hazards*, 23 (2-3), 231-246, 2001.
- Rosenfield, J.E., Effects of volcanic eruptions on stratospheric ozone recovery, in *Volcanism and the Earth's Atmosphere*, edited by A. Robock, and C. Oppenheimer, *Geophysical Monograph 139*, American Geophysical Union, 227-236, 2003.
- Rosenfield, J.E., A.R. Douglass, and D.B. Considine, The impact of increasing carbon dioxide on ozone recovery, *J. Geophys. Res.*, 107 (D6), 4049, doi: 10.1029/2001JD000824, 2002.
- Rosenlof, K.H., S.J. Oltmans, D. Kley, J.M. Russell III, E.-W. Chiou, W.P. Chu, D.G. Johnson, K.K. Kelly, H.A. Michelsen, G.E. Nedoluha, E.E. Remsburg, G.C. Toon, and M.P. McCormick, Stratospheric water vapor increases over the past half-century, *Geophys. Res. Lett.*, 28 (7), 1195-1198, 2001.
- Rozanov, E.V., M.E. Schlesinger, N.G. Andronova, F. Yang, S.L. Malyshev, V.A. Zubov, T.A. Egorova, and B. Li, Climate/chemistry effects of the Pinatubo volcanic eruption simulated by the UIUC stratosphere/troposphere GCM with interactive photochemistry, *J. Geophys. Res.*, 107 (D21), 4594, doi: 10.1029/2001JD000974, 2002.
- Santer, B.D., T.M.L. Wigley, C. Doutriaux, J.S. Boyle, J.E. Hansen, P.D. Jones, G.A. Meehl, E. Roeckner, S. Sengupta, and K.E. Taylor, Accounting for the effects of volcanoes and ENSO in comparisons of modeled and observed temperature trends, *J. Geophys. Res.*, 106 (D22), 28033-28059, 2001.
- Santer, B.D., M.F. Wehner, T.M.L. Wigley, R. Sausen, G.A. Meehl, K.E. Taylor, C. Ammann, J. Arblaster, W.M. Washington, J.S. Boyle, and W. Brüggemann, Contributions of anthropogenic and natural forcing to recent tropopause height changes, *Science*, 301 (5632), 479-483, doi: 10.1126/science.1084123, 2003.
- Santer, B.D., T.M.L. Wigley, A.J. Simmons, P.W. Kållberg, G.A. Kelly, S.M. Uppala, C. Ammann, J.S. Boyle, W. Brüggemann, C. Doutriaux, M. Fiorino, C. Mears, G.A. Meehl, R. Sausen, K.E. Taylor, W.M. Washington, M.F. Wehner, and F.J. Wentz, Identification of anthropogenic climate change using a second-generation reanalysis, *J. Geophys. Res.*, 109, D21104, doi: 10.1029/2004JD005075, 2004.
- Santer, B.D., T.M.L. Wigley, C. Mears, F.J. Wentz, S.A. Klein, D.J. Seidel, K.E. Taylor, P.W. Thorne, M.F. Wehner, P.J. Gleckler, J.S. Boyle, W.D. Collins, K.W. Dixon, C. Doutriaux, M. Free, Q. Fu, J.E. Hansen, G.S. Jones, R. Ruedy, T.R. Karl, J.R. Lanzante, G.A. Meehl, V. Ramaswamy, G. Russell, and G.A. Schmidt, Amplification of surface temperature trends and variability in the tropical atmosphere, *Science*, 309 (5740), 1551-1556, doi: 10.1126/science.1114867, 2005.
- Santer, B.D., J.E. Penner, and P.W. Thorne, How well can the observed vertical temperature changes be reconciled with our understanding of the causes of these changes?, in *Temperature Trends in the Lower Atmosphere: Steps for Understanding and Reconciling Differences*, A Report by the U.S. Climate Change Science Program and the Subcommittee on Global Change Research, edited by T.R. Karl, S.J. Hassol, C.D. Miller, and W.L. Murray, 89-118, NOAA, National Climatic Data Center, Asheville, North Carolina, USA, 2006.
- Sassi, F., D. Kinnison, B.A. Boville, R.R. Garcia, and R. Roble, Effect of El Niño-Southern Oscillation on the dynamical, thermal, and chemical structure of the middle atmosphere, *J. Geophys. Res.*, 109, D17108, doi: 10.1029/2003JD004434, 2004.
- Scaife, A.A., J. Austin, N. Butchart, S. Pawson, M. Keil, J. Nash, and I.N. James, Seasonal and interannual variability of the stratosphere diagnosed from UKMO TOVS analyses, *Quart. J. Roy. Meteorol. Soc.*, 126 (568), 2585-2604, 2000.
- Scaife, A.A., J.R. Knight, G.K. Vallis, and C.K. Folland, A stratospheric influence on the winter NAO and North Atlantic surface climate, *Geophys. Res. Lett.*,

CLIMATE-OZONE CONNECTIONS

- 32, L18715, doi: 10.1029/2005GL023226, 2005.
- Scheele, M.P., P.C. Siegmund, and P.F.J. van Velthoven, Stratospheric age of air computed with trajectories based on various 3D-Var and 4D-Var data sets, *Atmos. Chem. Phys.*, 5, 1-7, 2005.
- Schmidt, G.A., R. Ruedy, J.E. Hansen, I. Aleinov, N. Bell, M. Bauer, S. Bauer, B. Cairns, V. Canuto, Y. Cheng, A. DelGenio, G. Faluvegi, A.D. Friend, T.M. Hall, Y. Hu, M. Kelley, N.Y. Kiang, D. Koch, A.A. Lacis, J. Lerner, K.K. Lo, R.L. Miller, L. Nazarenko, V. Oinas, Ja. Perlwitz, Ju. Perlwitz, D. Rind, A. Romanou, G.L. Russell, M. Sato, D.T. Shindell, P.H. Stone, S. Sun, N. Tausnev, D. Thresher, and M.-S. Yao, Present day atmospheric simulations using GISS ModelE: Comparison to in-situ, satellite and reanalysis data, *J. Clim.*, 19, 153-192, 2006.
- Schneider, T., The tropopause and the thermal stratification in the extratropics of a dry atmosphere, *J. Atmos. Sci.*, 61 (12), 1317-1340, 2004.
- Schoeberl, M.R., A.R. Douglass, Z. Zhu, and S. Pawson, A comparison of lower stratospheric age spectra derived from a general circulation model and two data assimilation systems, *J. Geophys. Res.*, 108 (D3), 4113, doi: 10.1029/2002JD002652, 2003.
- Schoeberl, M.R., A.R. Douglass, B. Polansky, C. Boone, K.A. Walker, and P. Bernath, Estimation of stratospheric age spectrum from chemical tracers, *J. Geophys. Res.*, 110, D21303, doi: 10.1029/2005JD006125, 2005.
- Scott, R.K., and L.M. Polvani, Stratospheric control of upward wave flux near the tropopause, *Geophys. Res. Lett.*, 31, L02115, doi: 10.1029/2003GL017965, 2004.
- Scott, R.K., and L.M. Polvani, Internal variability of the winter stratosphere. Part I: Time independent forcing, *J. Atmos. Sci.*, 63 (11), 2758-2776, doi: 10.1175/JAS3797.1, 2006.
- Scott, R.K., D.G. Dritschel, L.M. Polvani, and D.W. Waugh, Enhancement of Rossby wave breaking by steep potential vorticity gradients in the winter stratosphere, *J. Atmos. Sci.*, 61 (8), 904-918, 2004.
- Seidel, D.J., and J.R. Lanzante, An assessment of three alternatives to linear trends for characterizing global atmospheric temperature changes, *J. Geophys. Res.*, 109, D14108, doi: 10.1029/2003JD004414, 2004.
- Seidel, D.J., R.J. Ross, J.K. Angell, and G.C. Reid, Climatological characteristics of the tropical tropopause as revealed by radiosondes, *J. Geophys. Res.*, 106 (D8), 7857-7878, 2001.
- Seidel, D.J., J.K. Angell, J. Christy, M. Free, S.A. Klein, J.R. Lanzante, C. Mears, D. Parker, M. Schabel, R. Spencer, A. Sterin, P. Thorne, and F. Wentz, Uncertainty in signals of large-scale climate variations in radiosonde and satellite upper-air temperature datasets, *J. Clim.*, 17 (11), 2225-2240, 2004.
- Sexton, D.M.H., The effect of stratospheric ozone depletion on the phase of the Antarctic Oscillation, *Geophys. Res. Lett.*, 28 (19), 3697-3700, 2001.
- Shaw, T.A., and T.G. Shepherd, Angular momentum conservation and gravity wave drag parameterization: Implications for climate models, *J. Atmos. Sci.*, 64 (1), 190-203, 2007.
- Shepherd, T.G., Issues in stratosphere-troposphere coupling, *J. Meteorol. Soc. Japan*, 80 (4B), 769-792, 2002.
- Sherwood, S.C., and A.E. Dessler, A model for transport across the tropical tropopause, *J. Atmos. Sci.*, 58 (7), 765-779, 2001.
- Shibata, K., H. Yoshimura, M. Ohizumi, M. Hosaka, and M. Sugi, A simulation of troposphere, stratosphere and mesosphere with an MRI/JMA98 GCM. Papers in *Meteorol. Geophys.*, 50, 15-53, 1999. (Available from Meteorological Research Institute, Nagamine 1-1, Tsukuba, Ibaraki, 305-0052, Japan.)
- Shindell, D.T., Climate and ozone response to increased stratospheric water vapor, *Geophys. Res. Lett.*, 28 (8), 1551-1554, 2001.
- Shindell, D., and G.A. Schmidt, Southern Hemisphere climate response to ozone changes and greenhouse gas increases, *Geophys. Res. Lett.*, 31, L18209, doi: 10.1029/2004GL020724, 2004.
- Shindell, D.T., D. Rind, N. Balachandran, J. Lean, and P. Lonergan, Solar cycle variability, ozone, and climate, *Science*, 284 (5412), 305-308, 1999.
- Shindell, D.T., G.A. Schmidt, R.L. Miller, and D. Rind, Northern Hemisphere winter climate response to greenhouse gas, ozone solar and volcanic forcing, *J. Geophys. Res.*, 106 (D7), 7193-7210, 2001.
- Shine, K.P., M.S. Bourqui, P.M.F. Forster, S.H.E. Hare, U. Langematz, P. Braesicke, V. Grewe, M. Ponater, C. Schnadt, C.A. Smith, J.D. Haigh, J. Austin, N. Butchart, D.T. Shindell, W.J. Randel, T. Nagashima, R.W. Portmann, S. Solomon, D.J. Seidel, J. Lanzante, S. Klein, V. Ramaswamy, and M.D. Schwarzkopf, A comparison of model-simulated trends in stratospheric temperatures, *Quart. J. Roy. Meteorol. Soc.*, 129 (590), 1565-1588, 2003.
- Sigmond, M., P.C. Siegmund, E. Manzini, and H. Kelder, A simulation of the separate climate effects of middle-atmospheric and tropospheric CO₂ doubling, *J. Clim.*, 17 (12), 2352-2367, 2004.
- Smith, A.K., An investigation of resonant waves in a numer-

- ical model of an observed sudden stratospheric warming, *J. Atmos. Sci.*, 46 (19), 3038-3054, 1989.
- Solomon, S., R.W. Portmann, T. Sasaki, D.J. Hofmann, and D.W.J. Thompson, Four decades of ozonesonde measurements over Antarctica, *J. Geophys. Res.*, 110, D21311, doi: 10.1029/2005JD005917, 2005.
- Song, Y., and W.A. Robinson, Dynamical mechanisms for stratospheric influences on the troposphere, *J. Atmos. Sci.*, 61 (14), 1711-1725, 2004.
- SPARC (Stratospheric Processes And their Role in Climate), *SPARC Assessment of Upper Tropospheric and Stratospheric Water Vapour*, edited by D. Kley, J.M. Russell III, and C. Phillips, *World Climate Research Program Report 113*, SPARC Report No. 2, 312 pp., Verrières le Buisson, France, 2000.
- SPARC (Stratospheric Processes And their Role in Climate), *SPARC Assessment of Stratospheric Aerosol Properties (ASAP)*, edited by L. Thomason, and Th. Peter, *World Climate Research Program Report 124*, SPARC Report No. 4, 346 pp., Verrières le Buisson, France, 2006.
- Steinbrecht, W., H. Claude, U. Köhler, and K.P. Hoinka, Correlations between tropopause height and total ozone: Implications for long-term changes, *J. Geophys. Res.*, 103 (D15), 19183-19192, 1998.
- Stenchikov, G., I. Kirchner, A. Robock, H.-F. Graf, J.C. Artuña, R.G. Grainger, A. Lambert, and L. Thomason, Radiative forcing from the 1991 Mount Pinatubo volcanic eruption, *J. Geophys. Res.*, 103 (D12), 13837-13857, 1998.
- Stenchikov, G.L., A. Robock, V. Ramaswamy, M.D. Schwarzkopf, K. Hamilton, and S. Ramachandran, Arctic Oscillation response to the 1991 Mount Pinatubo eruption: Effects of volcanic aerosols and ozone depletion, *J. Geophys. Res.*, 107 (D24), 4803, doi: 10.1029/2002JD002090, 2002.
- Stenke, A., and V. Grewe, Simulation of stratospheric water vapor trends: impact on stratospheric ozone chemistry, *Atmos. Chem. Phys.*, 5, 1257-1272, 2005.
- Stohl, A., H. Wernli, P. James, M. Bourqui, C. Forster, M.A. Liniger, P. Seibert, and M. Sprenger, A new perspective of stratosphere-troposphere exchange, *Bull. Amer. Meteorol. Soc.*, 84 (11), 1565-1573, 2003.
- Sudo, K., M. Takahashi, and H. Akimoto, Future changes in stratosphere-troposphere exchange and their impacts on future tropospheric ozone simulations, *Geophys. Res. Lett.*, 30 (24), 2256, doi: 10.1029/2003GL018526, 2003.
- Tabazadeh, A., M.L. Santee, M.Y. Danilin, H.C. Pumphrey, P.A. Newman, P.J. Hamill, and J.L. Mergenthaler, Quantifying denitrification and its effect on ozone recovery, *Science*, 288 (5470), 1407-1411, 2000.
- Taguchi, M., and D.L. Hartmann, Increased occurrence of stratospheric sudden warmings during El Niño as simulated by WACCM, *J. Clim.*, 19 (3), 324-332, 2006.
- Tett, S.F.B., G.S. Jones, P.A. Stott, D.C. Hill, J.F.B. Mitchell, M.R. Allen, W.J. Ingram, T.C. Johns, C.E. Johnson, A. Jones, D.L. Roberts, D.M.H. Sexton, and M.J. Woodage, Estimation of natural and anthropogenic contributions to twentieth century temperature change, *J. Geophys. Res.*, 107 (D16), 4306, doi: 10.1029/2000JD000028, 2002.
- The GFDL Global Atmospheric Model Development Team (GAMDT), The new GFDL global atmosphere and land model AM2-LM2: Evaluation with prescribed SST simulations. *J. Clim.*, 17, 4641-4673, 2004.
- Thomason, L.W., S.P. Burton, N. Iyer, J.M. Zawodny, and J. Anderson, A revised water vapor product for the Stratospheric Aerosol and Gas Experiment (SAGE) II version 6.2 data set, *J. Geophys. Res.*, 109, D06312, doi: 10.1029/2003JD004465, 2004.
- Thompson, D.W.J., and S. Solomon, Interpretation of recent Southern Hemisphere climate change, *Science*, 296 (5569), 895-899, 2002.
- Thompson, D.W.J., and S. Solomon, Recent stratospheric climate trends as evidenced in radiosonde data: Global structure and tropospheric linkages, *J. Clim.*, 18 (22), 4785-4795, 2005.
- Thompson, D.W.J., and J.M. Wallace, The Arctic Oscillation signature in the wintertime geopotential height and temperature fields, *Geophys. Res. Lett.*, 25 (9), 1297-1300, 1998.
- Thompson, D.W.J., and J.M. Wallace, Annular modes in the extratropical circulation. Part I: Month-to-month variability, *J. Clim.*, 13 (5), 1000-1016, 2000.
- Thompson, D.W.J., J.M. Wallace, and G.C. Hegerl, Annular modes in the extratropical circulation. Part II: Trends, *J. Clim.*, 13 (5), 1018-1036, 2000.
- Thompson, D.W.J., J.C. Furtado, and T.G. Shepherd, On the tropospheric response to anomalous stratospheric wave drag and radiative heating, *J. Atmos. Sci.*, 63 (10), 2616-2629, 2006.
- Thorne, P.W., P.D. Jones, T.J. Osborn, T.D. Davies, S.F.B. Tett, D.E. Parker, P.A. Stott, G.S. Jones, and M.R. Allen, Assessing the robustness of zonal mean climate change detection, *Geophys. Res. Lett.*, 29 (19), 1920, doi: 10.1029/2002GL015717, 2002.
- Thuburn, J., and G.C. Craig, On the temperature structure of the tropical substratosphere, *J. Geophys. Res.*, 107 (D2), 4017, doi:10.1029/2001JD000448, 2002.

CLIMATE-OZONE CONNECTIONS

- Tian, W., and M.P. Chipperfield, A new coupled chemistry-climate model for the stratosphere: The importance of coupling for future O₃-climate prediction, *Quart. J. Roy. Meteorol. Soc.*, 131 (605), 281-303, 2005.
- Tie, X., and G. Brasseur, The response of stratospheric ozone to volcanic eruptions: Sensitivity to atmospheric chlorine loading, *Geophys. Res. Lett.*, 22 (22), 3035-3038, 1995.
- Tilmes, S., R. Müller, J.-U. Grooß, and J.M. Russell III, Ozone loss and chlorine activation in the Arctic winters 1991-2003 derived with the tracer-tracer correlations, *Atmos. Chem. Phys.*, 4, 2181-2213, 2004.
- Timmreck, C., H.-F. Graf, and B. Steil, Aerosol chemistry interactions after the Mt. Pinatubo eruption, in *Volcanism and the Earth's Atmosphere*, edited by A. Robock and C. Oppenheimer, *Geophysical Monograph 139*, 214-225, American Geophysical Union, Washington, D.C., 2003.
- van Loon, H., and K. Labitzke, The Southern Oscillation, Part V: The anomalies in the lower stratosphere of the Northern Hemisphere in winter and a comparison with the Quasi-Biennial Oscillation, *Mon. Wea. Rev.*, 115 (2), 357-369, 1987.
- Varotsos, C., C. Cartalis, A. Vlamakis, C. Tzanis, and I. Keramitsoglou, The long-term coupling between column ozone and tropopause properties, *J. Clim.*, 17 (19), 3843-3854, 2004.
- Volodin, E.M., and V.Y. Galin, Interpretation of winter warming on Northern Hemisphere continents in 1977-94, *J. Clim.*, 12 (10), 2947-2955, 1999.
- Walter, B.P., and M. Heimann, A process-based, climate-sensitive model to derive methane emissions from natural wetlands: Application to five wetland sites, sensitivity to model parameters, and climate, *Global Biogeochem. Cycles*, 14 (3), 745-766, 2000.
- Walter, K., and H.-F. Graf, The North Atlantic variability structure, storm tracks, and precipitation depending on the polar vortex strength, *Atmos. Chem. Phys.*, 5, 239-248, 2005.
- Wennberg, P.O., R.C. Cohen, R.M. Stimpfle, J.P. Koplów, J.G. Anderson, R.J. Salawitch, D.W. Fahey, E.L. Woodbridge, E.R. Keim, R.S. Gao, C.R. Webster, R.D. May, D.W. Toohey, L.M. Avallone, M.H. Proffitt, M. Loewenstein, J.R. Podolske, K.R. Chan, and S.C. Wofsy, Removal of stratospheric O₃ by radicals: In situ measurements of OH, H₂O, NO, NO₂, ClO, and BrO, *Science*, 266 (5184), 398-404, 1994.
- Wennberg, P.O., T.F. Hanisco, L. Jaeglé, D.J. Jacob, E.J. Hints, E.J. Lanzendorf, J.G. Anderson, R.-S. Gao, E.R. Keim, S.G. Donnelly, L.A. Del Negro, D.W. Fahey, S.A. McKeen, R.J. Salawitch, C.R. Webster, R.D. May, R.L. Herman, M.H. Proffitt, J.J. Margitan, E.L. Atlas, S.M. Schauffler, F. Flocke, C.T. McElroy, and T.P. Bui, Hydrogen radicals, nitrogen radicals, and the production of O₃ in the upper troposphere, *Science*, 279 (5347), 49-53, 1998.
- Wigley, T.M.L., C.M. Amman, B.D. Santer, and S.C.B. Raper, Effect of climate sensitivity on the response to volcanic forcing, *J. Geophys. Res.*, 110, D09107, doi: 10.1029/2004JD005557, 2005.
- Wittman, M.A.H., L.M. Polvani, R.K. Scott, and A.J. Charlton, Stratospheric influence on baroclinic life-cycles and its connection to the Arctic Oscillation, *Geophys. Res. Lett.*, 31, L16113, doi: 10.1029/2004GL020503, 2004.
- WMO (World Meteorological Organization), *Scientific Assessment of Ozone Depletion: 1998, Global Ozone Research and Monitoring Project-Report No. 44*, Geneva, Switzerland, 1999.
- WMO (World Meteorological Organization), *Scientific Assessment of Ozone Depletion: 2002, Global Ozone Research and Monitoring Project-Report No. 47*, Geneva, Switzerland, 2003.
- Wu, D.L., Mesoscale gravity wave variances from AMSU-A radiances, *Geophys. Res. Lett.*, 31, L12114, doi: 10.1029/2004GL019562, 2004.
- Yokohata, T., S. Emori, T. Nozawa, Y. Tsusima, T. Ogura, and M. Kimoto, Climate response to volcanic forcing: Validation of climate sensitivity of a coupled atmosphere-ocean circulation model, *Geophys. Res. Lett.*, 32, L21710, doi: 10.1029/2005GL023542, 2005.
- Zeng, G., and J.A. Pyle, Changes in tropospheric ozone between 2000 and 2100 modeled in a chemistry-climate model, *Geophys. Res. Lett.*, 30 (7), 1392, doi: 10.1029/2002GL016708, 2003.
- Zhou, X.-L., M.A. Geller, and M. Zhang, Cooling trend of the tropical cold point tropopause temperatures and its implications, *J. Geophys. Res.*, 106 (D2), 1511-1522, 2001.
- Zhou, X.-L., M.A. Geller, and M. Zhang, Temperature fields in the tropical tropopause transition layer, *J. Clim.*, 17 (15), 2901-2908, 2004.

Appendix 5A

AOGCMs USED IN THIS CHAPTER

The coupled atmosphere-ocean general circulation models (AOGCMs) used in this chapter, and the country of the sponsoring organization. The model simulations were completed to support the Fourth Assessment Report of the Intergovernmental Panel on Climate Change (IPCC, in preparation for 2007). The models submitted 21st century simulations using the A2 (high) and B1 (low) emission scenarios. Also listed is the key reference for the atmospheric model, the approximate altitude in kilometers of the model top, and the number of stratospheric levels at or above 16 km. The experiments include various emission scenarios of the 20th and 21st century and focus on simulating the surface and tropospheric climate. The stratosphere of most of these models tends to be poorly resolved. While all models include changes in well-mixed greenhouse gases, other forcings such as changes in ozone, volcanic and other aerosols, and changes in solar radiation are only included in a subset of the models. This set of experiments was produced by 15 modeling groups from 9 countries and represents one of the most comprehensive international climate model efforts ever attempted.

Model	Key Reference	Model Top	Stratospheric Levels
BCCR-BCM2.0, Norway	Déqué et al., 1994	33	5
CCSM3, USA	Collins et al., 2004	40	7
CGCM3.1(T47), Canada	Flato, 2005	49	11
CNRM-CM3, France	Déqué et al., 1994	76	17
CSIRO-Mk3.0, Australia	Gordon et al., 2002	38	3
ECHAM5/MPI-OM, Germany	Roeckner et al., 2003	29	4
GFDL-CM2.0, USA	GFDL GAMDT, 2004	35	3
GFDL-CM2.1, USA	GFDL GAMDT, 2004	35	3
GISS-ER, USA	Schmidt et al., 2006	67	9
INM-CM3.0, Russia	Galim et al., 2003	32	6
IPSL-CM4, France	Hourdin et al., 2006	32	7
MIROC3.2-M, Japan	K-1 Developers, 2004	67	6
MRI-CGCM2.3.2, Japan	Shibata et al., 1999	54	8
PCM, USA	Kiehl et al., 1998	43	7
UKMO-HadGEM1, UK	Martin et al., 2004	39	10